Final Report

ENHANCED CHARACTERIZATION OF RAP FOR CRACKING PERFORMANCE

UF Project No.: P0034549
Contract No.: BDV31-977-70

Submitted to:

Florida Department of Transportation
605 Suwannee Street MS-30
Tallahassee, FL, 32399

Dr. Reynaldo Roque, P.E.
Bongsuk Park
Dr. Jian Zou
George Lopp

Department of Civil and Coastal Engineering
College of Engineering
365 Weil Hall, P.O. Box 116580
Gainesville, FL, 32611-6580
Tel: (352) 392-9537 extension 1458
Fax: (352) 392-3394

February 2020

DISCLAIMER

The opinions, findings, and conclusions expressed in this publication are those of the authors and not necessarily those of the State of Florida Department of Transportation.

Prepared in cooperation with the State of Florida Department of Transportation.

SI* (MODERN METRIC) CONVERSION FACTORS

APPROXIMATE CONVERSIONS TO SI UNITS

SYMBOL	WHEN YOU KNOW	MULTIPLY BY	TO FIND	SYMBOL
		LENGTH		
in	inches	25.4	millimeters	mm
ft	feet	0.305	meters	m
yd	yards	0.914	meters	m
mi	miles	1.61	kilometers	km
		AREA		
in^2	square inches	645.2	square millimeters	mm^2
ft^2	square feet	0.093	square meters	m^2
yd^2	square yard	0.836	square meters	m^2
ac	acres	0.405	hectares	ha
mi^2	square miles	2.59	square kilometers	km^2
		VOLUME		
fl oz	fluid ounces	29.57	milliliters	mL
gal	gallons	3.785	liters	L
ft^3	cubic feet	0.028	cubic meters	m^3
yd^3	cubic yards	0.765	cubic meters	m^3
	NOTE: volumes greater than 1000 L shall be shown in m^3			
		MASS		
oz	ounces	28.35	grams	g
lb	pounds	0.454	kilograms	kg
T	short tons (2000 lb)	0.907	megagrams (or "metric ton")	Mg (or "t")
		TEMPERATURE (exact degrees)		
°F	Fahrenheit	5 (F-32)/9 or (F-32)/1.8	Celsius	°C
		ILLUMINATION		
fc	foot-candles	10.76	lux	lx
fl	foot-Lamberts	3.426	candela/m^2	cd/m^2
		FORCE and PRESSURE or STRESS		
lbf	poundforce	4.45	newtons	N
lbf/in^2	poundforce per square inch	6.89	kilopascals	kPa

APPROXIMATE CONVERSIONS FROM SI UNITS

SYMBOL	WHEN YOU KNOW	MULTIPLY BY	TO FIND	SYMBOL
		LENGTH		
mm	millimeters	0.039	inches	in
m	meters	3.28	feet	ft
m	meters	1.09	yards	yd
km	kilometers	0.621	miles	mi
		AREA		
mm^2	square millimeters	0.0016	square inches	in^2
m^2	square meters	10.764	square feet	ft^2
m^2	square meters	1.195	square yards	yd^2
ha	hectares	2.47	acres	ac
km^2	square kilometers	0.386	square miles	mi^2
		VOLUME		
mL	milliliters	0.034	fluid ounces	fl oz
L	liters	0.264	gallons	gal
m^3	cubic meters	35.314	cubic feet	ft^3
m^3	cubic meters	1.307	cubic yards	yd^3
		MASS		
g	grams	0.035	ounces	oz
kg	kilograms	2.202	pounds	lb
Mg (or "t")	megagrams (or "metric ton")	1.103	short tons (2000 lb)	T
		TEMPERATURE (exact degrees)		
°C	Celsius	1.8C+32	Fahrenheit	°F
		ILLUMINATION		
lx	lux	0.0929	foot-candles	fc
cd/m^2	candela/m^2	0.2919	foot-Lamberts	fl
		FORCE and PRESSURE or STRESS		
N	newtons	0.225	poundforce	lbf
kPa	kilopascals	0.145	poundforce per square inch	lbf/in^2

*SI is the symbol for the International System of Units. Appropriate rounding should be made to comply with Section 4 of ASTM E380.

(Revised March 2003)

TECHNICAL REPORT DOCUMENTATION PAGE

1. Report No.	2. Government Accession No.	3. Recipient's Catalog No.	
4. Title and Subtitle Enhanced Characterization of RAP for Cracking Performance		5. Report Date February 2020	
		6. Performing Organization Code	
7. Author(s) Reynaldo Roque, Bongsuk Park, Jian Zou, and George Lopp		8. Performing Organization Report No. P0034549	
9. Performing Organization Name and Address University of Florida Department of Civil and Coastal Engineering 365 Weil Hall, PO Box 116580 Gainesville, FL 32611-6580		10. Work Unit No. (TRAIS)	
		11. Contract or Grant No. BDV31-977-70	
12. Sponsoring Agency Name and Address Florida Department of Transportation Research Center, MS 30 605 Suwannee Street Tallahassee, FL, 32399-0450		13. Type of Report and Period Covered Final 03/14/17-02/29/20	
		14. Sponsoring Agency Code	
15. Supplementary Notes			
16. Abstract: Even though reclaimed asphalt pavement (RAP) has economic and environmental benefits, the average percent usage of RAP in asphalt mixture in the United States is only 20.4%. Current Florida Department of Transportation (FDOT) specifications limit RAP usage to 20% in polymer-modified asphalt (PMA) mixtures and do not allow RAP in high-polymer (HP) mixtures. Literature indicated RAP binder stiffness and RAP gradation were important characteristics related to RAP mixture cracking performance. This study focused on evaluating the effect of these RAP characteristics on cracking resistance and on determining whether the current maximum RAP usage in PMA and HP mixtures may be increased with or without the need for RAP characterization. Twelve RAP sources were characterized using recovered RAP binder and aggregate to identify the range of RAP binder stiffness and RAP gradation for Florida RAP material. Eight out of 12 RAP sources, covering the range of these RAP characteristics encountered in Florida, were selected for further evaluation. The interstitial component fracture energy (FE_{IC}) obtained from IC direct tension tests was used as a surrogate for a mixture fracture energy (FE_{mix}) to assess all RAP mixture combinations. FE_{mix} obtained from Superpave indirect tensile (IDT) tests was used to evaluate findings from FE_{IC} results. Finer and stiffer RAP was more detrimental to cracking resistance than coarser and less stiff RAP. This indicated characterizing that RAP binder stiffness and RAP gradation was necessary to increase the current maximum RAP content in PMA mixture. A guideline to determine maximum RAP usage in PMA mixtures based on these two key RAP characteristics was developed to allow more than 20% RAP in PMA mixtures. Proposed guidelines which allow up to 40% RAP were validated by way of full mixture testing. Furthermore, it was concluded that incorporation of 20% RAP would sacrifice premium cracking performance expected of HP mixtures.			
17. Key Words: Reclaimed asphalt pavement (RAP), RAP characterization, cracking, polymer-modified asphalt binder, high-polymer binder, RAP binder stiffness, RAP fineness		18. Distribution Statement No restrictions	
19. Security Classif. (of this report) Unclassified	20. Security Classif. (of this page) Unclassified	21. No of Pages 135	22. Price

Form DOT F 1700.7 (8-72)

ACKNOWLEDGEMENT

The authors would like to acknowledge and thank the Florida Department of Transportation (FDOT) for providing technical and financial support and materials for this project. Special thanks go to project manager Howie Moseley and engineers and technicians of the Bituminous Section of the State Materials Office for their contributions throughout the various phases of this project.

EXECUTIVE SUMMARY

Reclaimed asphalt pavement (RAP) is a useful alternative to virgin aggregate and asphalt binder in the production of hot mix asphalt (HMA). Even though RAP has economic and environmental benefits, the average percent usage of RAP in asphalt mixtures is only 20.4% in the United States. Current Florida Department of Transportation (FDOT) specifications limit RAP usage to 20% in polymer-modified asphalt (PMA) mixtures, and RAP is not allowed in high-polymer (HP) mixtures. There is no requirement related to RAP characteristics. However, based on literature review, RAP binder stiffness and RAP aggregate gradation are related to cracking performance of RAP mixtures. Therefore, determination of these two characteristics may help increase the current limit for RAP usage in PMA mixtures. This study focused on evaluating an effect of these RAP characteristics on cracking resistance and on determining whether the current maximum RAP usage in PMA and HP mixtures may be increased with or without the need for RAP characteristics.

Twelve RAP sources were characterized using recovered RAP binder and aggregate to identify the range of RAP binder stiffness and RAP gradation for Florida RAP material. Eight out of 12 RAP sources, covering the range of these RAP characteristics encountered in Florida, were selected for further evaluation. High-temperature continuous grade was used to characterize RAP binder stiffness. The percent passing the No. 16 sieve size (1.18 mm), which was called RAP fineness in this study, was selected to characterize RAP gradation based on the dominant aggregate size range-interstitial component (DASR-IC) theory. DASR-IC theory indicates that 1.18 mm is the smallest size that contributes to aggregate interlocking. For each RAP source, an existing mix design (PMA mixture with 20% RAP) was used as a reference to design higher RAP mixtures (30% and 40%) and a control mixture (0% RAP). Use of existing mix design allowed evaluation of actual RAP mixtures currently used in Florida.

The experimental program consisted of two steps: (i) interstitial component direct tension (ICDT) test to evaluate all RAP mixture combinations and (ii) Superpave indirect tensile (IDT) tests to evaluate findings from the ICDT test results. IC fracture energy (FE_{IC}) obtained from the ICDT test was used as a surrogate for mixture fracture energy (FE_{mix}) because the ICDT test requires less effort in specimen preparation and testing than a mixture test. A previous study indicated that FE_{IC} correlated well with FE_{mix} of corresponding mixtures (Yan et al. 2017b).

Test results showed that finer and stiffer RAP was more detrimental to cracking resistance than coarser and less stiff RAP. Fine RAP sources (RAP fineness greater than 50%) resulted in lower FE_{IC} and FE_{mix} than coarser RAP. FE_{IC} of fine RAP appeared marginal, even at 20% RAP content. Lower FE_{IC} for fine RAP may be explained by the fact that finer RAP resulted in a greater amount of RAP, and therefore RAP binder, in the IC portion than coarser RAP at the same RAP content. In addition to the lower FE_{IC}, fine RAP caused a greater reduction in FE_{IC} with increasing %RAP as compared to coarse and intermediate RAP. Furthermore, stiffer RAP binder generally led to lower FE_{IC}. For the three intermediate RAP sources which had a similar RAP fineness level, stiffer RAP binder resulted in lower FE_{mix} at the same RAP content (20%). It was concluded that characterizing RAP binder stiffness and RAP fineness is necessary to increase the current maximum RAP content in PMA mixtures.

A preliminary guideline for determining maximum RAP usage in PMA mixtures based on RAP binder stiffness and RAP fineness was developed to allow more than 20% RAP in PMA mixture. Coarser and less stiff RAP allowed for greater maximum RAP content (up to 40%) in PMA mixtures than finer and stiffer RAP. A preliminary guideline was validated by way of full mixture testing. Furthermore, it was concluded that incorporation of 20% RAP in HP mixtures would sacrifice the premium benefits of using HP binder.

TABLE OF CONTENTS

LIST OF TABLES

LIST OF FIGURES

CHAPTER 1
INTRODUCTION

1.1 Background

Reclaimed asphalt pavement (RAP) consists of asphalt and aggregate commonly generated from the millings of damaged roads. Use of RAP results in both economic and environmental benefits, including: (i) cost savings from reducing the amount of virgin asphalt binder and virgin aggregate, (ii) reduced fuel usage and emissions associated with the extraction and transportation of virgin materials, (iii) reduced depletion of non-renewable resources, and (iv) reduced landfill space for disposal of used materials. Despite these benefits, the average percent usage of RAP in asphalt mixtures in the United States is only 20.4% (Williams et al. 2018). Since RAP contains aged and more brittle asphalt binder compared to virgin binders, there is a concern that increasing the amount of RAP in a mixture may increase its susceptibility to cracking. A review of studies of in-service pavements with diverse climates and traffic showed that pavements containing 30% RAP had more wheel path cracking than those with virgin materials, although the extent of cracking was acceptable (West et al. 2013). However, a more recent study indicated that RAP may not necessarily diminish cracking performance. At the National Center for Asphalt Technology (NCAT) test track, test sections containing Superpave mixtures with 50% RAP outperformed companion sections with all virgin materials for all measures of pavement performance through 17 million ESALs over a period of five years (Timm et al. 2016).

Polymer-modified binders have had proven success in mitigating rutting and cracking for asphalt pavements (Von Quintus et al. 2007; Yildirim 2007). Recently, high-polymer (HP) binder has been employed to mitigate severe rutting and cracking (Błażejowski et al. 2016; Chen et al. 2018; Kwon et al. 2019). However, benefits associated with these premium modified virgin binders may be diluted by the introduction of RAP, which often contains unmodified binder. In the Florida Department of Transportation (FDOT) current specifications, the maximum usage of RAP is limited to 20% when used in polymer-modified asphalt (PMA) mixtures, and RAP is not allowed for use in mixtures containing HP binder (FDOT 2018). Similarly, maximum usage of RAP in PMA mixtures in the range of 10%-20% has been adopted by the DOTs of other states (IDOT 2016; MnDOT 2016; ODOT 2013).

The literature has indicated mixed results regarding cracking performance of high RAP content mixtures with polymer-modified binders. Huang et al. (2004) reported that inclusion of RAP in the range of 10% to 30% into mixtures with a styrene-butadiene-styrene (SBS) polymer-modified binder PG 76-22 increased resistance to fracture failure by up to 100% based on results of the semi-circular notched fracture test. However, they recommended that inclusion of RAP should not exceed 20% due to a nearly 30% drop in fracture resistance observed when RAP was increased from 20% to 30%. Kim et al. (2009) found that PG 76-22 PMA mixtures with three RAP contents (15%, 25%, and 35%) performed well in the Superpave IDT tests, with all energy ratio (ER) values being greater than 4.0. Compared to the control PMA mixture without RAP, the 15% RAP mixture had slightly lower ER, while both 25% and 35% RAP mixtures exhibited higher ERs. The ER reduced slightly when the RAP content increased from 25% to 35%. Bending beam fatigue tests conducted by West et al. (2009) indicated that the PG 76-22 PMA mixtures with 45% RAP had much lower fatigue life compared to the PG 76-22 PMA mixtures with 20% RAP, but the authors attributed this to lower effective volume of asphalt in the higher RAP content mixtures.

More recently, Yan et al. (2017a) evaluated cracking performance of PMA mixtures with RAP for a combination of two RAP sources and three RAP contents using the Superpave IDT tests, including one fine RAP (44% passing 1.18 mm) with typical binder stiffness in Florida (about 100, 000 poises at 60°C) and one coarse RAP (17% passing 1.18 mm) with extremely high binder stiffness (about 600,000 poises at 60°C). They found it is important to characterize not only RAP binder but also RAP gradation when incorporating RAP into PMA mixtures. Specifically, they concluded RAP gradation affects the distribution of RAP binder within the RAP mixtures. The mixtures with coarse RAP exhibited better cracking performance than the ones with fine RAP for all three RAP contents (20%, 30%, and 40%), even though the coarse RAP binder was much stiffer than that of fine RAP. Overall, compared to the control mixture with no RAP, inclusion of up to 40% RAP did not negatively affect the cracking performance for all well-designed PMA mixtures satisfying dominant aggregate size range-interstitial component (DASR-IC) requirements (Kim et al. 2006).

In summary, limited research performed to date indicates it may be possible to use more than 20% RAP in PMA mixtures without jeopardizing cracking performance. However, there is limited insight regarding how RAP characteristics contribute to the properties and performance of PMA and HP mixtures. Therefore, there is a need to identify RAP characteristics that affect asphalt

mixture performance and to determine whether these key characteristics are needed for increased RAP usage, while maintaining acceptable performance of PMA mixtures and premium performance of HP mixtures.

1.2 Objectives

The primary objectives of this research are summarized as follows:

- Determine whether the current 20% maximum RAP content in PMA mixture may be increased without adversely affecting cracking performance.
- Determine whether additional RAP characterization is needed to implement the increase.
- Determine whether 20% RAP can be used with HP mixture without significant loss of premium cracking performance associated with HP binder

1.3 Scope

Twelve RAP sources were characterized using recovered RAP binder and aggregate to identify the range of key RAP characteristics for Florida RAP material. Eight out of 12 RAP sources, covering the range of key RAP characteristics encountered in Florida, were selected to assess the effect of these RAP characteristics on cracking performance. Figure 1-1 shows overall scope of this study, including two virgin binder types (PG 76-22 PMA and HP binder) typically used in Florida, four RAP contents for PG 76-22 PMA binder and two RAP contents for HP binder.

Laboratory testing plan consisted of two steps: (i) interstitial component direct tension (ICDT) test to evaluate all RAP mixture combinations and (ii) Superpave indirect tensile (IDT) tests to evaluate preliminary findings from ICDT test results. The ICDT test was used as a surrogate for mixture test, because it requires less effort in specimen preparation and testing than a mixture test. According to the DASR-IC theory, the IC is combination of fine aggregates, effective binder, and air voids. It has been reported that IC properties are related to mixture cracking resistance. Recently, Yan et al. (2017b) found that IC fracture energy values obtained from ICDT test correlated well with fracture energy of corresponding mixtures from Superpave IDT tests.

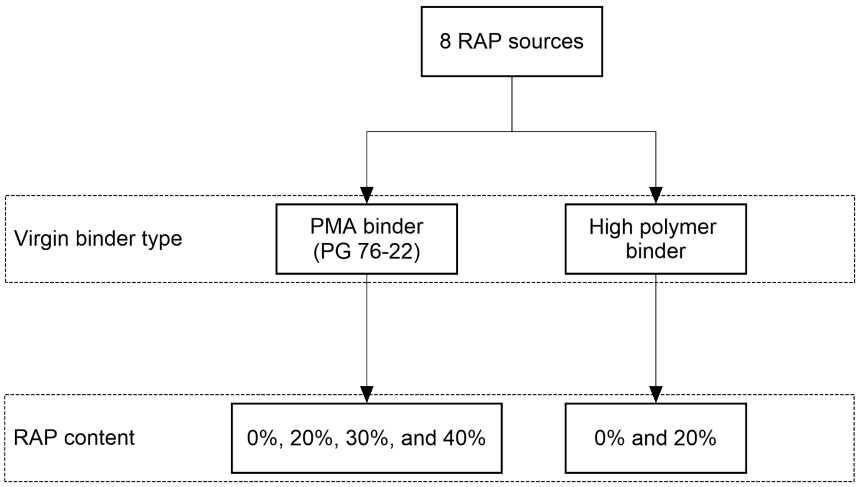

Figure 1-1. Overall scope

1.4 Research Approach

This research mainly focused on developing preliminary guidelines to determine maximum RAP content in PMA mixtures and determining whether RAP can be used for HP mixtures. The overall research approach is presented in Figure 1-2.

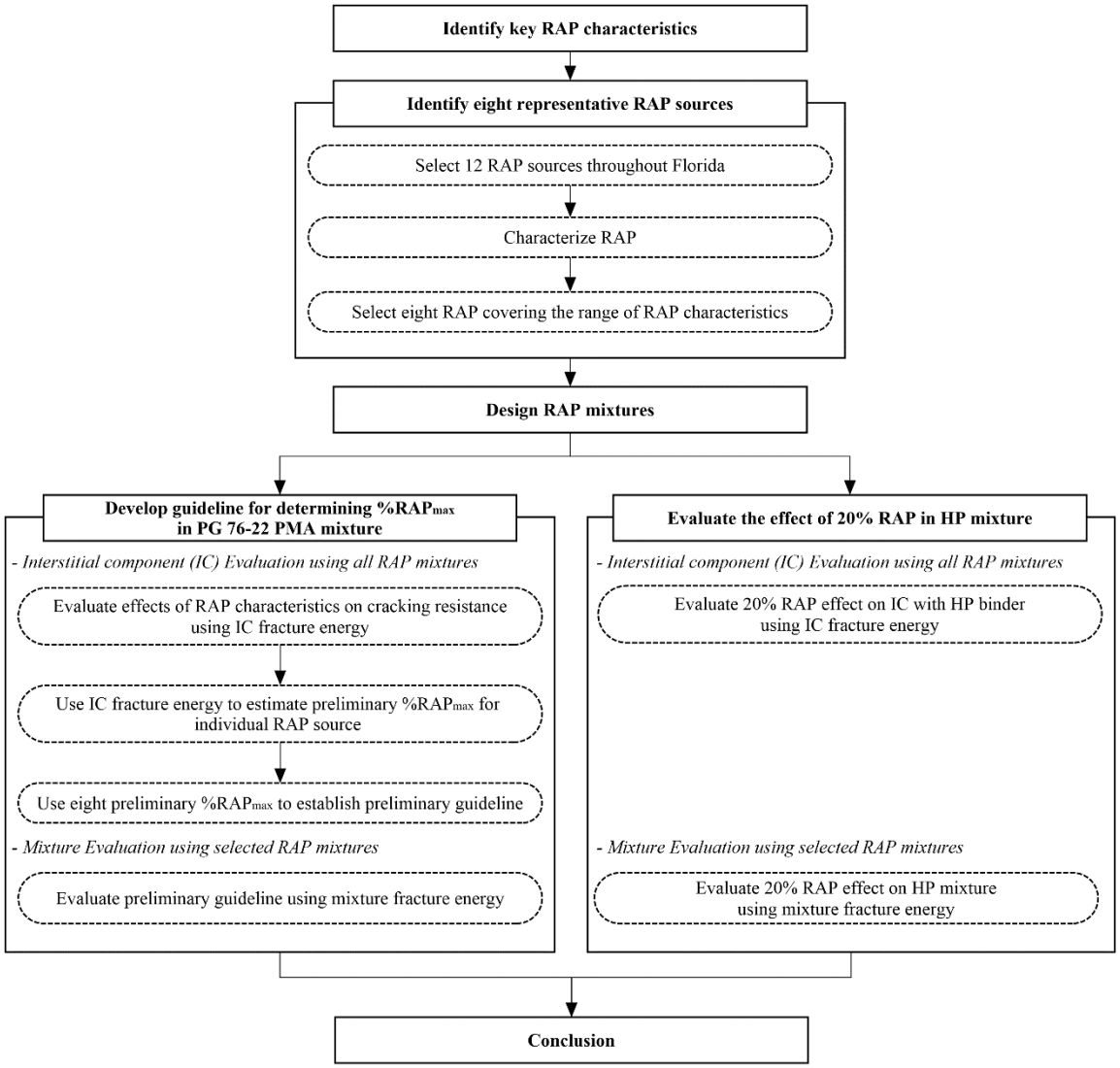

Figure 1-2. Overall research approach

Additional details are presented in the following subsection:

Identify key RAP characteristics

- Review available literature to identify key RAP characteristics which may affect cracking and rutting performance of asphalt mixtures.

Identify eight representative RAP sources

- Characterize 12 RAP sources using recovered RAP binder and aggregate to identify the range of key RAP characteristics for Florida RAP material.
- Select eight RAP sources, which cover the range of key RAP characteristics encountered in Florida.

Design RAP mixtures

- Design 24 RAP mixtures consisting of eight RAP sources and three RAP contents (0%, 30% and 40%) using existing mix design (PMA mixture containing 20% RAP) for each RAP source.
- Maintain the same job mix formula (JMF) gradation as reference mix design (20% RAP) for 0%, 30% and 40% RAP mixtures to minimize different gradation effects.
- Conduct dominant aggregate size range-interstitial component (DASR-IC) analysis to assess potential influence of gradation.

Develop guideline for determining $\%RAP_{max}$ in PG 76-22 PMA mixture

- Conduct interstitial component direct tension (ICDT) test on all RAP mixture combinations (eight RAP sources and four RAP contents: 0%, 20%, 30% and 40%) to evaluate effect of key RAP characteristics on cracking resistance.
- Identify preliminary IC fracture energy (FE_{IC}) limit, and estimate preliminary maximum RAP content for individual RAP source using FE_{IC}, along with preliminary FE_{IC} limit.
- Using estimated preliminary maximum RAP content, establish preliminary guideline for determining maximum RAP content in PMA mixture.
- Perform Superpave indirect tensile (IDT) tests on selected RAP mixtures to evaluate proposed guideline and preliminary findings from ICDT test results.

Evaluate 20% RAP effect in HP mixture

- Conduct ICDT test on all RAP mixture combinations (eight RAP sources and two RAP contents: 0% and 20%) to determine whether HP binder can provide premium cracking resistance, even with 20% RAP.
- Perform Superpave IDT tests on selected RAP mixtures to evaluate preliminary findings from ICDT test results.

CHAPTER 2
LITERATURE REVIEW

This chapter presents a summary of research on characteristics of reclaimed asphalt pavement (RAP) and associated characterization methods, current understanding on blending of RAP binders and virgin binders, and key findings on effects of RAP on polymer-modified asphalt (PMA) mixture performance based on both binder-level and mixture-level studies. Although RAP management is not within the scope of this study, it is part of the logical progression in which RAP materials are obtained, tested, and used in the mix design. Therefore, information on good RAP management practices obtained from the literature review is summarized in APPENDIX A.

2.1 Reclaimed Asphalt Pavement (RAP) Characteristics and Characterization Methods

Characteristics of RAP materials that are important for asphalt mixtures are asphalt content, RAP gradation, and RAP aggregate properties, which include bulk specific gravity and Superpave aggregate consensus properties. The continuous grade of RAP binder is needed if blending charts are required to select an appropriate virgin binder grade for higher RAP content mixtures (McDaniel et al. 2000). In addition, penetration and viscosity have been traditionally employed to provide information about stiffness of the RAP binder at an intermediate temperature (25°C) and viscous behavior at high temperatures (60°C and 135°C), respectively.

There are two major ways of determining the asphalt content of the RAP and at the same time recovering RAP aggregates: the ignition method (AASHTO T 308) and the solvent extraction method (AASHTO T 164). The ignition method is the most common method, but requires correction factors calculated or assumed based on local experience. The extraction method requires the use of solvents, which is an inconvenience. The asphalt content of RAP is generally in the range of 4% to 6%. Research has shown that when RAP particles get finer, asphalt content of the RAP increases (Al-Qadi et al. 2009). The recovered aggregates are typically tested to obtain gradation, bulk specific gravity (G_{sb}), and consensus properties, including coarse aggregate angularity, fine aggregate angularity, and flat and elongated particles.

Results of a joint study conducted by NCAT and the University of Nevada-Reno (UNR) showed that for high RAP content mix designs, the best method to recover the aggregate for determining the RAP aggregate specific gravity was to use a solvent extraction method and then

test the coarse and fine parts of the recovered aggregate using AASHTO T 85 and T 84, respectively (Kvasnak et al. 2010). The ignition method may also be used to recover the RAP aggregate for determining the RAP aggregate specific gravity except for some aggregate types that undergo significant changes in specific gravity when subjected to the extreme temperatures. West et al. (2013) pointed out that both methods used to recover the RAP aggregate were likely to cause small errors in the G_{sb} results. As RAP contents approached 50 percent, the effect of the small G_{sb} error could cause the voids in mineral aggregate (VMA) to be off by ± 0.4 percent.

A recently completed UF study funded by FDOT evaluated cracking performance of PMA mixtures with RAP for a combination of two RAP sources and three RAP contents using the Superpave IDT tests (Roque et al. 2015). It was found that RAP gradation affects the distribution of RAP binder within the PMA mixtures, because RAP binder tends to stay close to the RAP aggregate. The mixtures with coarse RAP exhibited better cracking resistance than the ones with fine RAP for all three RAP contents (20%, 30%, and 40%), even though the coarse RAP was much stiffer than the fine RAP.

RAP binder properties mainly include continuous grade determined using Superpave performance grade (PG) binder tests, and penetration and viscosity determined using conventional binder tests for consistency. Beeson et al. (2011) measured true low and high-temperature grades for 33 RAP samples taken across Indiana and for over 200 virgin asphalt binder samples that covered three PG-22 grades and three PG-28 grades. The average low-temperature grade was determined to be -11.1°C for the RAP samples, and -25.1°C and -28.7°C for the PG-22 and PG-28 virgin samples, respectively. Using the blending charts approach, the maximum amount of RAP (binder replacement) was determined to be 22.7% with a PG-22 binder and 38.1% with a PG-28 binder. Beeson et al. (2011) reported that these results were supported by findings of a concurrent mixture study conducted at the North Central Superpave Center (Shah et al. 2007), which evaluated stiffness and cracking potential of mixtures containing up to 40% RAP. Therefore, Indiana Department of Transportation (INDOT) changed the standard specifications to allow 25% binder replacement without changing the virgin asphalt binder grade and 40% binder replacement with one grade decrease in both high and low temperatures.

In addition, a Delta T_c parameter has been used to measure loss in relaxation or increase in brittleness of asphalt binder due to increased asphalt binder replacement (ABR) levels or increased aging (Sharma et al. 2017). The Delta T_c parameter is defined as the difference between the low

continuous grade temperatures of stiffness and m-value determined from the Superpave bending beam rheometer (BBR) test. The parameter was first proposed by Anderson et al. (2011) to measure loss in ductility (or relaxation) of aged asphalt binder as part of a study examining relationships between asphalt binder properties and block cracking in airport pavements. A minimum Delta T_c of -5°C (minimum Delta T_c criterion) was used to identify binders that were susceptible to non-load related cracking. Asphalt binders were found to be more likely to crack as their Delta T_c became more negative below the limit. Results of recent studies have indicated that the minimum Delta T_c criterion can be used for evaluating the impact of recycled engine oil bottoms (REOB) and recycled asphalt shingles (RAS) on performance of asphalt binders (Li et al. 2017; Sharma et al. 2017), and the effectiveness of rejuvenators with mixtures containing RAP and RAS (Xie et al. 2017).

For high RAP content mixtures, most studies followed the current standard that recommends recovering the RAP binder using a solvent extraction and recovery procedure, then determining properties of the RAP binder. However, solvent extraction and recovery has long been criticized for altering binder properties due to presence of residual solvent after recovery, aging of binder at high temperature, and for labor intensity (Mehta et al. 2012). In addition, the health and environmental impact of the chemicals used in the process is of concern. Therefore, methods for non-solvent based binder characterization have been developed to estimate properties of the RAP binder using mixture or mortar tests as described below.

Methods for estimating binder properties from mixture tests mainly include, but are not limited to, backcalculation from testing of gyratory-compacted mixture samples (Bonaquist 2007; Daniel and Mogawer 2010) and testing of thin beam samples cut from gyratory specimens (Zofka et al. 2005). The backcalculation process was introduced by Christensen Jr et al. (2003) after they refined the Hirsch model to predict the dynamic modulus of HMA using the shear modulus of the asphalt binder and volumetric properties of the mixture. Although successful in obtaining reasonable binder stiffness values from the measured mixture modulus, this type of method requires creation of a mix design for gyratory specimens, which may be more labor intensive than solvent extraction and recovery. It should be noted that a mix design with RAP may not be available during the RAP characterization stage.

Recently, research conducted at the University of Wisconsin (Ma et al. 2010; Swiertz et al. 2011) resulted in a mortar testing procedure to quantify the effect of RAP binder on the continuous

grades of virgin binder, allowing for an estimation of binder properties at critical pavement temperatures. This approach eliminates the need for binder extraction as well as for mix design and mixture testing. Only mortar and virgin binder samples are tested in the bending beam rheometer (BBR) and dynamic shear rheometer (DSR). Figure 2-1 illustrates the mortar preparation process for low-temperature characterization (Swiertz et al. 2011). The R100 RAP material consists of the RAP material passing the No.50 sieve and retained on the No.100 sieve. The burned R100 material consists of extracted RAP aggregate using an ignition oven. RTFO denotes rolling thin-film oven and PAV denotes pressure aging vessel.

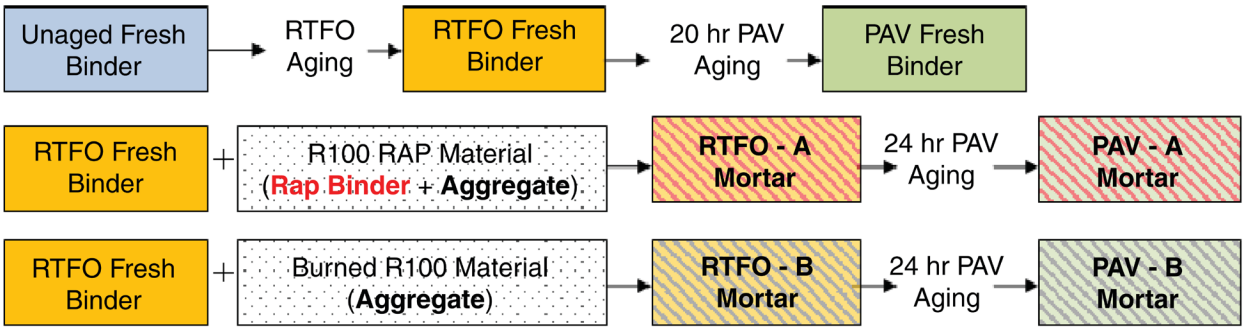

Figure 2-1. Sample preparation for RAP binder characterization (Swiertz et al. 2011)

Using the mortar approach, Hajj et al. (2012) determined the effective binder properties for two mixtures manufactured with PG 58-28 binder containing 15% and 50% RAP respectively, and one mixture produced with PG 52-34 binder containing 50% RAP. They found that the low critical temperatures of binder blends estimated from the mortar procedure were consistent with fracture temperatures of mixtures measured using the thermal stress restrained specimen test (TSRST). Furthermore, all critical temperatures (low, intermediate, and high temperatures) obtained from the mortars were lower than those determined from the recovered asphalt binders from the mixtures. In other words, the effective binder from the mortars is softer than the recovered binder, indicating only partial blending occurred between the virgin and RAP binders in the evaluated mortars (Hajj et al. 2012).

2.2 Blending of RAP Binders and Virgin Asphalt Binders

One of the key issues regarding mix designs containing RAP is how much blending occurs between the RAP binder and the virgin binder. The state-of-the-practice uses a three-tiered system to determine when to change binder grade based on RAP content used in the mixture (AASHTO M 323). The three-tiered system assumes that complete blending occurs between the RAP and virgin binders. For RAP contents greater than 25%, a blending chart analysis is recommended to determine the proper virgin binder grade as shown in Table 2-1 below.

Table 2-1. Binder selection guidelines for RAP mixtures (AASHTO M 323)

RAP Percentage	Recommended Virgin Asphalt Binder Grade
< 15	No change in binder selection
15 to 25	Select virgin binder one grade softer than normal
> 25	Follow recommendations from blending charts

Several studies have been conducted to determine the degree of blending. One approach relied on the stiffness |G*| measured on recovered binders. Huang et al. (2005) investigated how much virgin binder was blended into the RAP binder through a staged extraction process. Twenty percent fine RAP (passing No.4 sieve) was blended with coarse virgin aggregate (retained on No.4 sieve) and PG 64-22 virgin binder at a mixing temperature of 190°C for three minutes. Four layers of asphalt were extracted from the fine RAP mixture sequentially using trichloroethylene (TCE). The results showed that from the outer to the inner layers, the thickness of asphalt layers extracted from the RAP particles was 2.0, 1.1, 1.8, and 1.6 microns. The binder in the two inner layers had stiffness similar to the RAP binder, indicating that no blending occurred. The virgin binder appeared to only blend with the RAP binder in the two outer layers where the stiffness of the binder was lower than that of the RAP binder. It was estimated that about 40% RAP binder was blended with virgin binder. As a continuation of Huang's work, Shirodkar et al. (2011) developed an experimental procedure to quantify the degree of blending. To demonstrate the proof of concept, one mixture design (JMF), one RAP source at two contents (25% and 35% by weight of aggregates), and two virgin binders (PG 70-28 and PG 58-28) were selected. It was found that the degree of blending was 70% for PG 70-28 virgin binder with 25% RAP and 96% for PG 58-28 virgin binder with 35% RAP. It is important to note that in both studies mentioned above, fine

RAP material (– No.4 or – No.8 sizes) and coarse virgin aggregates (+ No.4 sieve size) were used to produce the mixtures such that they can be separated after mixing. This approach is not suitable to quantify the degree of blending in real mixtures.

Copeland et al. (2010) took another approach to determine the degree of blending by comparing measured and predicted dynamic modulus of a Superpave structural mixture containing 45% RAP fractionated on the 1/4-inch sieve size. The coarse fraction was graded as PG 82-16, and the fine fraction was PG 82-10. The virgin binder, which was the designated recycling agent (RA) 800, was a PG 52-28 binder. Their approach involved measuring the mixture dynamic modulus, |E*| over a range of temperatures and frequencies with the asphalt mixture performance tester (AMPT). The binder was extracted and recovered from the mixture, during which the virgin binder and RAP binder became completely blended. The recovered binders were tested in a DSR using a frequency sweep to determine the binder shear moduli, |G*|. Using the Hirsch model, with inputs of the binder shear moduli, VMA, and voids filled with asphalt (VFA) from the compacted specimens, the dynamic moduli, |E*|, of virtual specimens with completely blended binders were calculated. The predicted |E*| was plotted with the measured |E*|. The results showed predicted and measured values fell along the line of equality, indicating the Hirsch model succeeded in predicting the measured values within experimental error. This also indicated that complete blending occurred in the HMA with high RAP content (Copeland et al. 2010).

In a recently completed FDOT study, Roque et al. (2015) evaluated properties of PMA mixtures containing high RAP content. Two RAP sources with distinctively different characteristics were selected: one fine RAP with typical binder stiffness in Florida (PG 94-24) and one coarse RAP with extremely stiff binder (graded as PG 100-12). It was found that RAP gradation had a dominant effect on mixture properties. Although coarse RAP was much stiffer than fine RAP, it resulted in lower mixture resilient modulus than fine RAP, indicating full blending between virgin and RAP binder did not occur in the mixtures; instead, the RAP binder tended to stay close to the RAP aggregate. Furthermore, coarse RAP resulted in higher mixture fracture energy than fine RAP. This indicates that greater degree of blending is not necessarily favorable for mixture cracking resistance since the finer portion of the mixtures with coarse RAP was primarily virgin aggregate and virgin binder.

Overall, the literature has indicated that complete blending may occur when soft virgin binder was used with slightly aged RAP in asphalt mixtures. However, complete blending of RAP

binder and virgin binder did not always occur in asphalt mixtures. When partial blending occurred, RAP binder tended to stay close to RAP aggregate, which resulted in non-uniform distribution of RAP binder in the asphalt mixture.

2.3 Effect of RAP Binder on Properties of Polymer-Modified Asphalt (PMA) Binder

The age and stiffness of RAP binder may affect the performance of PMA mixtures. Furthermore, there is a concern that RAP binder may dilute PMA binders and reduce their effectiveness. Therefore, the effect of RAP binder on PMA binder viscosity and other properties related to various distresses including rutting, fatigue cracking, and thermal cracking will be reviewed in this section. It is noted that all binder tests described below were conducted for PMA binders fully blended with recovered RAP binders.

2.3.1 Viscosity

As expected, research has indicated that the introduction of RAP binder resulted in higher viscosity relative to virgin PMA binder (Kim et al. 2009; Roque et al. 2015; Singh and Sawant 2016). In addition, stiffer RAP binders, in comparison to softer RAP binders, resulted in a greater increase in viscosity.

Singh and Sawant (2016) performed the rotational viscometer (RV) test to measure the viscosity of SBS PMA binder blended with different contents of RAP binder recovered from six-year-old asphalt pavement in India. Table 2-2 presents the PG grades of RAP and virgin binders employed, and results of the RV test at 135°C. As expected, increasing the percentage of RAP binder led to increased values of viscosity, although the effect was relatively small. Additionally, Singh and Sawant measured the viscosity of the same blended binders at four different temperatures (120°C, 150°C, 165°C, and 180°C), and found that the rate of change in viscosity was inversely proportional to temperature. As the temperature decreased, the effect of RAP binder on the viscosity was greater.

Kim et al. (2009) measured viscosity of PMA binder blended with RAP binder at different percentages using the RV test as shown in Table 2-2. Test results showed higher viscosity of all blended binders was observed as compared to that of virgin PMA binder. However, they found relatively little increase in viscosity as RAP binder content was increased from 15% to 35%.

Table 2-2. Viscosity results in previous studies (at 135°C)

Authors		Singh and Sawant (2016)	Kim et al. (2009)	Roque et al. (2015)	
PMA binder grade		PG 76-xx	PG 76-22	PG 76-22	
RAP binder grade		PG 88-xx	PG 82-16	PG 100-12	PG 94-24
Viscosity at 135°C (Pa·s)	**RAP %**				
	0%(1)	1.25	1.73	1.46	
	15%	1.34	1.81	-	-
	20%	-	-	1.78	1.64
	25%	1.36	1.79	-	-
	30%	-	-	1.98	1.70
	35%	-	1.82	-	-
	40%	1.38	-	2.24	1.90
	100%	1.54	2.24	-	-

Note: (1) 0% means virgin PMA binder

Roque et al. (2015) found that viscosity of PMA blended binders increased as the RAP binder percentage increased as shown in Table 2-2. Two recovered RAP binders were investigated: one graded as PG 100-12, and the other as PG 94-24. Both were stiffer than the RAP binders employed by the other researchers (Kim et al. 2009; Singh and Sawant 2016). PMA binders blended with stiffer RAP binder showed greater viscosity than PMA binders blended with lower stiffness RAP binder.

2.3.2 Binder properties related to rutting

In general, PMA binder properties or indexes regarding rutting resistance were positively affected by the inclusion of recovered RAP binder. Kim et al. (2009) and Roque et al. (2015) used the dynamic shear rheometer (DSR) test to evaluate the effect of recovered RAP binder on the rutting potential of PMA virgin binder. The same PMA binder grade (PG 76-22) was used in both studies. RAP binder employed by Roque et al. (2015) had higher PG grade than those used by Kim et al. (2009) as shown in Table 2-3. Details of DSR test results from both studies are also summarized in Table 2-3. As expected, recovered RAP binder with higher PG grade led to a greater increase in $G^*/\sin\delta$ as RAP binder percentage increased. This finding implied stiffer RAP binder may be more beneficial to rutting resistance of PMA binder.

Table 2-3. Binder test results related to rutting in previous studies

Authors	Kim et al. (2009)	Roque et al. (2015)					
PMA binder grade	PG 76-22	PG 76-22					
RAP binder grade	PG 82-16	PG 100-12			PG 94-24		
Test type	DSR	DSR	MSCR		DSR	MSCR	
Aging condition	RTFO[(1)]	Unaged	RTFO		Unaged	RTFO	
Testing temperature	76°C[(2)]	76°C	67°C		76°C	67°C	
Parameter	G*/sinδ	G*/sinδ	$J_{nr,3.2}$	%Rec	G*/sinδ	$J_{nr,3.2}$	%Rec
RAP %	(kPa)	(kPa)	(kPa^{-1})	(%)	(kPa)	(kPa^{-1})	(%)
0%[(3)]	2.50	1.23	0.41	56.07	1.23	0.41	56.07
15%	2.55	-	-	-	-	-	-
20%	-	2.07	0.30	52.40	1.72	0.35	50.27
25%	2.60	-	-	-	-	-	-
30%	-	2.27	0.17	55.99	2.02	0.28	48.65
35%	3.25	-	-	-	-	-	-
40%	-	3.01	0.13	54.15	2.41	0.23	49.07
100%	18.50	-	-	-	-	-	-

Note: (1) RTFO is rolling thin-film oven aging
(2) 100% RAP binder was tested at 82°C
(3) 0% means virgin PMA binder

Roque et al. (2015) conducted the multiple stress creep and recovery (MSCR) test mainly to evaluate RAP binder effect on elastomeric behavior of virgin PMA binder. The average percent recovery parameter from the MSCR test results was employed to determine the elasticity of PMA binder. According to their results, all blended binders including the one with 40% RAP binder exhibited good elastomeric behavior based on the requirements of AASHTO TP-70. In other words, the contribution of PMA binder was still evident after blending with high stiffness RAP binder at 40% RAP content. Furthermore, the addition of RAP binder resulted in lower non-recoverable creep compliance (J_{nr}) at 3.2 kPa creep stress level, indicating improved rutting resistance (See Table 2-3). Similar to findings from the DSR test results, a greater improvement in rutting resistance was observed from the MSCR test when stiffer RAP binder was added to PMA binder.

Singh and Sawant (2016) found that increased amount of RAP binder led to higher values of the G*/sinδ parameter at various temperatures, although the RAP binder effect was insignificant

above 76°C. The DSR test was conducted at six different temperatures (58°C, 64°C, 70°C, 76°C, 82°C, and 88°C). PMA virgin binder (PG 76-xx) was blended with the RAP binder (PG 88-xx) at four RAP contents (0%, 15%, 25%, and 40%). The effect of the addition of RAP binder was diminished as the temperature increased. Specifically, the value of G*/sinδ was minimally affected by the RAP binder at 82°C and 88°C, even for 40% RAP binder.

In summary, the addition of RAP binder resulted in enhanced rutting resistance according to the G*/sinδ and J_{nr}. Furthermore, stiffer RAP binder had greater influence on rutting resistance of PMA binders. It was also found that PMA binder retained good elastomeric behavior, even when blended with 40% of high stiffness RAP binder.

2.3.3 Binder properties related to fatigue cracking

Several researchers have reported that inclusion of RAP binder has a negative influence on PMA binder properties regarding fatigue cracking resistance (Kim et al. 2009; Mohammad et al. 2003; Roque et al. 2015; Singh and Girimath 2016; Singh and Sawant 2016). These findings were based on results from various binder tests including the DSR, the linear amplitude sweep (LAS), the double edge notched tension (DENT), and binder fracture energy (BFE) test.

Kim et al. (2009) and Roque et al. (2015) found that addition of RAP binder resulted in increased G*sinδ indicating reduced fatigue cracking resistance (See Table 2-4). The PG binder parameter G*sinδ measured using the DSR test at intermediate service temperature was used to assess fatigue cracking resistance. The asphalt binder needs to be elastic but not too stiff, in order to achieve good fatigue cracking resistance. According to Superpave specifications, G*sinδ must be less than 5,000 kPa. Furthermore, a greater effect of RAP binder on increase in G*sinδ was observed when higher PG grade RAP binder was used.

Mohammad et al. (2003) employed much stiffer RAP binder that was recovered from eight-year-old polymer modified asphalt pavement. RAP binder was blended with virgin PMA binder (PG 70-22) at different proportions (0%, 20%, 40%, and 60%). According to the G*sinδ parameter, all PMA binders blended with RAP binder exceeded the maximum Superpave requirement of 5,000 kPa at 25°C, whereas those of Kim et al. (2009) and Roque et al. (2015) did not (See Table 2-4). The results showed that the fatigue cracking resistance of PMA binder was greatly reduced by the addition of RAP binder recovered from aged PMA pavement.

Table 2-4. DSR test results related to fatigue cracking in previous studies

Authors	Mohammad et al. (2003)		Kim et al. (2009)	Roque et al. (2015)	
PMA binder grade	PG 70-22		PG 76-22	PG 76-22	
RAP binder grade	Unknown(1)		PG 82-16	PG 100-12	PG 94-24
Testing temperature	25°C	28°C	25°C	26.5°C	26.5°C
Parameter	G*sinδ	G*sinδ	G*sinδ	G*sinδ	G*sinδ
RAP %	(kPa)	(kPa)	(kPa)	(kPa)	(kPa)
0%(2)	-	1,036	3,500	1,545	1,545
15%	-	-	3,900	-	-
20%	5,229	3,716	-	2,690	2,305
25%	-	-	4,000	-	-
30%	-	-	-	2,860	2,240
35%	-	-	4,100	-	-
40%	6,911	6,911	-	4,025	2,925
60%	8,889	7,064	-	-	-
100%	-	-	8,000(3)	-	-

Note: (1) RAP binder was recovered from PMA asphalt pavement
(2) 0% means virgin PMA binder
(3) 100% RAP binder was tested at 82°C

Recently, Singh and Sawant (2016) also found that recovered RAP binder negatively affected the fatigue life of PMA binder through the LAS test conducted at intermediate temperature (25°C). PMA binder (PG 76-xx) was mixed with recovered RAP binder (PG 88-xx) at four contents (0%, 15%, 25%, and 40%). The parameter N_f (Number of cycles to failure) was calculated using results from the LAS test as an indicator for the binder fatigue cracking performance. It was found that the increasing amount of RAP binder reduced N_f of PMA binder.

Singh and Girimath (2016) employed the DENT test to evaluate fatigue cracking potential of PMA binder (PG 76-xx) combined with different RAP binder contents (0%, 15%, 25%, and 40%). Two RAP sources were used: RAP-A binder with a viscosity of 2.15 Pa·s and RAP-S binder with a viscosity of 1.57 Pa·s, both measured at 135°C. Results from the DENT test showed the second peak in the load-displacement curve for the control PMA disappeared with the addition of both RAP sources, indicating damage to polymer interlinkage. The crack tip opening displacement (CTOD) value determined based on essential work of failure was used to indicate the binder's resistance to fatigue cracking. The greater the CTOD value, the better the fatigue resistance. They reported that addition of RAP binder decreased CTOD values for both RAP sources. This implied

that the adding RAP binder reduced the fracture resistance of PMA binder. Furthermore, the inclusion of stiffer RAP binder led to lower values of CTOD. At higher RAP binder content (25% and 40%), the difference between CTOD values of different RAP sources became greater. They concluded that PMA binder blended with stiffer RAP binder may be more fracture susceptible than those with less stiff RAP binder.

Roque et al. (2015) found that the addition of RAP binder decreased the fracture energy density (FED) of PMA binder. The BFE test was employed to measure the FED of binder as an indicator of the fracture tolerance at intermediate temperatures (Niu et al. 2014). Two types of RAP binder (WHI: PG 100-12 and ATL: PG 94-24) were blended with the virgin PMA binder (PG 76-22) at four different percentages (0%, 20%, 30%, and 40%). PMA binder blended with RAP binder exhibited lower FED as compared to virgin PMA binder as shown in Table 2-5. This indicated that recovered RAP binders had an adverse influence on FED of PMA binder. Furthermore, based on the true stress-true strain curves, it was observed that inclusion of RAP binder resulted in dilution of the polymer modification. The second peak of true stress, which is an indicator of elastomeric behavior, became less pronounced as the percentage of RAP binder increased.

Table 2-5. BFE test results by Roque et al. (2015)

Authors	Roque et al. (2015)	
RAP binder grade	PG 100-12	PG 94-24
Parameter **RAP binder %**	Fracture energy density (psi)	Fracture energy density (psi)
0%[(1)]	1,192	1,192
20%	1,103	932
30%	1,014	823
40%	625	623

Note: (1) 0% means virgin PMA binder

In summary, various binder performance indexes have indicated that use of recovered RAP binder typically reduced the resistance of PMA binder to fatigue cracking. Fatigue resistance of PMA binder was affected by RAP binder stiffness. The higher the stiffness of the RAP binder, the greater the effect on fatigue resistance of the blended binders. Furthermore, it was shown by several researchers that addition of RAP binder reduced the effectiveness of elastomeric behavior.

2.3.4 Binder properties related to thermal cracking

Previous studies based on BBR test results have reported that PMA blended with recovered RAP binder typically showed lower resistance to low-temperature cracking relative to control PMA binder (Roque et al. 2015; Singh and Girimath 2016). The BBR test provides parameters to assess the resistance of binders to low-temperature cracking: m-value (rate of stress relaxation) and S (creep stiffness). Singh and Girimath (2016) observed that the addition of RAP binder increased the stiffness of SBS PMA binder (PG 76-xx) while decreasing m-value for both RAP sources employed. These results indicated that recovered RAP binder negatively affected the low-temperature performance of PMA binders.

Roque et al. (2015) also found that addition of recovered RAP binder (PG 100-12 and PG 94-24) increased the BBR creep stiffness of PG 76-22 PMA binder and decreased m-value. However, it is important to note that all blended binders satisfied the Superpave specification: (i) a maximum stiffness of 300 MPa; (ii) a minimum m-value of 0.3.

2.3.5 Summary

Generally, the effects of RAP binder on PMA binder have been found to be similar to effects on unmodified binder. As the amount of RAP binder in PMA binder increased, rutting resistance increased, while fatigue cracking and thermal cracking resistance decreased. Furthermore, several researchers found that addition of RAP binder reduced the effectiveness of elastomeric behavior. However, results of the MSCR test indicated that elastomeric behavior remained in blended binder even with the addition of high stiffness RAP binder at a high percentage (40%). Furthermore, it was found that the addition of stiffer RAP binder had a greater effect on properties of PMA binder. Therefore, it is important to characterize RAP binder to achieve a better estimation of its effect on PMA binder.

2.4 Effect of RAP on PMA Mixture Performance

Recent research has indicated that complete blending of RAP binder and virgin binder may not occur in asphalt mixtures at typical temperatures and mixing times used in production (Roque et al. 2015). Therefore, effect of RAP on mixture performance determined based on studies of mixtures should be inherently more reliable than studies of binder blends, where complete blending is assumed. Furthermore, RAP materials have two major components: RAP binder and RAP aggregate. Studies of asphalt blends clearly cannot address the effect of RAP aggregate on mixture performance. Only studies of mixtures can provide a complete and more accurate picture in this regard. Therefore, research conducted to evaluate effect of RAP on PMA mixture performance through analysis and testing of mixtures were reviewed, including resistance to rutting, fatigue cracking, and thermal cracking.

2.4.1 Resistance to rutting

Several researchers (Bernier et al. 2012; Hajj et al. 2009; Kim et al. 2009; West et al. 2009) have performed the asphalt pavement analyzer (APA) test on laboratory-fabricated specimens to assess rutting resistance of PMA mixtures containing RAP. Specimens were typically compacted with a Superpave gyratory compactor to 7% air voids and 75 mm in height or 4% air voids and 115 mm in height, and tested at around 60°C. The rut depth was measured at 8000 cycles of loading (AASHTO TP63). Results associated with these studies are described below.

Kim et al. (2009) evaluated rutting resistance of PG 76-22 PMA mixtures containing 0%, 15%, 25% and 35% RAP. The RAP material was graded as PG 82-16. Florida limestone was used as the virgin aggregates. All four mixtures had the same gradation. The control mixture (with 0% RAP) exhibited a rut depth of 2 mm. All RAP-containing mixtures had a similar rut depth as the control. It appeared that addition of RAP up to 35% did not reduce the already low rut depth of the PMA mixture, although binder tests in the same study showed that addition of RAP binder increased the stiffness of the PMA binder (See Section 2.3). West et al. (2009) compared rutting resistance of PG 76-22 PMA mixtures containing 20% and 45% RAP without a control PMA mixture. The RAP material had a similar PG as the one used by Kim et al. (2009). They reported that the PMA mixture containing 45% RAP had a rut depth of 2-4 mm, which is close to the values determined by Kim et al. (2009). However, the PMA mixture containing 20% RAP had a much

higher rut depth of 4-7 mm. It is important to note that rutting resistance of asphalt mixtures is dominated by the aggregate structure of the mixture (Roque et al. 2011), and West et al. (2009) did not keep the same gradation between the PMA mixtures containing different RAP contents. Therefore, the difference between rut depths of the two RAP-containing mixtures may have been caused by different mixture gradations rather than different RAP contents.

Hajj et al. (2009) evaluated the impact of the RAP source and content on rutting resistance of PMA mixtures. Three RAP sources (plant waste material, 15-year old pavement, and 20-year old pavement) located in Reno, Nevada, and three RAP contents (0%, 15%, and 30%) were selected. Interestingly, all three recovered RAP binders had the same Superpave PG grade 82-16 with continuous grades of 83.5-19.7, 82.2-16.7, and 83.5-18.7, respectively. All mixtures were designed with the same target binder grade of PG 64-28 and similar gradations. Using the blending charts, the required virgin binder grades for the 15% and 30% RAP contents were determined to be PG 64-34 and PG 58-34, respectively. The APA test results showed that the PMA mixtures containing RAP exhibited rut depths similar to that of the control mixture (2 mm) regardless of the RAP sources.

Bernier et al. (2012) examined the effect of PMA type and RAP source on rutting resistance of mixtures containing 10% RAP. Four polymer-modified binders (PG 58-34, PG 64-28, PG 70-28, and PG 76-22) and four RAP sources (basalt, granite, schist, and limestone RAP) were used in the study. The basalt RAP had the finest gradation and exhibited the highest binder stiffness among all RAP sources. For the same RAP source, the PG 76-22 PMA mixture exhibited higher rut depth than the PG 70-28 and PG 64-28 PMA mixtures. This unexpected result may have been caused by the heating procedure used before APA testing, where specimens were maintained at the high PG temperature of asphalt binder for six hours. For the same PMA binder type, the basalt RAP binder with the highest stiffness only showed a clear reduction in rutting in the PG 58-34 mixture. It should be noted that PMA mixtures with different RAP sources had different gradations and that only 10% RAP was used. The effect of RAP binder stiffness on rutting resistance of the other PMA mixtures may have been overwhelmed by the effect of aggregate structure. In addition, the results showed that rutting resistance of the PG 76-22 PMA mixtures were the least sensitive to the RAP sources.

In summary, PMA mixtures are known to have good rutting resistance, which was confirmed based on this part of the review. Furthermore, it was found that for well-controlled APA

testing programs where mixture gradations were kept the same, PMA mixtures containing RAP had equivalent or better rutting resistance than the virgin PMA mixtures. It appeared that addition of RAP would not diminish rutting resistance of PMA mixtures.

2.4.2 Resistance to fatigue cracking

Various tests and methods have been used to evaluate load-related cracking resistance of PMA mixtures containing RAP, including beam fatigue tests, semi-circular bending fracture tests, and Superpave indirect tensile tests. Due to different cracking mechanisms simulated by different tests, inconsistent results were reported with respect to the effect of RAP on cracking resistance of PMA mixtures.

The beam fatigue tests were generally intended to simulate traditional bottom-up fatigue cracking. Samples were typically compacted in a kneading compactor and then cut to obtain 50 by 63 by 380 mm beam specimens. The beam specimens with air voids in the range of 5% to 7% were long-term aged and then subjected to repeated loading at a constant strain level at around 20°C. Fatigue life or failure was defined as the cycle corresponding to a 50% reduction in the initial stiffness taken at the 50^{th} cycle (AASHTO T 321).

West et al. (2009) conducted beam fatigue tests at a strain level of 500 μstrain to evaluate fatigue-cracking resistance of PG 76-22 PMA mixtures containing 20% and 45% RAP. The RAP material was graded as PG 88-16. The results showed that the increased RAP content from 20% to 45% led to a reduction in the fatigue life of PMA mixtures from around 200,000 to 50,000 cycles. Huang et al. (2011) also evaluated fatigue-cracking resistance of PG 76-22 PMA mixtures containing RAP. Limestone was used as the virgin aggregate. Screened RAP materials (passing No. 4 sieve size) were added to the mixtures at four RAP contents (0%, 10%, 20%, and 30%). The recovered RAP binder was determined to have a $G^*\sin\delta$ value of 3,200 kPa. Beam fatigue tests were conducted at a strain level of 600 μstrain. The results showed that all mixtures failed at 400,000 cycles regardless of the RAP contents, which did not agree with the trend of reduced fatigue life with increasing RAP content observed by West et al. (2009).

Hajj et al. (2009) evaluated the impact of the RAP source and content on fatigue-cracking resistance of PMA mixtures. Three RAP sources (plant waste material, 15-year old pavement, and 20-year old pavement) located in Reno, Nevada and three RAP contents (0%, 15%, and 30%) were selected. All mixtures were designed with the same target binder grade of PG 64-28. Beam fatigue

tests were conduct on each mixture at five strain levels in the range of 400 μstrain to 1,000 μstrain. A fatigue model in the form of $N_f = k_1 \cdot (1/\varepsilon)^{k_2}$ was developed for each mixture based on the testing results. It was found that the ranking for fatigue-cracking resistance was affected by the strain level of loading. In other words, the resistance of one mixture may be ranked higher than the other one at one strain level but lower at a different strain level. A mechanistic-empirical analysis was conducted along with resilient modulus determined using indirect tensile tests and fatigue characteristic data. First, layered elastic analysis was conducted to obtain tensile strain at the bottom of the asphalt layer. All pavements were assumed to have the same structure (4-inch asphalt layer on top of 10-inch granular base course) subjected to the same axle load representing the legal load limits in Nevada. Resilient modulus measured on each mixture was used as input for the asphalt layer, while typical values of 30 ksi and 10 ksi were assumed for the base layer and subgrade, respectively. The calculated tensile strain was then input into the corresponding fatigue model to determine the fatigue life. Results showed that PMA mixtures with 15% and 30% RAP had lower fatigue resistance compared to the virgin PMA mixtures regardless of RAP sources. However, the fatigue resistances of PMA mixtures with 15% and 30% RAP were significantly better than the virgin mixtures with neat binder. The authors concluded that RAP could be used in PMA mixtures to offset the additional cost of the polymer while achieving higher fatigue resistance than neat mixtures without RAP.

The Superpave indirect tensile (IDT) test system includes a series of three tests: resilient modulus test, creep test, and fracture energy test conducted at an intermediate service temperature to determine mixture's stiffness, creep compliance rate, and energy-based failure limits: fracture energy limit (FE_f) and dissipated creep strain energy limit ($DCSE_f$). Samples were prepared to a thickness around 38 mm with a target air voids content of 7±0.5%. Three aging levels: short-term oven aging (STOA), long-term oven aging (LTOA), and LTOA plus cyclic pore pressure conditioning (CPPC) have been employed to condition the samples before testing. CPPC of mixtures after LTOA was found necessary to more properly simulate field aging (Isola et al. 2014).

The energy ratio (ER) parameter integrates key mixture properties measured using the Superpave IDT test system. It was developed based on a detailed analysis and evaluation of 22 field test sections throughout the state of Florida (Roque et al. 2004). An ER less than 1 is considered to have high potential for top-down cracking. The higher the ER, the better the expected

cracking resistance of the mixture. It is important to note that ER should not be used to evaluate brittle mixtures as reflected by a $DCSE_f$ lower than 0.75 kJ/m^3.

Kim et al. (2009) conducted Superpave IDT tests on STOA samples to evaluate cracking resistance of PG 76-22 PMA mixtures containing 0%, 15%, 25%, and 35% RAP. The RAP material was graded as PG 82-16. It was found that all mixtures had a similar $DCSE_f$ value except for the one containing 35% RAP, which exhibited a lower value. ER results showed that mixtures containing 25% and 35% RAP exhibited slightly better performance than the ones with 0% and 15% RAP mainly due to lower creep compliance rates. West et al. (2009) conducted IDT tests on cores taken from the NCAT test track to compare cracking performance of PG 76-22 PMA mixtures containing 20% and 45% RAP. The RAP material had a similar PG as the one used by Kim et al. (2009). They reported that the PMA mixture with 45% RAP exhibited lower ER than the one with 20% RAP, indicating reduced cracking performance. However, the authors attributed this to lower effective volume of asphalt (V_{be}) in the higher RAP content mixtures.

Recently, Yan et al. (2017a) evaluated cracking performance of PG 76-22 PMA mixtures with four RAP contents (0%, 20%, 30%, and 40%) using the Superpave IDT tests. Two RAP sources with distinctively different characteristics were selected: one fine gradation RAP with typical binder stiffness in Florida (PG 94-24) and one coarse gradation RAP with extremely stiff binder (graded as PG 100-12). The fine RAP (with 75% passing the 4.75 mm sieve) was mainly composed of granite, while the majority of the coarse RAP (with only 25% passing the 4.75 mm sieve) was Florida limestone. Both RAP sources had similar RAP binder contents, i.e., 4.8% for the fine RAP and 4.6% for the coarse RAP. Before testing, one group of samples was subjected to STOA to simulate aging due to the mixing and construction process, and the other was subjected to LTOA plus CPPC to simulate field aging. Results of specimens tested at both aging levels generally showed the same trend, i.e. increased RAP content led to stronger (higher tensile strength) but more brittle (lower fracture energy limit) mixtures. More importantly, it was found that RAP gradation had a dominant effect on mixture properties. Although coarse RAP was much stiffer than fine RAP, it resulted in lower mixture resilient modulus than fine RAP, indicating full blending between virgin and RAP binder did not occur in the mixtures; instead, the RAP binder tended to stay close to the RAP aggregate. Furthermore, coarse RAP resulted in higher mixture FE_f than fine RAP. This indicates that greater degree of blending is not necessarily favorable for

mixture cracking resistance since the finer portion of the mixtures with coarse RAP was primarily virgin aggregate and virgin binder.

Mixture cracking performance was evaluated based on samples conditioned with LTOA plus CPPC. Results showed that the mixtures with coarse RAP exhibited higher ER values than the ones with fine RAP for all three RAP contents (20%, 30%, and 40%), even though the coarse RAP was much stiffer than the fine RAP. All mixtures exhibited ER values greater than 1.0. The addition of RAP generally resulted in higher ER values, which was consistent with findings reported by Kim et al. (2009). The authors concluded that RAP gradation affects the distribution of RAP binder within the PMA mixtures. Therefore, it is important to characterize not only RAP binder but also RAP gradation for proper PMA mixture designs containing RAP. This work appeared to indicate that up to 40% RAP could be used in well-designed PMA mixtures without negatively affecting the cracking performance.

Semi-circular bending (SCB) tests have also been used by researchers to evaluate fracture resistance of PMA mixtures containing RAP. Two semi-circular specimens were obtained by slicing along the central axis of each gyratory compacted sample. A notch was introduced along the symmetrical axis for each specimen. The notched specimens were then subjected to a constant loading rate of 0.5 mm/min until failure in a three-point bending load configuration (Mull et al. 2002). Typically, specimens with three notch depths were tested to determine the critical strain energy release rate J_c. High J_c values are desirable for fracture-resistant mixtures. Huang et al. (2004) conducted SCB fracture tests on long-term aged specimens of PG 76-22 PMA mixtures containing screened RAP (passing No.4 sieve size) in the range of 10% to 30%. Test results showed that addition of RAP led to higher J_c values indicating improved fracture resistance.

In summary, analysis based on beam fatigue test results showed that although PMA mixtures containing RAP exhibited better performance than virgin mixtures with neat binder, incorporation of RAP reduced fatigue life (or cracking performance) relative to virgin PMA mixtures. However, the ranking of fatigue-cracking resistance was affected by the strain level employed in the test. Furthermore, since the majority of cracking distress in Florida asphalt pavements is top-down (or near-surface) cracking, not traditional bottom-up cracking, use of beam fatigue tests does not appear to be appropriate. Analysis based on ER and Superpave IDT results showed that addition of RAP into virgin PMA mixtures led to improved cracking performance as long as key RAP characteristics (RAP gradation and binder stiffness) were considered to achieve

proper mix designs. This trend was also supported by the results of SCB fracture tests. It is important to note that the ER was calibrated using field-aged cores taken from pavements throughout Florida. Furthermore, it has been verified that ER reliably evaluated top-down cracking performance of asphalt mixtures in the NCAT test track and in the field, respectively (Timm et al. 2009; Zou et al. 2013). Therefore, use of ER to evaluate the cracking performance of PMA mixtures containing RAP appears to be better warranted for success than the other approaches.

2.4.3 Resistance to thermal cracking

Very little research has been conducted to evaluate the effect of RAP on thermal-cracking resistance of PMA mixtures. Hajj et al. (2009) showed that the addition of 15% or 30% RAP resulted in better resistance to thermal cracking regardless of RAP sources. All PMA mixtures were designed with the same target binder grade of PG 64-28. Using the blending charts, virgin binder grades with a colder low performance temperature, i.e. PG 64-34 and PG 58-34 were used for the mixtures containing 15% and 30% RAP, respectively. The thermal stress restrained specimen test (TSRST) was conducted on 50 by 50 by 254 mm beam specimens. The specimens were placed vertically and restrained at the two ends when temperature cools down at a rate of 10°C/hour. During the cooling process, tensile stresses develop in the specimen. The specimen will fracture as the internally generated stress exceeds its tensile strength. The temperature at which fracture occurs is referred to as fracture temperature, which was used as an indicator of thermal-cracking resistance. The lower the fracture temperature, the higher the thermal-cracking resistance. It was found that the addition of RAP resulted in a colder fracture temperature than the virgin PMA mixture, hence an increase in thermal-cracking resistance. The authors concluded that the change in the virgin binder grade had a positive impact on the thermal-cracking resistance of the RAP-containing PMA mixtures.

2.4.4 Summary

PMA mixtures are known to have better rutting and cracking resistance than unmodified mixtures with neat binder. However, the impact of RAP on performance of PMA mixtures is not as clear. A literature review was conducted and the results on performance of PMA mixtures containing RAP are summarized below.

APA test results of several independent studies clearly showed that PMA mixtures containing RAP had equivalent or better rutting resistance than the control PMA mixtures containing no RAP. Results were less clear regarding the effect of RAP on fatigue cracking performance of PMA mixtures. The beam fatigue test, which simulates traditional bottom-up cracking, had variable results. Fatigue lives determined from the test were found to be dependent on the strain level of loading. The ER approach addresses the predominant failure mode in Florida: top-down cracking. Results of ER have consistently showed that addition of RAP into virgin PMA mixtures led to improved cracking performance. This trend was supported by results of the SCB fracture test. ER results also indicated that distribution of RAP binder in PMA mixtures was affected by RAP gradation. This implied that RAP gradation should be considered in addition to RAP binder stiffness for proper mix designs containing RAP. Limited data from one study using the TSRST test showed that addition of RAP led to increased resistance to thermal cracking. Softer virgin binder grades, which were used to achieve the same target grade as the control mixture, appeared to have contributed to the improved thermal-cracking resistance.

2.5 Concluding Remarks

A literature review was conducted to gather and examine available information regarding RAP characteristics, methods of RAP characterization, and effects of RAP on PMA mixture performance. The literature review was mainly focused on obtaining the understanding necessary to help identify key RAP characteristics that affect PMA mixture performance and promising methods for RAP characterization and for performance evaluation of PMA mixtures containing RAP. A summary of findings is described below:

- A similar trend was observed in terms of the effect of RAP binder on properties and performance indexes of PMA binder as compared to those of unmodified binder. As the amount of RAP binder increased in PMA binder, rutting resistance increased, while resistance to fatigue cracking and thermal cracking was reduced. Generally, a stiffer RAP binder resulted in greater change in PMA binder properties.
- This confirmed that RAP binder stiffness is an important characteristic for use in mix designs containing RAP. Performance grade testing of recovered binders obtained from a solvent extraction and recovery procedure has been the most widely used characterization method.

Recently, a mortar testing procedure without the need for binder extraction was shown to be promising in determining effective RAP binder properties.

- BFE test results showed that incorporation of RAP led to dilution of polymer modification. However, all PMA binders containing RAP binder exhibited higher fracture energy values than those of unmodified binders. In addition, results of MSCR testing showed that elastomeric behavior of PMA binder was still evident after blending with stiff RAP binder at 40% RAP content.
- Various studies have indicated that complete blending of RAP binder and virgin binder may not occur in asphalt mixtures during standard production. When partial blending occurred, RAP binder tended to stay close to RAP aggregate, which resulted in non-uniform distribution of RAP binder in the asphalt mixture.
- The APA test results of several independent studies clearly showed that PMA mixtures containing RAP had equivalent or better rutting resistance than the control PMA mixtures.
- Results were less clear regarding the effect of RAP on fatigue cracking performance of PMA mixtures. Various tests and methods intended for different cracking mechanisms have been employed in different studies.
  - The beam fatigue test, which simulates traditional bottom-up cracking, had variable results. In addition, very high strain levels were applied in the studies reviewed to complete the test in a reasonable time. Fatigue lives determined from the test were found to be dependent on the strain level of loading.
  - The ER approach addresses top-down cracking, which is the predominant failure mode in Florida. Results of ER have consistently shown that addition of RAP into virgin PMA mixtures led to improved cracking performance. This trend was also observed based on results of the SCB fracture test.
  - ER results also indicated that distribution of RAP binder in PMA mixtures was affected by RAP gradation. This implied that RAP gradation should be considered in addition to RAP binder stiffness for proper mix designs containing RAP.

Overall, both RAP binder stiffness and RAP gradation were found to be important characteristics for proper PMA mix designs containing RAP. The mortar testing procedure without the need for binder extraction appeared to be more suitable than the conventional approach for use

during RAP binder characterization. Furthermore, there is no consensus as to the best test for evaluating fatigue cracking performance of PMA mixtures containing RAP. Since the ER approach was calibrated and validated to field performance in Florida, the Superpave IDT tests and ER approach were proposed for use to provide reference for top-down cracking performance. A detailed experimental plan to determine whether these selected characteristics are needed for increased RAP usage in PMA mixtures are presented in the CHAPTER 4.

CHAPTER 3
IDENTIFICATION OF REPRESENTATIVE RAP SOURCES

3.1 Introduction

According to the literature review, both RAP binder stiffness and RAP gradation appeared to be important characteristics for PMA mix designs containing RAP. In this study, the need for these RAP characteristics to achieve high RAP content in PMA mixture was assessed using eight RAP sources that cover a broad range of RAP binder stiffness and gradation. This chapter documents the process of selecting these RAP stockpiles.

Twelve RAP stockpiles were identified in consultation with the Florida Department of Transportation (FDOT) research panel as representative RAP sources throughout Florida (See Figure 3-1). Details of sampled RAP sources, including product names, contractors, and locations are presented in Table 3-1. Recovered RAP binders of the 12 RAP sources were evaluated to confirm that the RAP sources covered the reference range of RAP binder stiffness from the FDOT 2015 inventory in terms of both absolute viscosity and high-temperature continuous grade. Also, recovered RAP aggregate gradation of the 12 RAP sources was evaluated to identify its range and distribution. In addition, 12 PMA mix designs with 20% RAP corresponding to each RAP stockpile were evaluated using the dominant aggregate size range-interstitial component (DASR-IC) analysis system to assess the potential influence of gradation deficiency. As a result, eight of the 12 RAP stockpiles were selected for further evaluation.

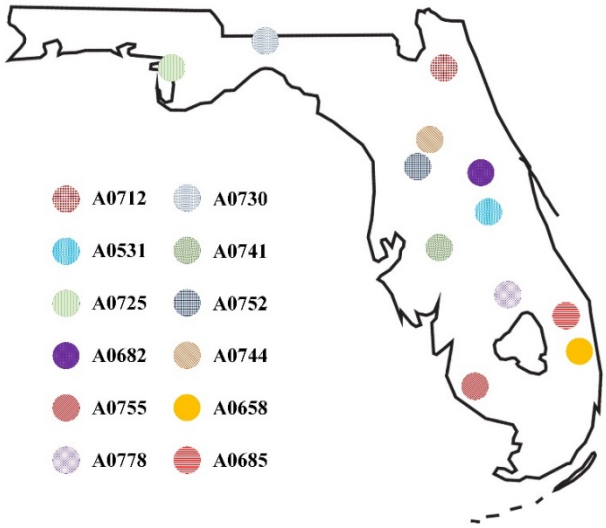

Figure 3-1. Location of collected RAP sources

Table 3-1. Information of sampled RAP sources

RAP material		Location	Contractor
Plant No.	**Name**		
A0712	1-12	Jacksonville, FL	Duval Asphalt Products, Inc.
A0531	2-12	Taft, FL	Orlando Paving Company
A0725	1-14	Panama City, FL	C.W. Roberts Contracting, Inc.
A0682	1-16	Debary, FL	Ranger Construction Industries, Inc.
A0755	1-14	Naples, FL	Preferred Materials, Inc.
A0778	1-17	Okeechobee, FL	Lynch Paving, Inc.
A0730	1-16	Havana, FL	Peavy & Construction Company, Inc.
A0741	1-13	Eaton park, FL	The Lane Construction Corporation
A0752	1-13	Gainesville, FL	Preferred Materials, Inc.
A0744	1-16	Gainesville, FL	V.E. Whitehurst & Sons, Inc.
A0658	1-15	Delray beach, FL	Hardrives, Inc.
A0685	2-12	West palm beach, FL	J.W. Cheatham, LLC

3.2 RAP Characterization

3.2.1 RAP binder and aggregate recovery

A solvent extraction and recovery process was conducted by FDOT to obtain recovered RAP binder and aggregate and to determine RAP binder content. Recovered RAP binder and aggregate were used to determine important characteristics for all RAP sources, including RAP binder stiffness and RAP gradation. RAP binder content and recovered RAP aggregate gradation were used to verify the PMA mix design containing 20% RAP associated with each RAP source and to design PMA mixtures containing other RAP contents (0%, 30%, and 40%).

A reflux method was used to extract RAP binders following Florida Method of Test FM 5-524. Trichloroethylene (TCE) was used as a solvent. RAP binders were recovered following Florida Method of Test FM 3-D5404. The entire procedure, from the reflux extraction to the recovery, needs to be completed within eight hours. Table 3-2 shows the resulting RAP binder content, which ranged from 4.4% to 6.6% for all 12 sampled RAP sources.

Table 3-2. RAP binder contents of the 12 sampled RAP sources

RAP material	RAP binder content (%)
A0712	5.7
A0531	5.8
A0725	4.9
A0682	5.2
A0755	5.7
A0778	5.8
A0730	6.6
A0741	4.9
A0752	5.9
A0744	5.9
A0658	4.4
A0685	5.0

3.2.2 Characterization of RAP binder stiffness

Stiffness of recovered RAP binders was obtained by measuring absolute viscosity and high-temperature continuous grade to confirm that collected RAP sources included a broad range of RAP binder stiffness. High-temperature continuous grade was used as the preferred indicator of RAP binder stiffness because it can be measured without need of binder extraction and recovery process using the mortar approach and PG grade, not viscosity, is the current approach by FDOT for characterization of binders. Details of mortar approach are described in APPENDIX B. High-temperature continuous grade results were compared with the results of viscosity to verify that both parameters exhibited a similar trend of RAP binder stiffness.

RAP binder viscosity

Absolute viscosity is a measure of fluid resistance to flow and is defined by the following equation.

$$\mu = \frac{\tau}{\dot{\gamma}} \qquad Eq.3.1$$

where,

μ = viscosity, τ = shear stress, $\dot{\gamma}$ = shear strain rate.

The absolute viscosity of recovered RAP binder was determined by vacuum capillary viscometer at 60°C following ASTM D2171-07. Figure 3-2 shows the binder viscosity of the 12 recovered RAP binders ranged from 200,000 to 1,400,000 poises. In addition, Figure 3-3 shows a histogram of RAP binder viscosity from FDOT 2015 inventory, along with the viscosity values of the 12 collected RAP sources. The 12 viscosity values covered the range of FDOT 2015 inventory histogram except for values below 200,000 poises. Therefore, the sampled RAP sources appeared to be representative of the viscosity range of Florida RAP material.

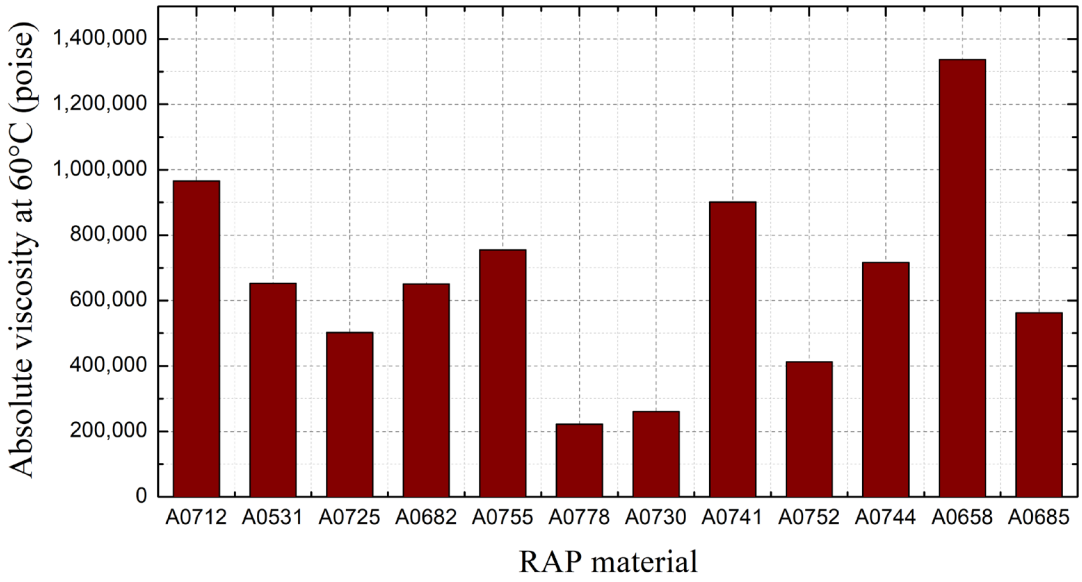

Figure 3-2. Absolute viscosity of recovered RAP binder

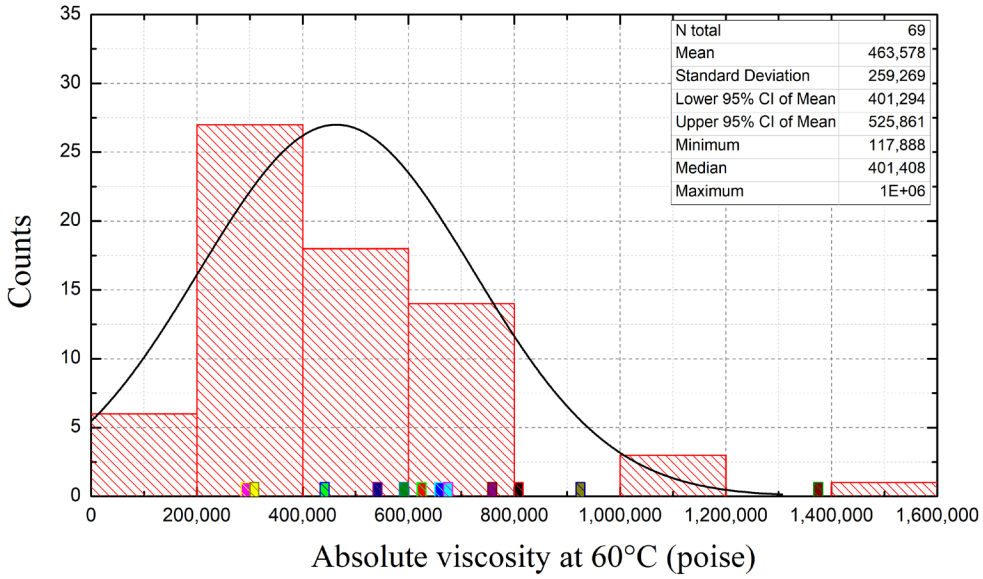

Figure 3-3. Histogram of RAP binder viscosity from FDOT 2015 inventory

RAP binder high-temperature continuous grade

High-temperature continuous grade of recovered RAP binder was determined based on the minimum requirement on G*/sinδ (1.0 kPa) for virgin binder and 12% strain level for RTFO-aged binder in the Superpave specification. The complex shear modulus, G* and phase angle (δ) of recovered binder were measured using dynamic shear rheometer (DSR).

Figure 3-4 shows high-temperature continuous grade for the 12 recovered RAP binders ranged from 95°C to 108°C. Additionally, Figure 3-5 shows high-temperature continuous grades of the 12 recovered RAP binders covered a range above the mean value of FDOT 2015 inventory (93.7°C). However, a higher minimum requirement of G*/sinδ (2.2 kPa) was used in 2015, which is the likely reason for the difference in range.

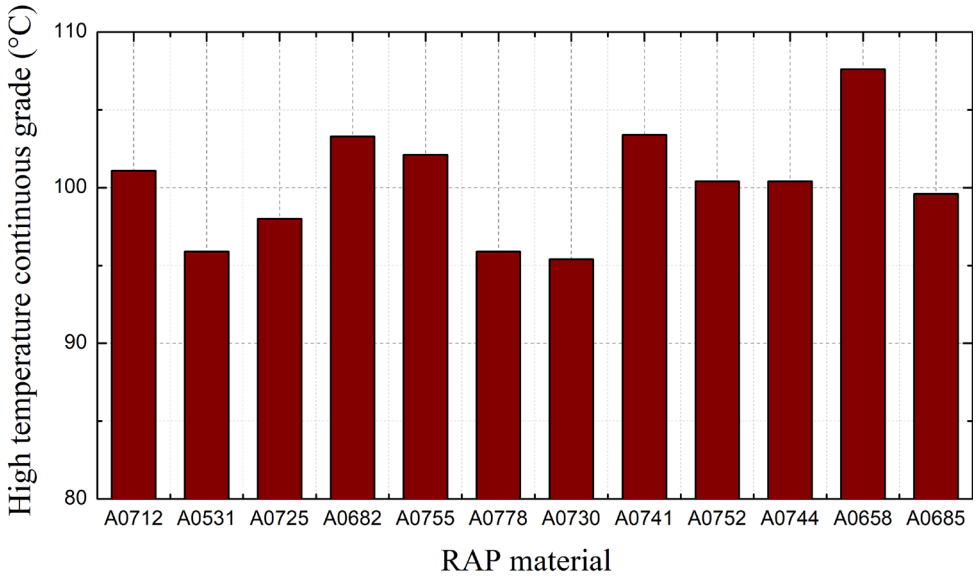

Figure 3-4. High-temperature grade of recovered RAP binder

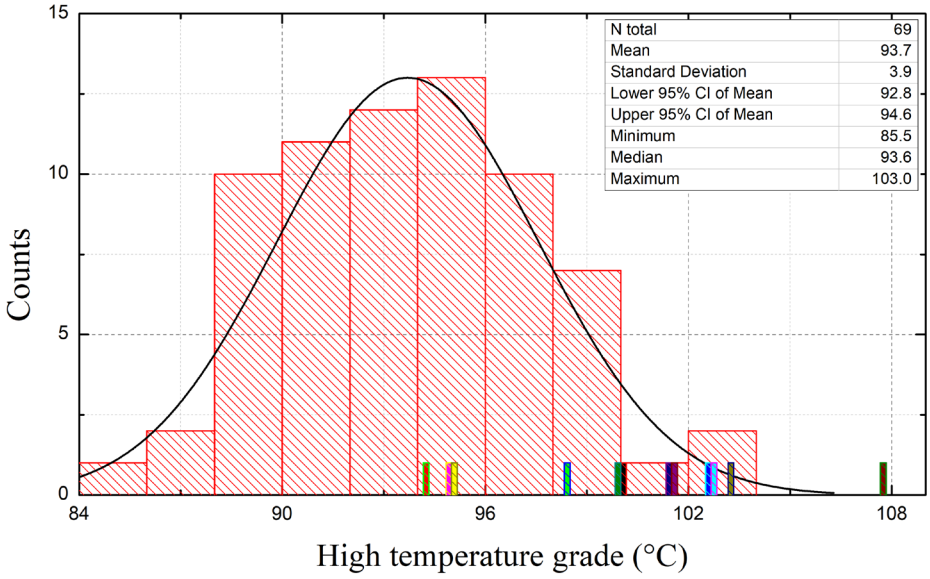

Figure 3-5. Histogram of high-temperature grade of RAP binder from FDOT 2015 inventory

Comparison between viscosity and high-temperature continuous grade for RAP binders

The comparisons presented in Figure 3-6 indicate that RAP binder viscosity and high-temperature continuous grade appeared to be correlated. Therefore, it appears that high-temperature continuous grade can be used in lieu of absolute viscosity as an indicator of RAP binder stiffness.

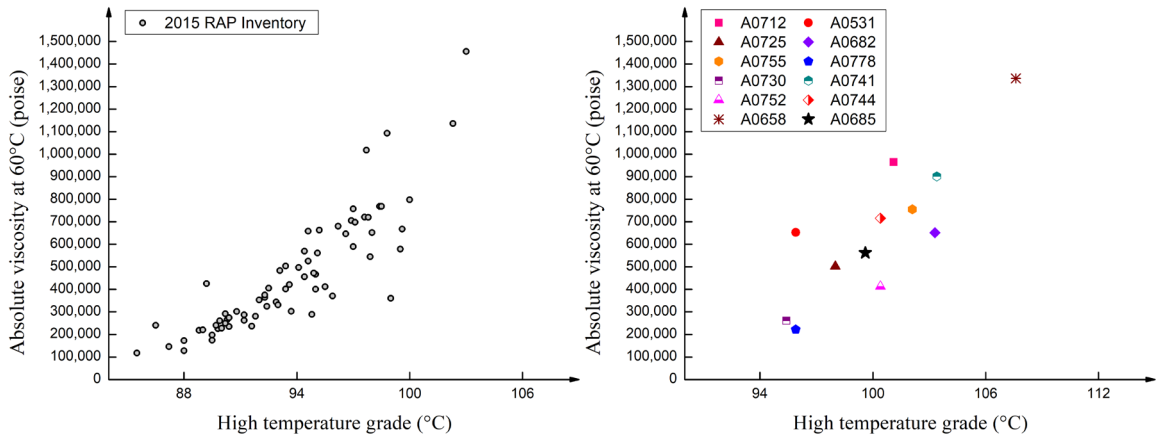

(a) (b)

Figure 3-6. Comparison between absolute viscosity at 60°C and high-temperature grade: (a) 2015 FDOT inventory and (b) the 12 sampled RAP sources in 2017

3.2.3 Characterization of RAP aggregate gradation

In a recent study conducted to determine effects of RAP on cracking performance of asphalt mixtures, it was found that mixtures with coarse RAP exhibited higher cracking resistance than the ones with fine RAP for all three RAP contents (20%, 30%, and 40%) evaluated, even though the coarse RAP was much stiffer than the fine RAP (Roque et al. 2015). It appeared that the RAP binder tended to stay close to the RAP aggregate, indicating that RAP gradation affected the distribution of RAP binder within the RAP mixtures. In other words, the mixtures with coarse RAP had almost no RAP binder (primarily virgin aggregate and virgin binder) in the finer portion, while the ones with fine RAP contained more RAP binder in the finer portion. Therefore, when incorporating RAP into asphalt mixtures it is important to characterize RAP gradation, particularly to determine the percent of fine particles in the RAP gradation, which is called RAP fineness for purpose of this study.

The percent passing No. 16 sieve size (1.18 mm) was selected for determination of RAP fineness because it is used in the dominant aggregate size range-interstitial component (DASR-IC) system to separate fine particles from the coarser ones. According to the DASR-IC theory (Chun et al. 2012; Kim et al. 2009; Kim et al. 2006), the behavior of a mixture is mainly dominated by two components: the DASR and the IC. The DASR is composed of coarse aggregates that provide the structural interactive network of aggregate to resist shear. The IC is the combination of fine aggregates, binder, and air voids that fill the interstitial volume (IV) within the DASR. The IC primarily resists tension and, to a lesser extent, resists shear. Results from a recent study showed that fracture-related properties of ICs correlated well with those of the corresponding mixtures (Yan et al. 2017b). Specifically, it was found that ICs containing coarsely graded stiff RAP exhibited higher fracture energy than those with finely graded RAP that was less stiff. This trend agreed well with the results at the mixture level mentioned earlier (Roque et al. 2015).

Two types of RAP aggregate gradation, black and white curves, are typically determined. The black curve is the stockpile gradation of RAP material which containing RAP binder, and the white curve is the recovered RAP aggregate gradation. It should be noted that neither curve may exactly represent the actual gradation of RAP material in the final mixture, which depends on the degree of blending during mixing (Roque et al. 2015). Figure 3-7 which shows the black and white curves for one of the RAP sources (A0712) used in this study, indicates that these can be significantly different from each other. Al-Qadi et al. (2009) found that black curve tends to contain more large particles and less amounts of fine particles as compared to white curve. This observation indicates fine particles do remain on the surface of larger particles. The use of white curve is typically suggested for RAP mixture design because it is assumed that RAP particles are completely broken down during production (Roque et al. 2015). Therefore, the recovered RAP aggregate gradation (white curve) was selected for gradation characterization.

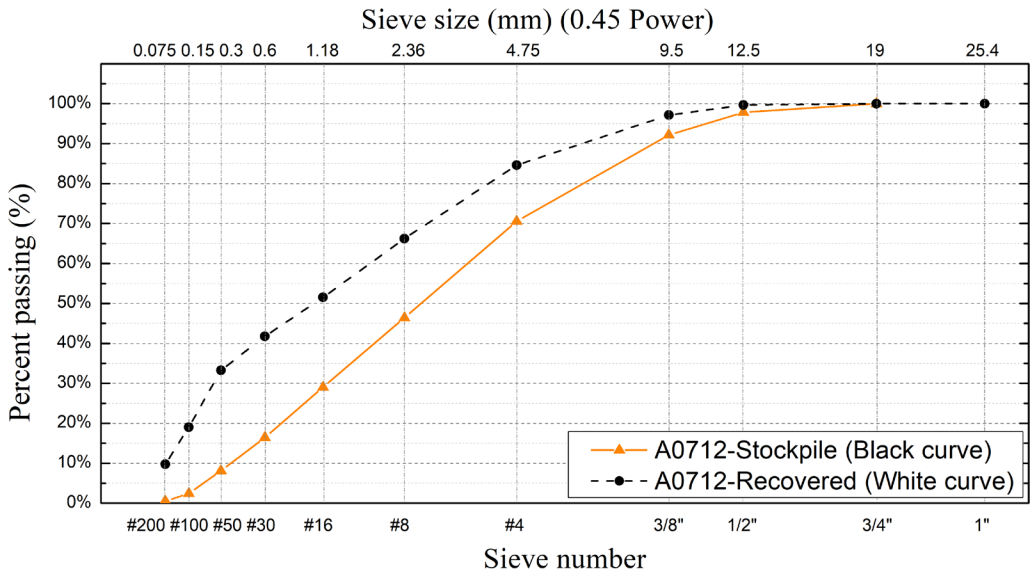

Figure 3-7. Comparison between black and white curve (A0712 RAP)

Recovered RAP aggregate gradation (white curve) was used to identify the range and distribution of RAP gradation for the 12 sources collected. Recovered RAP aggregate acquired from solvent extraction was washed, dried and sieved to determine the recovered RAP aggregate gradation (white curve). The gradations shown in Figure 3-8 represent the range of the 12 recovered RAP gradations obtained in this study. Recovered RAP gradations for all 12 RAP sources is presented in APPENDIX C.

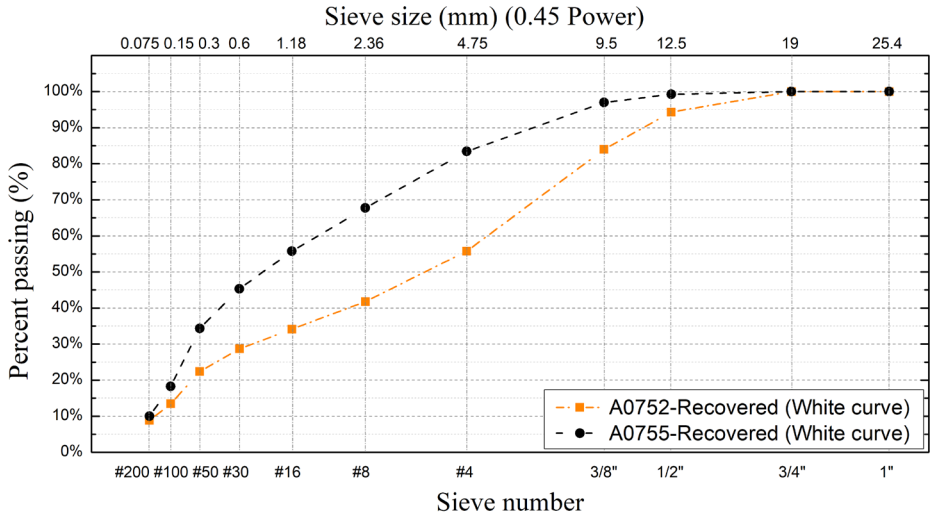

Figure 3-8. Example of recovered RAP gradation (A0752 and A0755)

3.3 Mixture Gradation Analysis

Twelve existing PMA mix designs with 20% RAP corresponding to each RAP stockpile were provided by FDOT and were evaluated using the DASR-IC analysis system to assess the potential influence of gradation deficiency. Results of DASR-IC analysis were considered in the selection of the final eight RAP sources for further evaluation.

3.3.1 Dominant aggregate size range-interstitial component (DASR-IC) system

The DASR-IC system was developed to describe gradation characteristics and volumetric properties of mixtures. The system provides a practical framework for the design and modification of gradation to ensure adequate shear resistance, durability and fracture resistance (Roque et al. 2011). According to the DASR-IC theory, behavior of mixture is mainly dominated by two components: the DASR and the IC. The DASR is composed of coarse aggregates that forms the primary structural interactive network of aggregate to resist shear. Particles larger than DASR will not play a major role in the aggregate structure because they float in the DASR matrix. On the other hand, particles finer than DASR will serve to fill the void space between DASR particles, which is called interstitial volume (IV). The IC is the combination of fine aggregates, binder, and air voids that fill the IV within the DASR. The IC resists primarily tension and to a lesser extent, shear. DASR can consist of one size or multiple contiguous sizes. (Kim et al. 2006). Figure 3-9 conceptually illustrates the DASR-IC system.

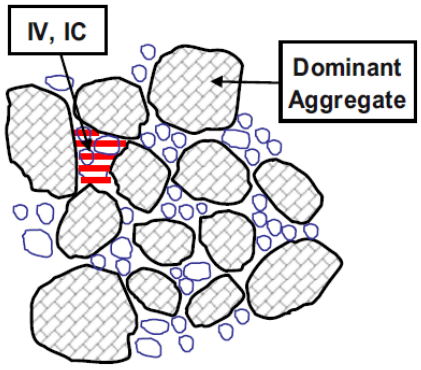

Figure 3-9. Schematic representation of DASR-IC system

Based on results from laboratory studies and long-term field evaluation of mixtures (nominal maximum aggregate size from 9.5 to 12.5 mm), three key parameters and associated criteria to ensure potentially good mixture performance have been identified: DASR porosity (η_{DASR}: 38-52%), disruption factor (DF: 0.50-0.95), and effective film thickness (EFT: 12.5-25.0 microns).

The DASR porosity (η_{DASR}) criterion was used to ensure adequate interlocking to provide resistance to deformation and fracture. DASR porosity can be calculated using Equation 3.2 based on volume of mixture components (See Figure 3-10).

$$\eta_{DASR} = \frac{V_{V(DASR)}}{V_{T(DASR)}} = \frac{V_{ICAGG} + V_{VMA}}{V_{TM} - V_{AGG(>DASR)}} \qquad Eq.3.2$$

where,

$V_{V(DASR)}$ = volume of voids within DASR (i.e., IV),

$V_{T(DASR)}$ = total volume available for DASR particles,

V_{ICAGG} = volume of IC aggregates,

V_{TM} = volume of total mixture,

$V_{AGG(>DASR)}$ = volume of particles greater than DASR

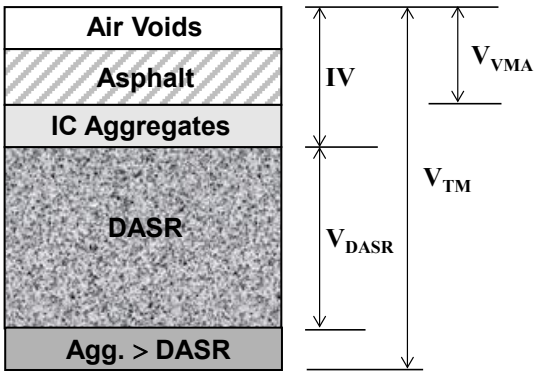

Figure 3-10. Mixture components for calculation of DASR porosity

The DF was developed to evaluate the IC aggregates that may potentially disrupt the DASR structure (Guarin et al. 2013). DF can be calculated using the following equation:

$$\mathrm{DF} = \frac{\text{Volume of IC Particles in the potentially disruptive range (PDR)}}{\text{Volume of DASR packing voids}} \qquad Eq.3.3$$

When DF is in the optimal range, the IC aggregates does not disrupt the DASR but it can assist the DASR particles to resist shear stresses. However, if DF is too high, the IC aggregate would disrupt the DASR structure. If DF is too low, the IC aggregates would not be involved in transferring load between the DASR particles.

The EFT criterion was established to ensure adequate durability and fatigue resistance of the mixture (Isola et al. 2014; Nukunya et al. 2002). EFT (in Microns) can be calculated using the following equation:

$$\mathrm{EFT} = \frac{\mathrm{V_{be}}}{\mathrm{SA_F} \cdot \mathrm{M_{TM}} \cdot \frac{\mathrm{P_{sF}}}{100}} \times 10^3 = \frac{\mathrm{P_{be}}}{\mathrm{SA_F} \cdot \mathrm{G_b} \cdot \mathrm{P_{sF}}} \times 10^3 \qquad Eq.3.4$$

where,

V_{be} = volume of effective asphalt binder (cm^3),

SA_F = surface area per unit mass (m^2/kg) for fine particles passing 2.36 mm sieve size,

M_{TM} = mass of total mixture (g),

P_{sF} = fine aggregate content,

P_{be} = effective asphalt content,

G_b = specific gravity of asphalt binder

It is important to note that fine particles for EFT was defined based on a slightly larger sieve size (#8) than the one used for RAP fineness (#16). Nukunya et al. (2002) found that EFT based on the percent passing No. 8 sieve size (2.36 mm) related well with binder age-hardening rate and mixture performance.

3.3.2 Implementation of gradation analysis for PMA mixtures containing 20% RAP

Table 3-3 summarizes DASR-IC parameters of existing mix designs containing 20 % RAP along with the recommended criteria. A range of DASR porosity was given for five RAP mix designs (A0741, A0682, A0531, A0658, and A0712) because the DASR was unclear due to marginal interaction between contiguous size aggregates.

Table 3-3. DASR-IC parameters of existing mix design containing 20% RAP

RAP material	η_{DASR} (38.0% to 52.0%)*	DF (0.50 to 0.95)*	EFT (12.5 to 25.0 μm)*
A0712	47.8% to 43.6%	0.81 to 0.78	17.0 μm
A0531	68.6% to 48.2%	0.91 to 0.65	19.1 μm
A0725	49.1%	0.95	18.9 μm
A0682	45.6% to 41.8%	0.64 to 0.62	25.4 μm
A0755	48.8%	0.84	19.9 μm
A0778	51.8%	0.87	12.0 μm
A0730	46.7%	0.89	20.5 μm
A0741	55.8% to 48.4%	0.58 to 0.69	26.6 μm
A0752	53.8%	0.65	15.8 μm
A0744	47.1%	0.63	16.8 μm
A0658	56.0% to 50.2%	0.84 to 0.80	16.2 μm
A0685	54.7%	0.64	13.3 μm

*DASR-IC requirement

3.4 Selection of Representative RAP Sources

The eight RAP sources selected for further evaluation should cover a broad range and distribution of RAP binder stiffness (high-temperature continuous grade) and RAP gradation (RAP fineness) to evaluate the need of RAP characterization for increased RAP usage in PMA mixtures. As mentioned in section 3.2.3, RAP fineness was defined by percent passing No. 16 sieve size (1.18 mm), which is the threshold between coarse and fine aggregate in DASR-IC theory. Figure 3-11a shows a RAP distribution chart which encompasses high-temperature continuous grade and RAP fineness, along with DASR porosity (η_{DASR}). RAP aggregate fineness was separated into three groups: (i) Coarse (less than 40% passing the No. 16 sieve (1.18 mm)); (ii) Intermediate (between 40% to 50% passing the No. 16 sieve (1.18 mm)); and (iii) Fine (greater than 50% passing the No. 16 sieve (1.18 mm)).

The selection of RAP sources was performed based on the following two conditions:

- DASR porosity should meet the DASR porosity criterion (38% to 52%)
- Each group of RAP fineness should include at least two levels of RAP binder stiffness

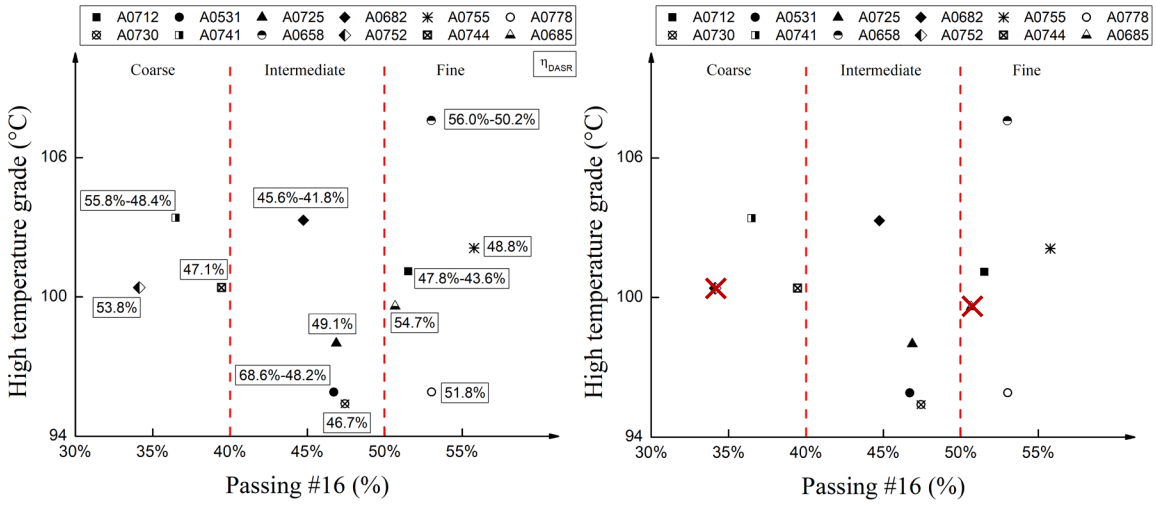

Figure 3-11. RAP material distribution chart: (a) for all 12 RAP sources collected, including DASR porosity and (b) for sampled RAP with the two eliminated RAP sources

As shown in Figure 3-11b, two RAP sources were excluded due to high DASR porosity, i.e., 53.8% for A0752 and 54.7% for A0685. The two remaining RAP sources (A0741 and A0744) in the coarse group were selected to include at least two levels of RAP binder stiffness. In the intermediate group, A0531 RAP source was eliminated because A0730 RAP had similar RAP characteristics while exhibiting better DASR porosity. The three remaining RAP sources (A0682, A0725, and A0730) were selected to cover the range of binder stiffness for this group. For the fine group, since A0712 and A0755 RAP had a similar RAP binder stiffness, A0755 RAP with finer gradation was selected. The two remaining RAP sources (A0658 and A0778) in the fine group were also selected to cover the range of binder stiffness. It should be noted that the two mix designs for A0741 and A0658 RAP sources, for which a range of DASR porosity was reported, were slightly modified during mix design to ensure good DASR porosity.

The circled data points in Figure 3-12 represent the eight RAP sources selected for further evaluation. These consist of two coarse, three intermediate, and three fine RAP sources. Moreover, the range of high-temperature continuous grade was broader as RAP aggregate fineness increased. It was hypothesized that finer and stiffer RAP may be more critical to cracking resistance of RAP mixtures. Therefore, the broader range of binder stiffness identified for finer RAP was advantageous for this study.

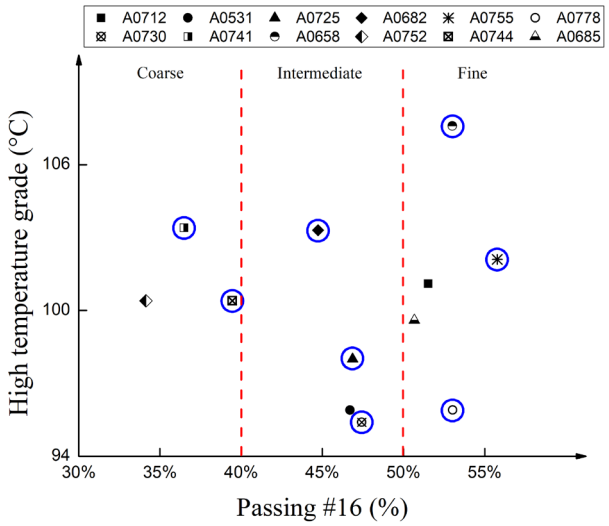

Figure 3-12. The eight selected RAP sources

3.5 Concluding Remarks

Twelve RAP stockpiles were identified in consultation with the FDOT research panel as representative RAP sources throughout Florida. Absolute viscosity, high-temperature continuous grade of RAP binder, and recovered RAP aggregate gradation were determined for all 12 RAP stockpiles. In addition, mixture gradation analysis was conducted for 12 PMA mix designs containing 20% RAP corresponding to each RAP stockpile using the DASR-IC system to assess the potential influence of gradation deficiency on performance. As a result, eight out of the 12 RAP stockpiles were selected for further evaluation. The selected RAP stockpiles covered a broad range and distribution of two important RAP characteristics: RAP binder stiffness represented by high-temperature performance grade and RAP fineness represented by percent passing No. 16 sieve size (1.18 mm) based on the RAP white curve gradation. No. 16 sieve size (1.18 mm) is employed by the DASR-IC system to separate fine aggregates from the coarser ones.

CHAPTER 4

DEVELOPMENT OF EXPERIMENTAL PLAN

4.1 Introduction

This study was conducted to achieve three primary objectives: (i) determine whether the 20% maximum usage of RAP with PMA mixture could be increased without adversely affecting cracking performance; (ii) determine whether additional RAP characterization is needed to implement the increase, and (iii) determine whether 20% RAP can be used with HP mixture without significant loss in premium cracking performance associated with HP binder. A complete laboratory experimental plan was developed for the purposes of this study.

Figure 4-1 shows the overall experimental plan for this study. RAP mixtures were designed using the eight RAP sources at four RAP contents (0%, 20%, 30%, and 40%). The interstitial component direct tension (ICDT) test was conducted on all RAP mixture combinations. The ICDT test provides interstitial component fracture energy (FE_{IC}) from which a preliminary maximum allowable RAP content ($\%RAP_{max}$) in PMA mixture was determined for individual RAP sources. Using $\%RAP_{max}$ of the eight RAP sources, a preliminary guideline for selection of $\%RAP_{max}$ in PMA mixtures was recommended based on RAP fineness and RAP binder stiffness. Furthermore, FE_{IC} was used to determine whether HP binder can maintain premium cracking resistance of mix designs with 20% RAP. Finally, Superpave indirect tension (IDT) tests were conducted on selected RAP mixtures to evaluate a preliminary guideline for $\%RAP_{max}$ in PMA mixtures as well as to evaluate the effect of 20% RAP on HP mixture cracking resistance at the mixture level.

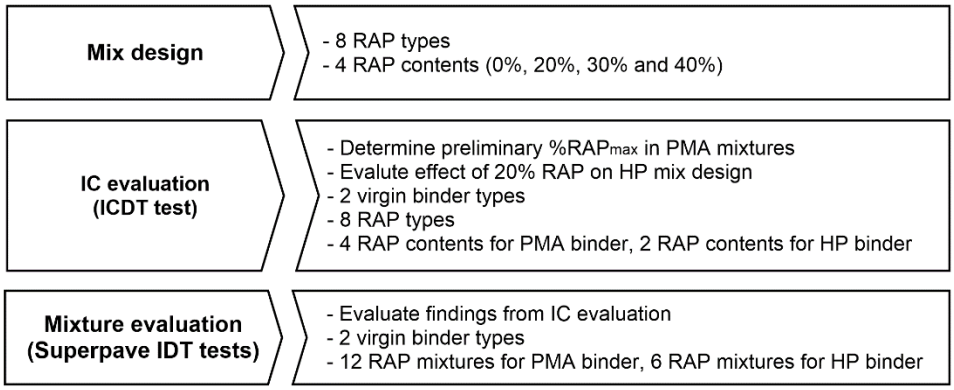

Figure 4-1. Overall experimental plan

4.2 Materials

The eight RAP sources selected in CHAPTER 3 are listed in Table 4-1. Existing mix designs (PMA mixture containing 20% RAP) for each RAP source were provided by FDOT. A list of virgin aggregate associated with each mix design is presented in Table 4-2. Two virgin binder types, PG 76-22 PMA binder and HP binder selected by FDOT, were used to evaluate the effect of virgin binder properties on RAP content.

Table 4-1. Eight RAP sources

RAP material		Location	Contractor
Plant No.	**Name**		
A0741	1-13	Eaton Park, FL	The Lane Construction Corporation
A0744	1-16	Gainesville, FL	V.E. Whitehurst & Sons, Inc.
A0682	1-16	Debary, FL	Ranger Construction Industries, Inc.
A0725	1-14	Panama City, FL	C.W. Roberts Contracting, Inc.
A0730	1-16	Havana, FL	Peavy & Construction Company, Inc.
A0658	1-15	Delray Beach, FL	Hardrives, Inc.
A0755	1-14	Naples, FL	Preferred Materials, Inc.
A0778	1-17	Okeechobee, FL	Lynch Paving, Inc.

Table 4-2. Virgin aggregate for each RAP mix design

RAP ID	Mine	FDOT code	Product name
A0741	GA 383	C43	#7 stone
	GA 383	C51	#89 stone
	GA 383	F21	Screenings
	-	334-LS	Davenport sand
A0744	GA 553	C47	#78 stone
	GA 553	C53	#89 stone
	GA 553	F22	W-10 screenings
	-	334-LS	Archer sand
A0682	GA 383	C43	#7 stone
	NS 315	C54	#89 stone
	GA 383	F21	Screenings
	-	334-LS	Tarmac sand
A0725	GA 178	C52	#89 stone
	GA 178	F21	W-12 screenings
	GA 178	F23	M-10 screenings
	-	334-LS	Panama City sand
A0730	GA 553	C53	#89 stone
	GA 553	F22	W-10 screenings
	-	334-LS	Hwy 267
A0658	93406	C44	S1A stone
	93406	C51	S1B stone
	93406	F20	Screenings
A0755	03616	C52	S1B stone
	03616	F20	W-10 screenings
	03677	334-MS	Asphalt sand
A0778	NS 315	C44	#7 stone
	NS 315	C54	#89 stone
	NS 315	F22	Screenings
	-	334-LS	Sand

4.3 Mix Design

Figure 4-2 shows a mix design flow chart for all RAP mixtures including eight RAP types and four RAP contents (0%, 20%, 30%, and 40%). Table 4-3 presents mix type, design traffic level and design number of gyrations (N_{design}) of the eight reference mixtures (20% RAP).

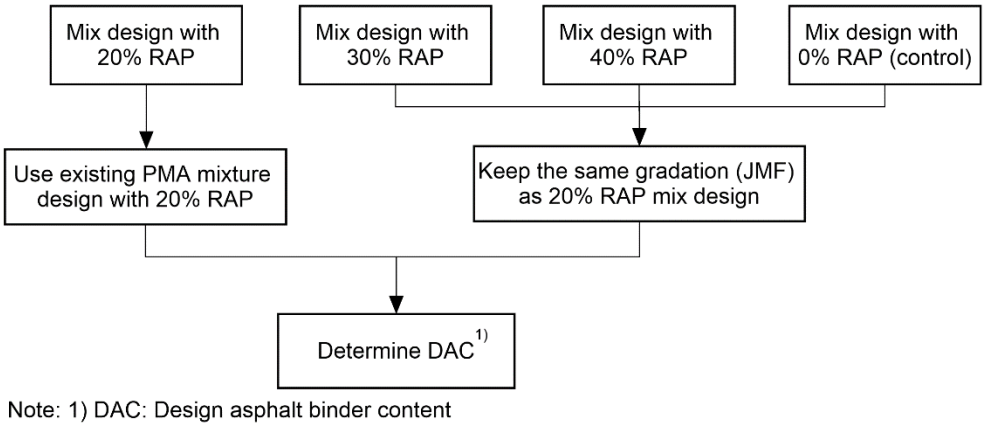

Figure 4-2. Flow chart of RAP mix design

Table 4-3. Reference PMA mixtures with 20% RAP

RAP type	Mix type	Traffic level(1)	Use of mix	PG binder	N_{design}
A0741	FC-12.5 Recycle	C	Friction course	PG 76-22 (PMA)	75
A0725	FC-9.5 Recycle	C	Friction course	PG 76-22 (PMA)	75
A0730	FC-9.5 Recycle	C	Friction course	PG 76-22 (PMA)	75
A0658	SP-12.5 Recycle	D	Structural	PG 76-22 (PMA)	100
A0744	SP-12.5 Recycle	D	Structural	PG 76-22 (PMA)	100
A0682	SP-12.5 Recycle	C	Structural	PG 76-22 (PMA)	75
A0778	SP-12.5 Recycle	C	Structural	PG 76-22 (PMA)	75
A0755	SP-9.5 Recycle	C	Structural	PG 76-22 (PMA)	75

Note: (1) Traffic level C: 3 to 10 million ESAL's (Equivalent single axle load) and D: 10 to 30 million ESAL's

For 30% and 40% RAP mixtures and control mixtures (0% RAP), virgin aggregate percentages were adjusted to maintain the gradation of the reference mixtures (20% RAP). Figure 4-3 shows one example (A0755) of blended aggregate gradations for four RAP contents. Complete results for all RAP sources are presented in APPENDIX F. Higher RAP mixtures (30% and 40%) and control mixtures for all eight RAP sources had almost identical blended aggregate gradation to the 20% RAP mixtures.

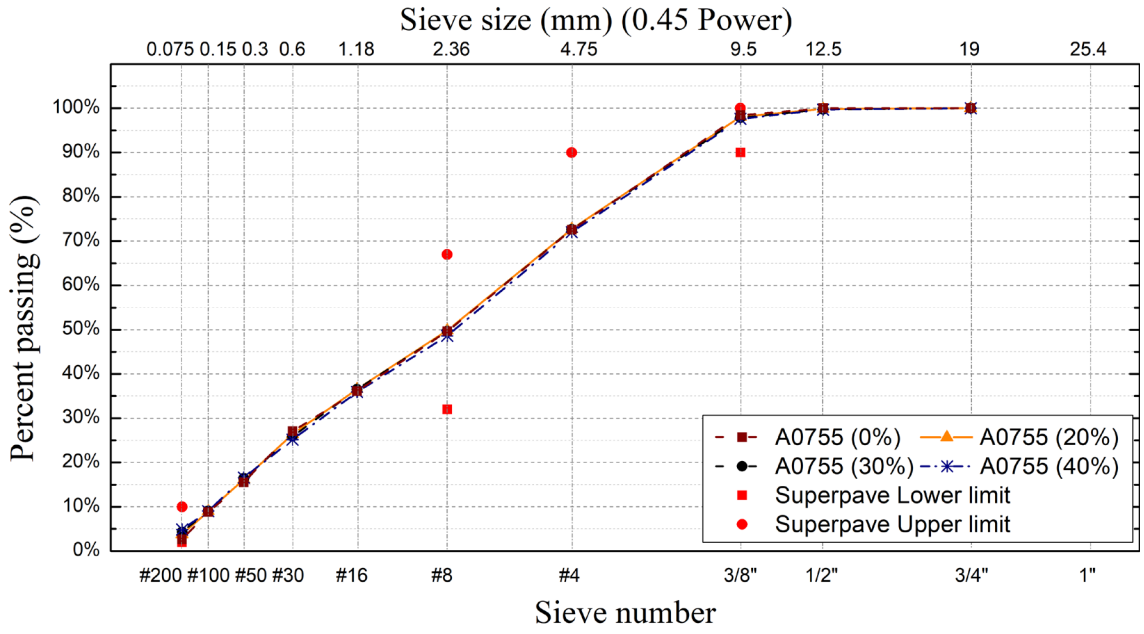

Figure 4-3. Blended aggregate gradations (JMF) of A0755 RAP mix design

The design asphalt binder content (DAC) for each RAP mix design was determined at 4% air voids at N_{design} following the Superpave mix design procedure (Asphalt Institute 2001). For all mixtures, PG 76-22 PMA binder was used for mix design and the same DAC was adopted for mixes with HP binder. Table 4-4 presents mix design results including Superpave volumetric properties, binder replacement ratio, and dominant aggregate size range (DASR) porosity for all 32 RAP mixtures. Almost all RAP mixtures satisfied the minimum voids in mineral aggregate (VMA) requirement (15% for 9.5 mm NMAS and 14% for 12.5 mm NMAS) except for two RAP mixtures (A0744-0% and A0778-40%) which had slightly lower VMA (13.8%). Most RAP mixtures met the voids filled with asphalt (VFA) requirement (65% to 75%), while eight out of 32 RAP mixtures exhibited slightly high VFA of 76% to 77%, which was considered to be negligible. DASR porosity values for most RAP mixtures were within the recommended range except for three mixtures associated with one RAP type (A0658). These mixtures had slightly high DASR porosity, which was considered to be negligible.

Table 4-4. Mix design results (Superpave volumetric properties, binder replacement ratio, and DASR porosity)

RAP type	%RAP	P_b[(1)]	G_{mm}[(2)]	VMA[(3)]	VFA[(4)]	BRR[(5)]	η_{DASR}[(6)] (38.0% to 52.0%)[(7)]
A0741	0%	5.4%	2.485	16.6%	76%	N/A	49.2% to 56%
	20%	5.1%	2.475	16.5%	76%	18.1%	49.0%
	30%	5.0%	2.473	16.0%	75%	27.8%	48.4%
	40%	4.9%	2.471	15.5%	75%	37.8%	48.0%
A0744	0%	4.7%	2.580	13.8%	71%	N/A	46.4% to 42.3%
	20%	4.9%	2.560	14.4%	72%	22.7%	47.3%
	30%	5.0%	2.551	14.6%	73%	33.4%	47.1% to 43.0%
	40%	4.9%	2.540	14.9%	73%	45.5%	47.6% to 46.5%
A0682	0%	5.9%	2.456	17.8%	77%	N/A	42.1% to 47.1%
	20%	5.2%	2.468	16.5%	76%	18.9%	46.0% to 42.2%
	30%	5.2%	2.468	16.4%	76%	28.3%	45.6% to 41.8%
	40%	5.1%	2.469	16.3%	75%	38.5%	46.0% to 42.1%
A0725	0%	5.8%	2.503	16.1%	75%	N/A	48.6%
	20%	5.6%	2.500	16.2%	75%	16.5%	48.6%
	30%	5.7%	2.498	16.3%	75%	24.3%	49.3%
	40%	5.7%	2.501	16.3%	76%	32.4%	48.6%
A0730	0%	6.3%	2.502	17.4%	77%	N/A	45.4%
	20%	6.0%	2.507	17.0%	76%	20.6%	45.7%
	30%	5.9%	2.513	16.6%	76%	31.5%	45.9%
	40%	5.8%	2.516	16.5%	75%	42.7%	46.2%
A0658	0%	7.8%	2.326	15.7%	75%	N/A	51.0% to 56.9%
	20%	7.7%	2.331	16.2%	75%	12.3%	52.9%
	30%	7.5%	2.343	15.8%	75%	18.4%	52.7%
	40%	7.1%	2.356	15.3%	74%	24.5%	52.7%
A0755	0%	7.7%	2.324	15.3%	74%	N/A	46.5%
	20%	7.5%	2.332	16.1%	75%	14.1%	47.5%
	30%	7.1%	2.345	16.0%	74%	22.4%	47.5%
	40%	6.8%	2.350	16.0%	75%	31.2%	47.5%
A0778	0%	5.8%	2.455	14.8%	73%	N/A	51.2%
	20%	5.4%	2.452	14.3%	72%	20.5%	51.3%
	30%	5.3%	2.456	14.1%	71%	31.3%	50.9%
	40%	5.3%	2.460	13.8%	71%	41.7%	50.3%

Note: (1) P_b: Design asphalt binder content (%)
(2) G_{mm}: Theoretical maximum specific gravity
(3) VMA: Voids in mineral aggregate (%)
(4) VFA: Voids filled with asphalt (%)
(5) BRR: Binder replacement ratio (%)
(6) η_{DASR}: DASR porosity (%)
(7) DASR porosity criterion

4.4 Interstitial Component Direct Tension (ICDT) Test

The interstitial component direct tension (ICDT) test was used as a surrogate for a mixture test to evaluate all RAP mixture combinations because it requires less effort in specimen preparation and testing than a mixture test (Yan et al. 2018b). According to the dominant aggregate size range-interstitial component (DASR-IC) theory, the interstitial component (IC) is the combination of fine aggregates, effective binder, and air voids (Kim et al. 2006). IC fills DASR voids and binds coarse aggregate. It has been reported that IC properties are related to mixture cracking resistance (Chun et al. 2012; Kim et al. 2009). Recently, Yan et al. (2017b) found that IC fracture energy values obtained from the ICDT test correlated well with fracture energy of corresponding mixtures from Superpave IDT tests. This section describes details of the ICDT test, including specimen preparation, testing procedure and data analysis.

4.4.1 ICDT test specimen preparation

Calculation of ICDT test specimen weight

According to DASR-IC theory, the IC aggregate was defined by aggregates finer than the DASR. All eight selected RAP mixtures had the same IC range (1.18 mm to -200, as shown in Figure 4-4).

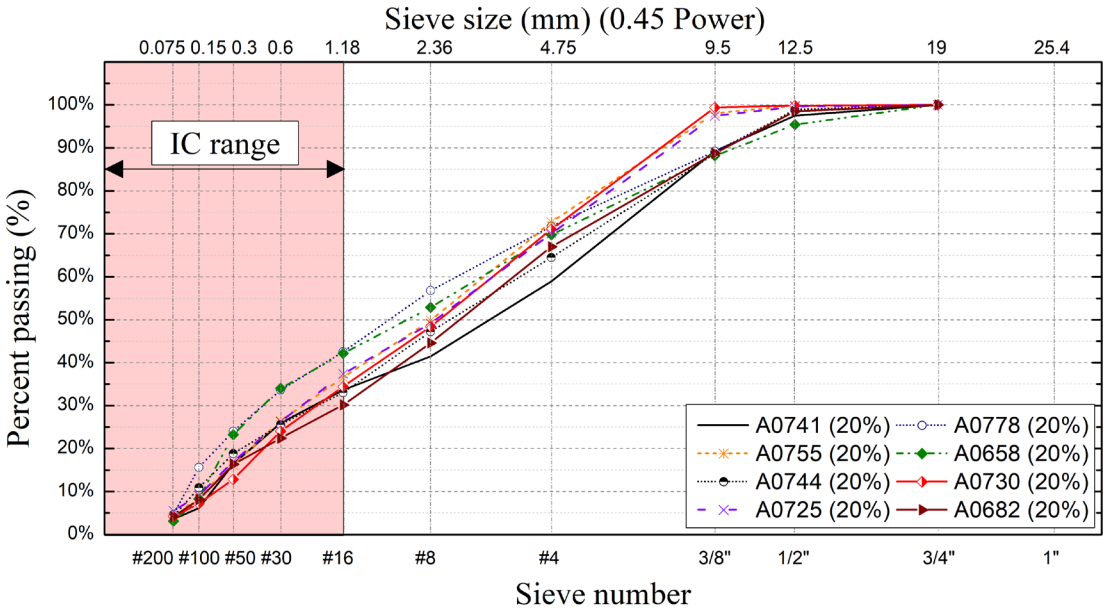

Figure 4-4. IC ranges of all eight reference mixtures with 20% RAP

For each mix design, the ratio of effective binder weight to IC aggregate weight in the Superpave pill is the same as the one in the ICDT specimen. It is important to note that the aggregates within the IC range (finer than 1.18 mm) have a much smaller pore area as compared to the larger aggregates in the mixture gradation. Therefore, the absorbed binder in the IC portion was assumed negligible. As a result, the effective binder weight was approximated by the total binder weight in the ICDT specimen as expressed in the following equation:

$$Ratio = \frac{W_{bIC}}{W_{sIC}} = \frac{W_{be-m}}{W_{IC-m}} \qquad Eq.\,4.1$$

where,

W_{bIC} = Total binder weight in ICDT test specimen (g);

W_{sIC} = IC aggregate weight in ICDT test specimen (g);

W_{be-m} = Effective binder weight in Superpave pill including 4,500-g batch weight (g);

W_{IC-m} = IC aggregate weight in Superpave pill including 4,500-g batch weight (g).

The volume of an ICDT test specimen (31.96 cm^3) is related to the specific gravity and weight of each material in an ICDT test specimen as follows:

$$V_{IC} = \frac{W_{sIC}}{G_{sb}} + \frac{W_{bIC}}{G_b} \qquad Eq.\,4.2$$

where,

V_{IC} = Volume of ICDT test specimen (31.96 cm^3);

G_{sb} = Bulk specific gravity of aggregate;

G_b = Bulk specific gravity of asphalt binder.

Solving Equation 4.1 and 4.2, the weight of aggregate and binder in ICDT test specimen can be calculated by the following equations:

$$W_{bIC} = \frac{V_{IC} \times G_{sb} \times G_b \times Ratio}{G_b + (G_{sb} \times Ratio)} \qquad Eq.\,4.3$$

$$W_{sIC} = \frac{V_{IC} \times G_{sb} \times G_b}{G_b + (G_{sb} \times Ratio)} \qquad Eq.\,4.4$$

Mixing and compaction

IC aggregates (RAP and virgin) were batched according to the IC aggregate gradation. Batched IC aggregates and virgin binder were mixed at mixing temperature (325°F for PMA binder and 335°F for HP binder). Short-term oven aging (STOA) was performed by subjecting the loose mixtures to two hours of oven aging at the mixing temperature. The loose mixtures were stirred after one hour to ensure uniform aging throughout the aging process.

The STOA loose mixtures were compacted into a stainless-steel mold (Figure 4-5a) at the mixing temperature. A needle gun with a steel foot (Figure 4-5b) was used to compact the ICDT test specimen. The needle gun is a compressed air powered tool operated in a vibratory mode. In a previous internal study, it was determined that a duration of two minutes for compaction resulted in uniform thickness of 0.5 in (12.7 mm) and approximately 0% air void content, which is the target for ICDT test specimens. Yan et al. (2018b) showed that the middle section of ICDT test specimens where fracture occurs had an air void content of 0.3% (near zero percent). It was further confirmed by X-ray computed tomography that no air voids were observed in the middle section, while some air voids appeared to concentrate near the two heads.

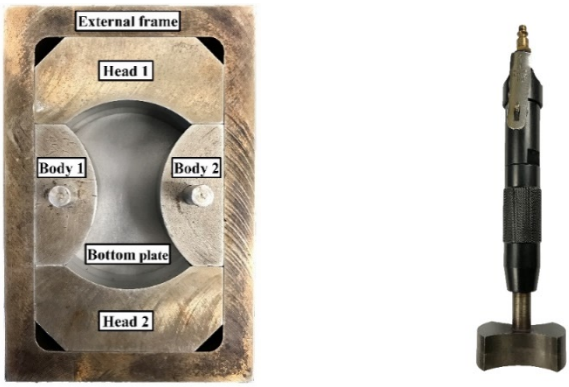

(a) (b)

Figure 4-5. Equipment for ICDT specimen compaction: (a) mold and (b) compactor

Loading head attachment

Figure 4-6a shows a compacted ICDT test specimen. Loading heads were glued to the top and bottom of the specimen using epoxy (LOCTITE E-20NS), as shown in Figure 4-6b. Asphalt film at the top and bottom surfaces of the specimen was removed using sandpaper to increase the effectiveness of bonding between loading heads and specimen. The specimen was kept at room

temperature for at least 12 hours to ensure that epoxy reaches full strength. The specimen was then placed in an environmental chamber at 50°F (10°C) for three hours before performing the ICDT test.

(a) (b)

Figure 4-6. ICDT specimen: (a) compacted ICDT specimen and (b) ICDT specimen with loading head

4.4.2 ICDT test procedure

The ICDT test was performed by applying a monotonic load at a displacement rate of 2 in/min (50.8 mm/min) using a material testing system (MTS, see Figure 4-7) until the specimen fails. For each mixture type, three replicates were tested at 50°F (10°C). Testing time, force and displacement data were collected.

Figure 4-7. Material testing system (MTS)

FE_{IC} can be determined as the area under the stress-strain curve. Stress can be calculated by the following equation:

$$\sigma = \frac{F}{A} \qquad Eq.4.5$$

where,

σ = Stress;

F = Force recorded during the test;

A = Cross-sectional area in the middle of specimen (322 mm^2).

Average tensile strain on the failure plane (middle of the specimen) can be calculated from displacement using the following relationship developed from finite element analysis (Yan et al. 2017b):

$$\varepsilon = 0.0199 \times \delta \qquad Eq.4.6$$

where,

ε = Average strain on failure plane;

δ = Displacement (mm).

4.5 Superpave Indirect Tensile (IDT) Tests

Superpave IDT tests were conducted on selected RAP mixtures to validate results obtained from the ICDT tests. This section describes details of Superpave IDT tests, including test specimen preparation, testing procedure and data analysis.

4.5.1 Superpave IDT test specimen preparation

Virgin and RAP aggregates were mixed with virgin asphalt binder at the mixing temperature (325°F for PMA binder and 335°F for HP binder) until the aggregates are completely coated by the binder. The STOA loose mixture was compacted using the Superpave gyratory compactor (SGC) shown in Figure 4-8 with a compaction stress of 600 kPa and a gyratory angle of 1.25° at the mixing temperature. The compacted sample (gyratory pill) was allowed to cool

down at least 12 hours, after which it was sliced using a masonry saw to obtain 38.1 mm (1.5 in) thick test specimens (two per gyratory pill). A sliced specimen was dried in a dehumidifier at room temperature for 48 hours. Figure 4-9 shows the complete test specimen with gauge points attached on both faces. The target air void content for the test specimen was 7% (± 0.5%) to simulate the initial air voids typically achieved in the field.

Figure 4-8. Superpave gyratory compactor

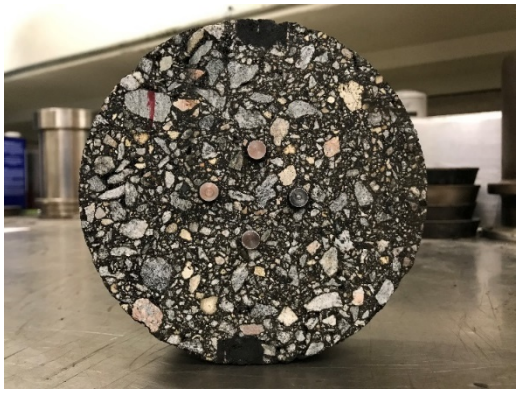

Figure 4-9. Superpave IDT test specimen

4.5.2 Superpave IDT test description

One set of Superpave IDT tests consists of resilient modulus (M_R), creep compliance and strength tests. The tests were conducted at 50°F (10°C) to measure the properties including resilient modulus, creep compliance, tensile strength (S_t), failure strain and fracture energy for determining the cracking performance of RAP mixtures.

Resilient modulus test

The resilient modulus (M_R) is defined as the ratio of the applied stress to recoverable strain when repeated loads are applied. The resilient modulus test was a nondestructive test conducted in a load-controlled mode to determine the resilient modulus (M_R) of asphalt mixtures. A repeated haversine waveform load was applied to the specimen for 0.1 seconds followed by a rest period of 0.9 seconds. The load was selected to keep the horizontal resilient deformations between 100 to 180 micro-inches to stay within the linear viscoelastic range.

Roque and Buttlar (1992) developed the following equations to calculate the resilient modulus and Poisson's ratio based on three-dimensional finite element analysis. These equations were incorporated in the Superpave Indirect Tension Test at Low Temperatures (ITLT) computer program, which was developed by Roque et al. (1997).

$$M_R = \frac{P \times GL}{\Delta H \times t \times D \times C_{cmpl}} \qquad Eq.4.7$$

$$\nu = -0.1 + 1.480 \times \left(\frac{X}{Y}\right)^2 - 0.778 \times \left(\frac{t}{D}\right)^2 \times \left(\frac{X}{Y}\right)^2 \qquad Eq.4.8$$

where,

M_R = resilient modulus; P = maximum load; GL = gauge length;

ΔH = horizontal deformation; t = thickness; D = diameter; $C_{cmpl} = 0.6345 \times (X/Y)^{-1} - 0.332$;

ν = Poisson's ratio; (X/Y) = ratio of horizontal to vertical deformation.

Creep test

Creep compliance is a function of time-dependent strain over stress. The creep compliance curve was originally developed to predict thermally induced stress in asphalt pavement. It can also be used to evaluate the rate of damage accumulation of an asphalt mixture (Roque et al. 1997). Mixture properties including D_0, D_1 and m-value can be obtained from the creep compliance curve shown in Figure 4-10. Using these properties, creep compliance rate can be calculated by following equation:

$$Creep\ compliance\ rate = \frac{dD(t)}{dt} = \mathrm{m} \times D_1 \times t^{m-1} \qquad Eq.\ 4.9$$

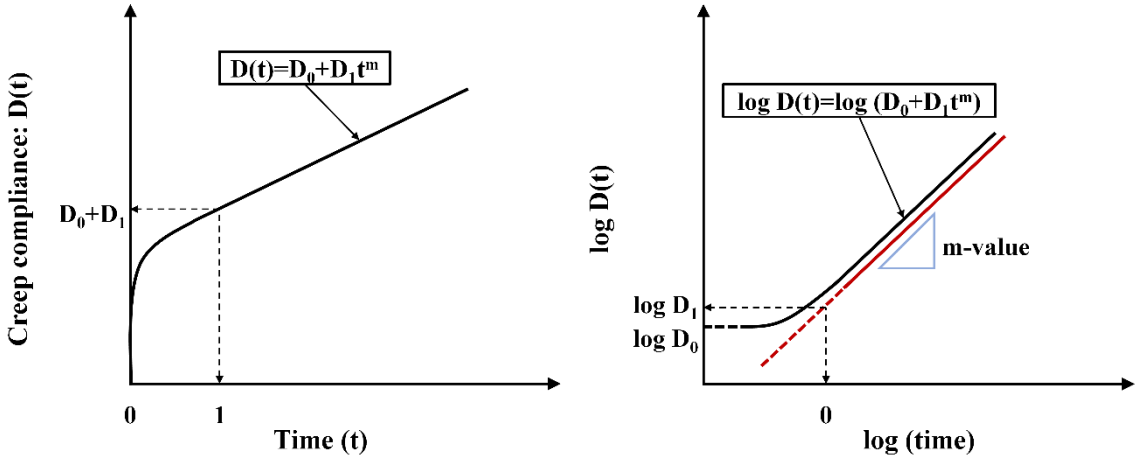

Figure 4-10. Creep compliance power model curve

The creep test was conducted in a load-controlled mode by applying a static load in the form of a step function to the specimen and then holding it for 1,000 seconds. The magnitude of the load was selected to maintain the accumulated horizontal deformations in the linear viscoelastic range, which is below the total horizontal deformation of 750 micro-inches. Even though the horizontal deformation range at 100 seconds can vary depending upon specimen type, a horizontal deformation of 100 to 130 micro-inches at 100 seconds was generally considered to be acceptable.

The ITLT computer program was used to determine creep properties using the load and deformation data. Creep compliance and Poisson's ratio are calculated by the following equations:

$$D(t) = \frac{\Delta H \times t \times D \times C_{cmpl}}{P \times GL} \qquad Eq.\,4.10$$

$$\nu = -0.1 + 1.480 \times \left(\frac{X}{Y}\right)^2 - 0.778 \times \left(\frac{t}{D}\right)^2 \times \left(\frac{X}{Y}\right)^2 \qquad Eq.\,4.11$$

where,

D(t) = creep compliance at time t (1/psi);

Others are the same as described above.

Tensile strength test

Failure limits including tensile strength, failure strain and fracture energy were determined from the strength test. These properties, along with those determined from the resilient modulus and creep compliance tests, can be used to estimate the cracking resistance of asphalt mixtures. The strength test was performed in a displacement controlled mode by applying a constant displacement rate of 2 in/min (50.8 mm/min) until the specimen fails. The maximum tensile strength was calculated by the following equation:

$$S_t = \frac{2 \times P \times C_{SX}}{\pi \times t \times D} \qquad Eq.\,4.12$$

where,

S_t = maximum indirect tensile strength; P = Failure load at first crack;

C_{SX} = Horizontal stress correction factor:

$0.948 - 0.01114 \times (t/D) - 0.2693 \times \nu + 1.436 \times (t/D) \times \nu$;

t = thickness; D = diameter; ν = Poisson's ratio.

Fracture energy (FE) and dissipated creep strain energy (DCSE) can be determined from the strength test and the resilient modulus test. Fracture energy, which is the total energy necessary to induce fracture, can be calculated as the area underneath the stress-strain curve until failure. Dissipated creep strain energy is the absorbed energy that damages the specimen, and the dissipated creep strain energy to failure ($DCSE_f$) is the absorbed energy to fracture. As shown in

Figure 4-11, elastic energy (EE), FE and $DCSE_f$ can be determined as described below. The ITLT program also computes FE automatically.

$$M_R = \frac{S_t}{\varepsilon_f - \varepsilon_0} \rightarrow \varepsilon_0 = \frac{M_R \cdot \varepsilon_f - S_t}{M_R} \qquad Eq.\,4.13$$

$$Elastic\ energy\ (EE) = \frac{1}{2} \cdot S_t \cdot (\varepsilon_f - \varepsilon_0) \qquad Eq.\,4.14$$

$$Fracture\ energy\ (FE) = \int_0^{\varepsilon_f} S(\varepsilon) d\varepsilon \qquad Eq.\,4.15$$

$$Dissipated\ creep\ strain\ energy\ to\ failure\ (DCSE_f) = FE - EE \qquad Eq.\,4.16$$

where,

S_t = tensile strength; ε_f = failure strain.

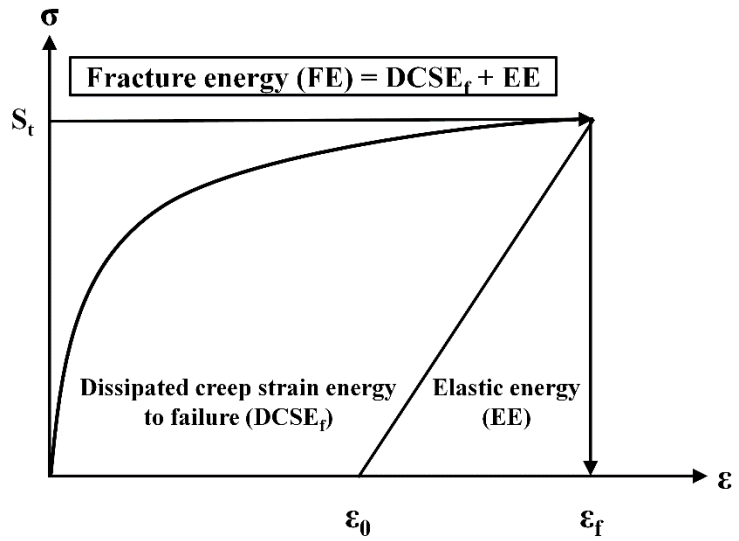

Figure 4-11. Determination of fracture energy and dissipated creep strain energy to failure

4.6 Concluding Remarks

A complete experimental plan was developed to determine whether the maximum usage of RAP in PMA and HP mixtures could be increased without adversely affecting cracking performance and whether additional RAP characterization is needed to implement the increase. Eight reference designs of PMA mixtures containing 20% RAP provided by FDOT were used and modified to include PMA mixtures containing 0%, 30% and 40% RAP. The ICDT test, which requires less efforts in specimen preparation and testing than mixture testing, was selected as a surrogate for mixture tests. Superpave IDT tests were selected to evaluate findings obtained from IC evaluation

CHAPTER 5
ICDT TEST RESULTS AND ANALYSIS

5.1 Introduction

As described in CHAPTER 4, the interstitial component direct tension (ICDT) test was employed to evaluate all RAP mix designs (and control mixtures with 0% RAP) because it requires less effort in specimen preparation and testing than a mixture test. According to the DASR-IC theory, the interstitial component (IC) is the combination of fine aggregates, effective binder, and air voids (Kim et al. 2006). IC fills DASR voids and binds coarse aggregate. It has been reported that IC properties are related to mixture cracking resistance (Chun et al. 2012; Kim et al. 2009). Recently, Yan et al. (2017b) found that IC fracture energy values obtained from ICDT tests correlated well with fracture energy of corresponding mixtures from Superpave IDT tests. Figure 5-1 shows experimental factors considered for the ICDT test, including eight RAP sources, two virgin binder types (PG 76-22 PMA and high-polymer), four RAP contents (0%, 20%, 30%, and 40%) with PMA binder, and two RAP contents (0% and 20%) with high-polymer (HP) binder.

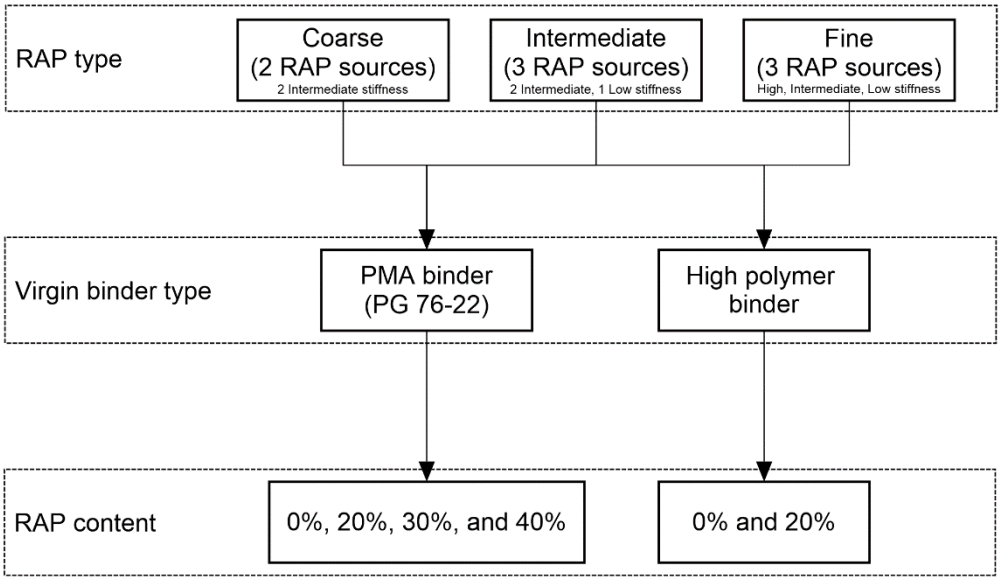

Figure 5-1. Experimental factors for ICDT test

Figure 5-2 presents RAP distribution zones defined based on RAP binder stiffness (high-temperature continuous grade) and RAP fineness (% passing #16 sieve) along with eight RAP sources selected for this study. Details regarding selection of RAP materials across the State of Florida are described in CHAPTER 3. As shown in Figure 5-2, coarse, intermediate and fine levels were defined for RAP fineness using a 10% interval within the range identified in this study. High, intermediate and low stiff ranges were defined for RAP binder stiffness following Superpave performance grading system (6°C interval). For convenience, a code was assigned for each RAP source (Figure 5-2), which were used throughout the rest of this study. Both coarse RAP sources (C-I-#1 and C-I-#2) are in the intermediate stiff range. At the intermediate fineness level, two RAP sources (I-L-#1 and I-L-#2) are in the low stiff range, and one (I-I) is in the intermediate stiff range. Three fine RAP sources (F-H, F-I and F-L) covered a broader range of stiffness, which are distributed evenly in the high, intermediate and low stiff ranges, respectively.

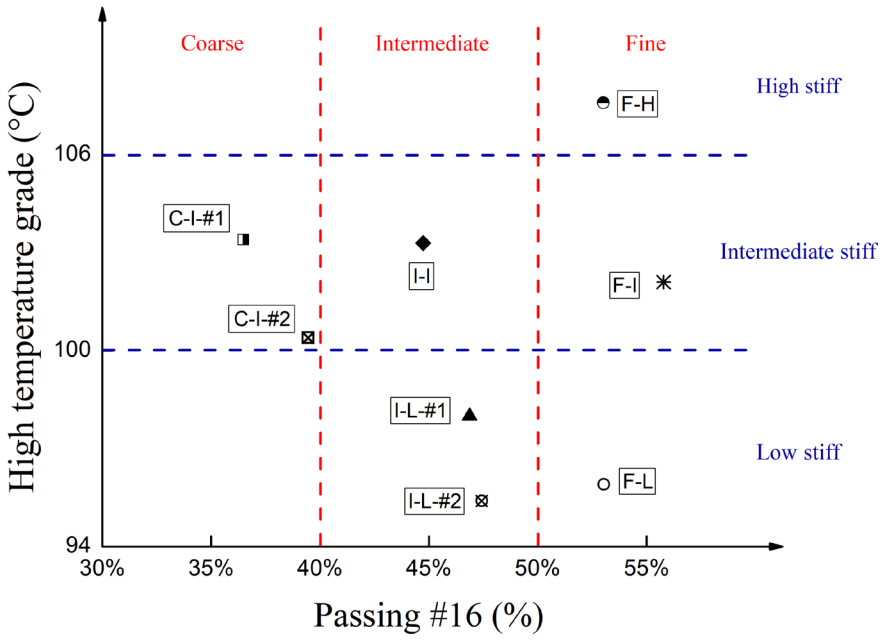

Figure 5-2. RAP distribution zones along with code assigned for each RAP source

5.2 Fracture Energy of IC Mixes with PG 76-22 PMA Binder

IC fracture energy (FE_{IC}) was obtained from the ICDT test for IC mixes with PMA binder containing 0%, 20%, 30%, and 40% RAP for each RAP source. FE_{IC} was used to evaluate the effect of RAP characteristics on cracking resistance of IC mixes with PMA binder as well as to estimate preliminary maximum RAP content in PMA mixtures for each RAP source.

5.2.1 Effect of RAP characteristics on IC mixes with PMA binder

Figure 5-3 shows FE_{IC} generally decreases as %RAP increases, which is consistent with results from mixture tests reported elsewhere (Yan et al. 2017b). Since RAP material contains aged and brittle RAP binder, higher RAP content resulted in lower FE_{IC}. This trend indicates that FE_{IC} may be used as a criterion to estimate maximum RAP content at a specified FE_{IC} limit. Furthermore, Figure 5-3 shows that IC mixes with fine RAP (i.e., RAP fineness greater than 50%) exhibited clearly lower FE_{IC} compared to those with coarse and intermediate RAP. Even at 20% RAP content, all three IC mixes with fine RAP exhibited distinctively lower FE_{IC}. As conceptually illustrated in Figure 5-4, fine RAP appeared to result in a greater amount of RAP in IC portion than coarse and intermediate RAP at the same RAP content, leading to lower FE_{IC}.

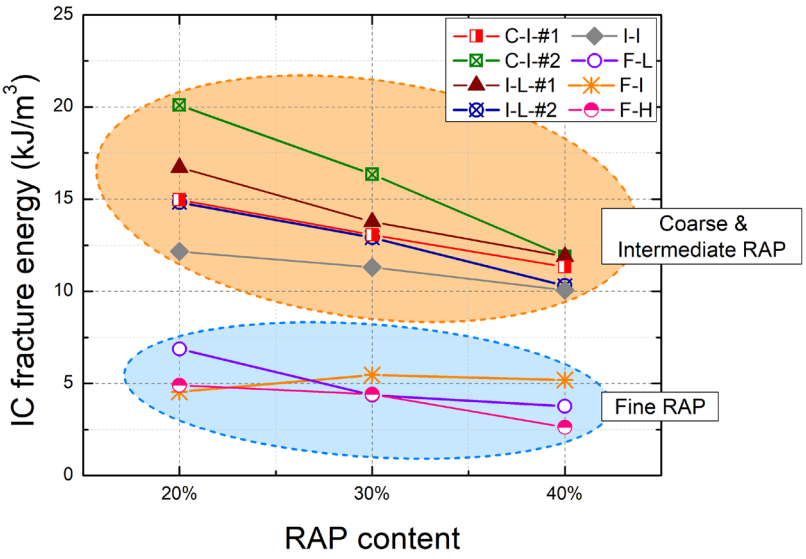

Figure 5-3. IC fracture energy results at a range of RAP contents (PMA binder)

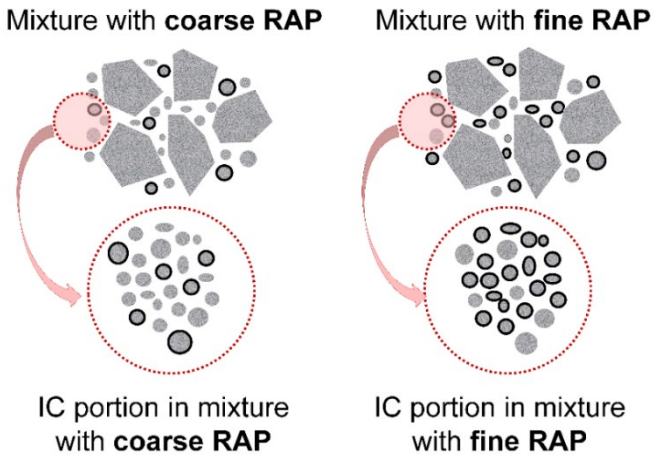

Figure 5-4. Schematic of RAP gradation effect on RAP distribution in IC mixes

Since the use of actual mix designs resulted in different gradations and design asphalt contents, RAP binder replacement ratio in IC (BRR_{IC}) may provide additional insight when comparing different IC mixes containing RAP. BRR_{IC} can be calculated as follows:

$$BRR_{IC} = \frac{RAP\ binder\ weight\ in\ IC}{Total\ binder\ weight\ in\ IC} \qquad Eq.5.1$$

Figure 5-5 shows all mix designs had different BRR_{IC} for the same RAP content. Mix designs with fine RAP appeared to have marginal FE_{IC}, which is consistent with the trend observed based on %RAP. In addition, the effect of RAP binder stiffness was more evident when compared at the same BRR_{IC} than at the same RAP content. For the coarse group, C-I-#1 RAP mix, which had a higher stiffness (represented by a higher high-temperature grade), exhibited lower FE_{IC} compared to C-I-#2 RAP mix. The same trend can be observed from the intermediate group, i.e., stiffer RAP binder led to lower FE_{IC}. Only coarse and intermediate RAP mix designs were used for evaluating RAP binder stiffness effects since mix designs with fine RAP had marginal FE_{IC}.

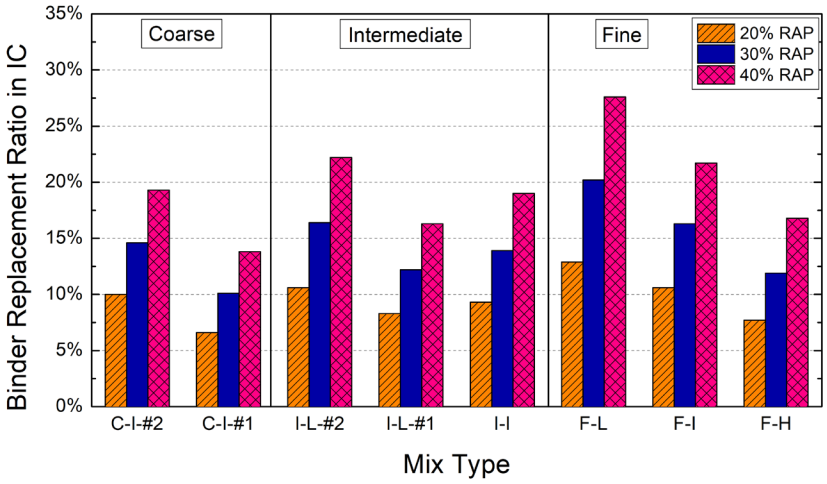

(a)

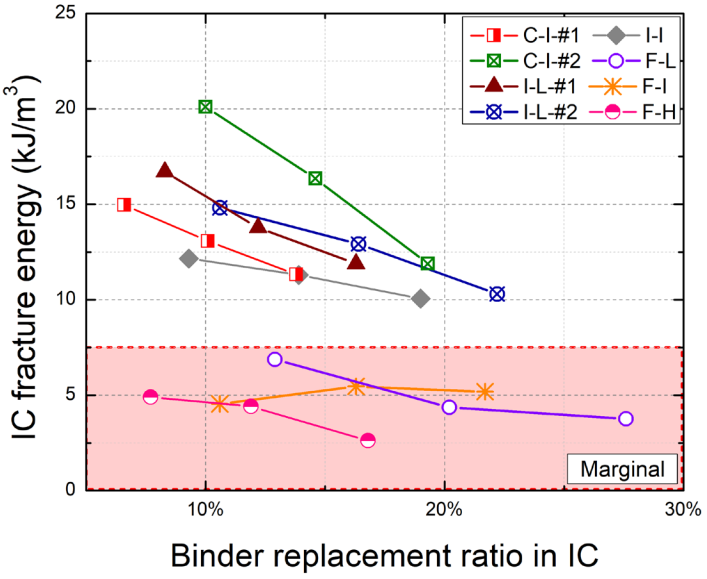

(b)

Figure 5-5. Binder replacement ratio in IC and IC fracture energy: (a) binder replacement ratio in IC for all mix types and (b) IC fracture energy results at a range of BRR_{IC} levels (PMA binder)

Furthermore, each RAP mix design with 20% RAP was adjusted to allow virgin aggregates only while keeping the JMF gradation unchanged, which resulted in eight control mix designs without RAP (i.e., 0% RAP). For each RAP source, FE_{IC} results were normalized with respect to the value obtained from the control mix design to evaluate the effect of RAP characteristics on reduction in FE_{IC} with increasing RAP content, so that the results would not be confounded by

different gradations and design asphalt contents associated with each RAP mix design. Figure 5-6 presents normalized FE_{IC} results for all eight RAP sources.

As shown in Figure 5-6, fine RAP sources generally resulted in greater reduction in FE_{IC} than coarse and intermediate RAP sources at all three RAP contents, which appeared to confirm the detrimental effects of fine RAP on cracking resistance at the IC mix level. Within three intermediate RAP sources, it was evident that stiffer RAP binder led to greater reduction in FE_{IC} at a similar RAP fineness level. I-I RAP with the highest RAP binder stiffness (103°C) showed the greatest FE_{IC} reduction, followed by I-L-#1 RAP (98°C) and I-L-#2 RAP (95°C). This observation confirmed that RAP binder stiffness is an important RAP characteristic affecting cracking resistance. Within coarse RAP sources, stiffer but coarser RAP (C-I-#1) led to greater reduction in FE_{IC} than softer but finer RAP (C-I-#2) at 20% and 30% RAP content. However, this trend was reversed between 30% and 40% RAP content, indicating that the negative effect of finer RAP became greater at 40% RAP content. It is important to note that C-I-#1 RAP showed the lowest reduction in FE_{IC} at 40% RAP content among all eight RAP sources, even though RAP binder stiffness was in the intermediate range. This indicated that coarsely graded RAP may be able to mitigate negative effects of stiff RAP binder. In other words, coarser RAP may allow a greater amount of stiff RAP in PMA mixture than finer ones, while maintaining adequate cracking resistance.

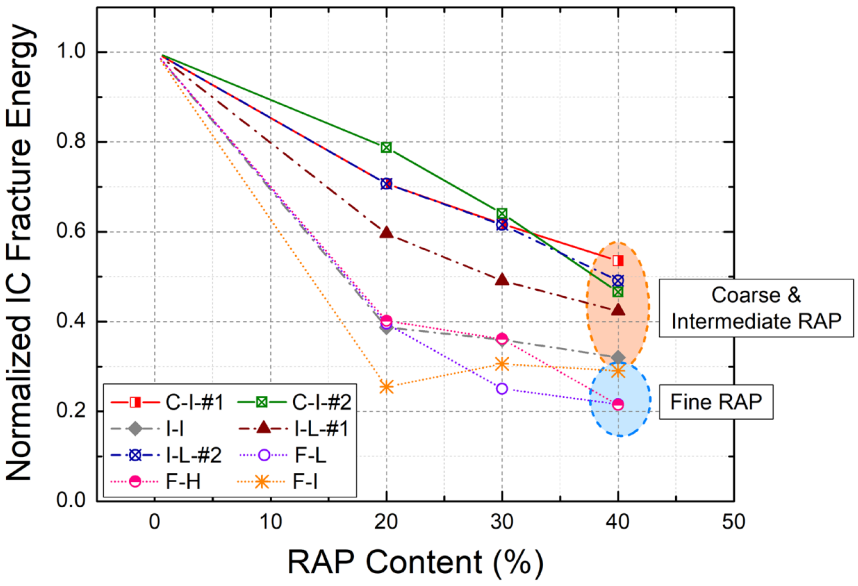

Figure 5-6. Normalized IC fracture energy results for PMA binder

5.2.2 Estimate preliminary maximum allowable RAP content in PMA mixture

Since mix designs with fine RAP appeared to have considerably lower FE_{IC}, only coarse and intermediate RAP sources were used to estimate preliminary maximum RAP content ($\%RAP_{max}$) in PMA mixtures. Figure 5-7 showed FE_{IC} decreased as %RAP increased. The effect of RAP type was clearly more evident at lower %RAP. It appeared FE_{IC} approached the lowest FE_{IC} (10 kJ/m^3) among all mix designs with coarse and intermediate RAP, over 40% RAP. This indicated that 40% RAP may be the upper limit for RAP usage in PMA mixture within the range of RAP sources tested in this study.

Maximum allowable RAP content can be estimated based on a preliminary FE_{IC} limit, as shown in Figure 5-7. The lowest FE_{IC} (12 kJ/m^3) among mix designs with 20% RAP sources was selected as the preliminary FE_{IC} limit, since 20% is the maximum RAP usage currently allowed by Florida Department of Transportation (FDOT). Figure 5-8 shows the resulting $\%RAP_{max}$ for each RAP source. All fine RAP sources remained at 20% due to marginal FE_{IC}. Within the coarse and intermediate stiff group (C-I), the stiffer but coarser RAP (C-I-#1) resulted in lower $\%RAP_{max}$ than C-I-#2 RAP (34.5% vs. 39.6%). RAP binder stiffness appeared to be a more dominant factor than RAP fineness for this group. Within the intermediate fineness and low stiff group (I-L), however, a stiffer RAP (I-L-#1) resulted in higher $\%RAP_{max}$ than I-L-#2 RAP (38.1% vs. 32.1%) at similar RAP fineness. Different binder replacement ratio (BRR), which resulted from different gradation and design asphalt content associated with these two RAP mix designs, confounded the results of $\%RAP_{max}$ for this group. The mix design with the stiffer RAP (I-L-#1) had a lower BRR than the one with I-L-#2 RAP at the maximum RAP content estimated for each RAP source (Figure 5-8). This implied BRR may be needed for better description of RAP binder stiffness effects on maximum RAP usage. However, it should be noted that %RAP is more practical for determination of RAP usage in PMA mixture, since BRR is unknown prior to the mix design stage.

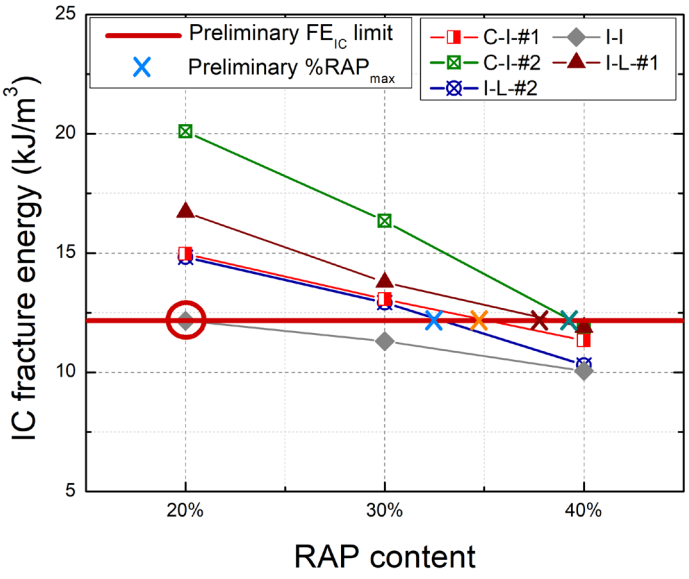

Figure 5-7. Determination of FE_{IC} limit and maximum RAP content for PMA mixture

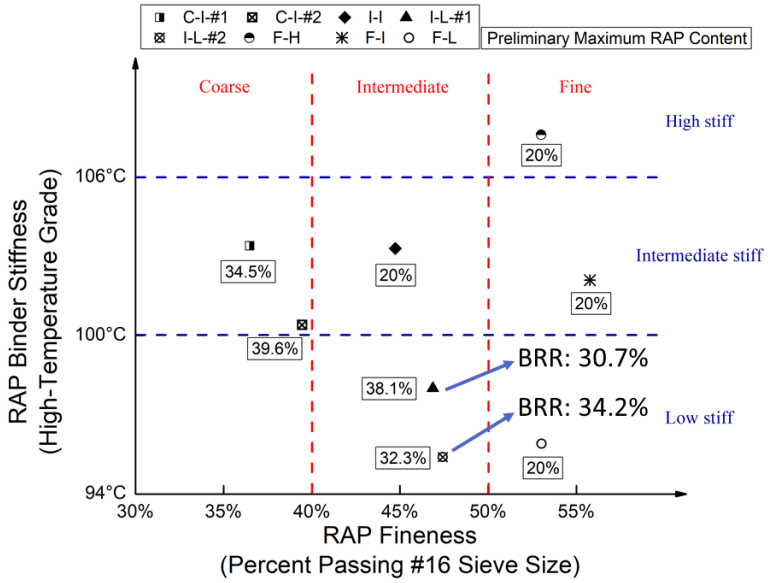

Figure 5-8. Estimated maximum allowable RAP content for PMA mixture

Compared to the intermediate fineness and intermediate stiff RAP (I-I), coarser (fineness no greater than 40%) or less stiff RAP (high-temperature grade no greater than 100°C) resulted in $\%RAP_{max}$ higher than 20% (Figure 5-8). Therefore, a preliminary guideline for selection of $\%RAP_{max}$ was recommended for each zone (defined based on RAP fineness and RAP binder stiffness), as shown in Figure 5-9. A maximum RAP content of 35% was recommended for Zone

C-I, which was obtained from the lower preliminary maximum RAP content of 34.5% determined for two RAP sources (C-I-#1 and C-I-#2) in the zone. Compared to Zone C-I, the maximum content was increased by 5% for Zone C-L (a maximum of 40%) due to decreased binder stiffness and decreased by 5% for Zone C-H (a maximum of 30%) due to increased binder stiffness at the same fineness level. Within the three intermediate fineness zones, a maximum RAP content of 30% was recommended for Zone I-L, which was taken from the lower preliminary maximum RAP content of 32.3% determined for two RAP sources (I-L-#1 and I-L-#2) in the zone and rounded it down to the nearest 5%. Maximum RAP contents remained at 20% for Zone I-I and Zone I-H based on preliminary maximum RAP content determined for RAP source I-I (20%). In addition, maximum RAP contents for RAP sources in three fine zones (F-H, F-I and F-L) remained at the current limit (20%) due to marginal FE_{IC} determined based on sampled RAP sources. Verification of the preliminary guidelines using mixture test results is included in CHAPTER 6.

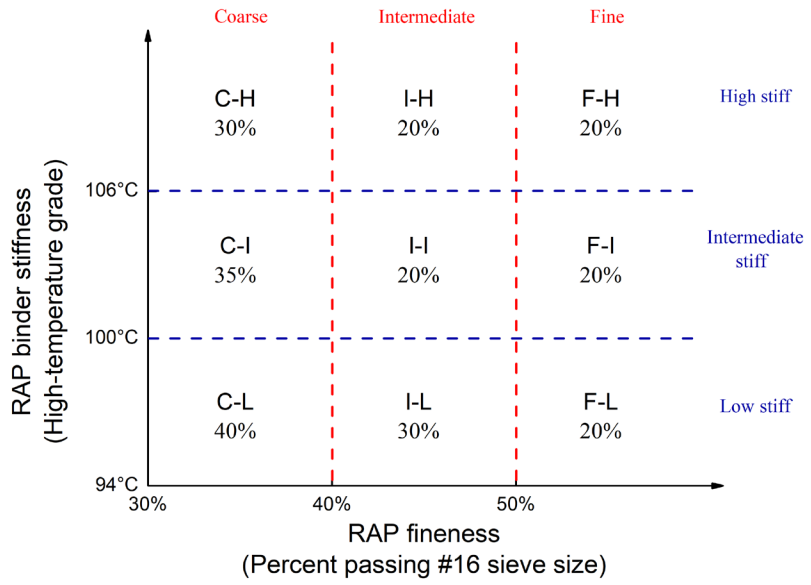

Figure 5-9. Preliminary guideline for maximum allowable RAP content in PMA mixture

5.3 Fracture Energy of IC Mixes with High Polymer (HP) Binder

IC fracture energy (FE_{IC}) was obtained from ICDT test for IC mixes with HP binder containing 0% and 20% RAP for each RAP source. FE_{IC} was used to evaluate effects of RAP characteristics on cracking resistance of IC mixes with HP binder as well as to determine whether HP binder can maintain premium cracking resistance of mix designs containing 20% RAP from various RAP sources.

5.3.1 Effect of RAP characteristics on IC mixes with HP binder

As compared to regular PMA binder, HP binder generally increased FE_{IC} for all IC mixes containing 20% RAP regardless of RAP sources (Figure 5-10). Higher polymer content in HP binder appeared to provide an enhanced polymer network leading to greater FE_{IC}. Also, Figure 5-10 shows that IC mixes with fine RAP exhibited clearly lower FE_{IC} compared to those with coarse and intermediate RAP, even though HP binder was used. It appeared that fine RAP resulted in a greater amount of RAP in IC portion than coarse and intermediate RAP at the same RAP content, leading to lower FE_{IC}. Furthermore, with the increasing amount of polymer from regular PMA to HP binder, FE_{IC} appeared to be less dependent on RAP binder stiffness, but more sensitive to total asphalt content in IC mixes. For all three RAP fineness levels, higher asphalt content generally resulted in greater FE_{IC}, and greater increase in FE_{IC} with respect to FE_{IC} values from PMA mix designs containing 20% RAP.

Normalization with respect to the FE_{IC} value from the control mix design (0% RAP) was conducted to identify effects of RAP characteristics on reduction in FE_{IC} without being confounded by individual mix design characteristics (e.g., JMF gradation and design asphalt content). Figure 5-11 presents normalized FE_{IC} results for all eight RAP sources with HP binder, along with PMA binder results. As shown in Figure 5-11, fine RAP sources resulted in greater reduction in FE_{IC} (up to 60%) than both coarse and intermediate RAP sources (about 20%). Compared to IC mixes with PMA binder, IC mixes with HP binder generally were able to better retain cracking resistance, represented by less reduction in FE_{IC} (Figure 5-11). More specifically, use of HP binder resulted in about 10% less reduction for coarse RAP, 10% to 40% less for intermediate RAP, and about 20% to 40% less for fine RAP. It should be noted that for the finest and stiffest RAP (F-H), IC mix with HP binder showed almost identical FE_{IC} reduction to IC mix with PMA binder. This implies

excessively fine and stiff RAP still have a negative effect on cracking resistance at IC level, even with HP binder.

In general, the beneficial effect of HP binder over regular PMA binder was evident in terms of better retaining cracking resistance at the IC mix level. However, even with 20% coarse RAP, the result of 20% reduction in FE_{IC} indicated that use of HP binder may not ensure premium cracking resistance of asphalt mixtures. Verification of the finding using mixture test results is included in CHAPTER 6.

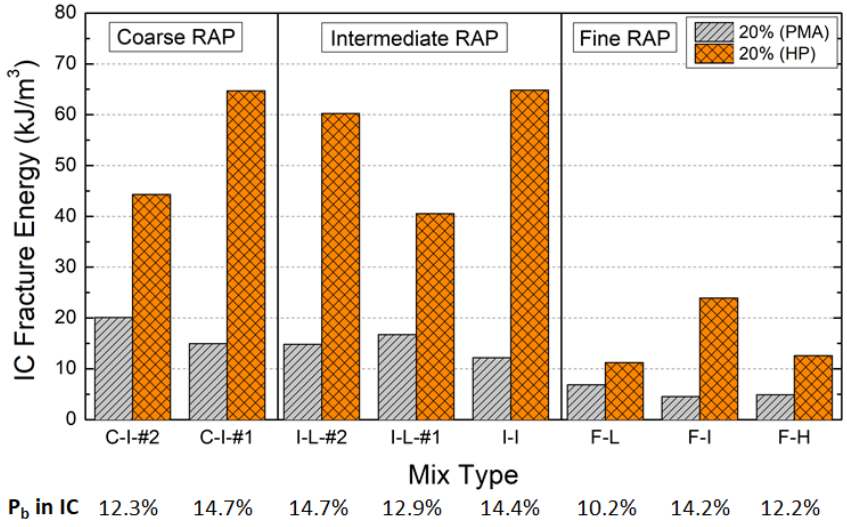

Figure 5-10. IC fracture energy for HP and PMA mix designs containing 20% RAP

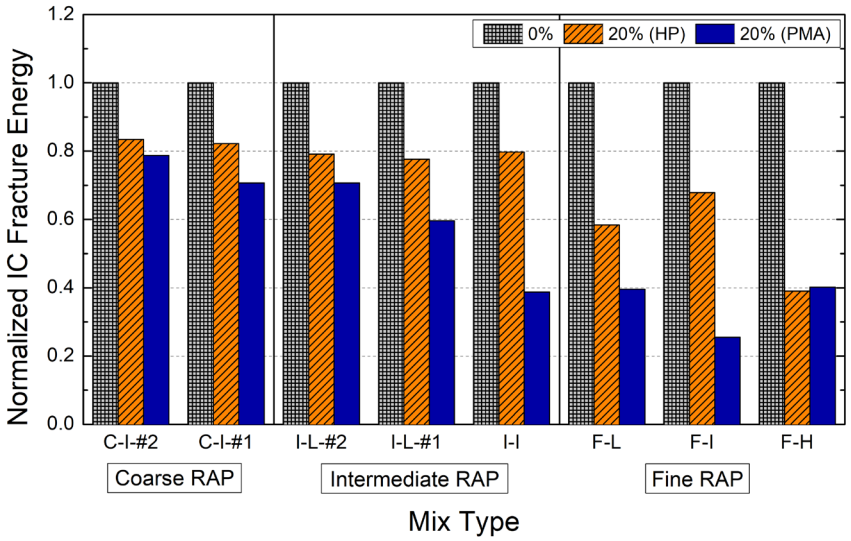

Figure 5-11. Normalized IC fracture energy for HP and PMA mix designs

5.4 Concluding Remarks

IC fracture energy results obtained from ICDT tests were employed to estimate preliminary maximum RAP content in PMA mixtures for each RAP source, as well as to determine whether HP binder can maintain premium cracking resistance of mixtures with 20% RAP. Generally, RAP sources with coarser and less stiff RAP characteristics were found promising for higher RAP content in PMA mixtures. As a result, a preliminary guideline for maximum RAP content in PMA mixtures was proposed based on RAP characteristics zones. Furthermore, HP binder was found to better retain cracking resistance than regular PMA binder at the IC level. However, even with 20% coarse RAP, 20% reduction in FE_{IC} indicated that use of HP binder may not ensure premium cracking resistance of asphalt mixtures.

CHAPTER 6
SUPERPAVE IDT TEST RESULTS AND ANALYSIS

6.1 Introduction

Superpave IDT tests were conducted on PMA and HP mixtures in this part of the study for the following two purposes: (i) verification of the preliminary guideline for maximum RAP content in PMA mixtures developed, based on FE_{IC} results; and (ii) verification of cracking resistance of HP mix designs with 20% RAP observed at the IC level. Prior to testing, all mixtures were conditioned using the long-term oven aging (LTOA) plus the cyclic pore pressure conditioning (CPPC) procedure (Roque et al. 2012). This procedure was shown to be essential for simulation of long-term field aging effects on mixture failure limits. Therefore, LTOA plus CPPC is required to obtain mixture properties appropriate for evaluation of cracking performance (Isola et al. 2014).

6.2 Cracking Performance Indicator

The hot mix asphalt fracture mechanics (HMA-FM) is a viscoelastic fracture mechanics-based system developed to provide a comprehensive framework for practical implementation of mechanisms of pavement cracking into an evaluation and prediction model (Roque et al. 2002; Zhang et al. 2001). The system considers both fundamental failure limits and rate of damage for crack initiation and growth. For typical asphalt mixtures with relatively low polymer and low RAP contents, failure of the mixture is dominated by dissipated creep strain energy limit ($DCSE_f$) and rate of damage. As shown in Figure 6-1a, cracking occurs when accumulated DCSE (function of damage rate) reaches the $DCSE_f$. This failure mode is the fundamental premise for the energy ratio (ER) approach (Roque et al. 2004). Recently, use of more RAP and/or more polymer in asphalt mixtures has resulted in changes in key mixture properties as described below:

- Incorporation of more RAP, which is stiff and brittle due to presence of aged RAP binder, led to lower failure limits (both $DCSE_f$ and fracture energy) and lower creep compliance rate (directly related to lower rate of damage)
- Introduction of more polymer, which is elastic and enhances stiffness, led to lower creep compliance rate without affecting mixture failure limits

Change in mixture properties resulted in change in mixture failure mode. As shown in Figure 6-1b, cracking occurred when accumulated FE (i.e., a combination of accumulated DCSE and elastic energy) reached the FE limit. This failure mode is clearly dominated by elastic energy, since accumulated DCSE is minimized due to extremely low damage rate. Therefore, for stiffer and more brittle mixtures, it is rational to set a failure criterion based on FE limit.

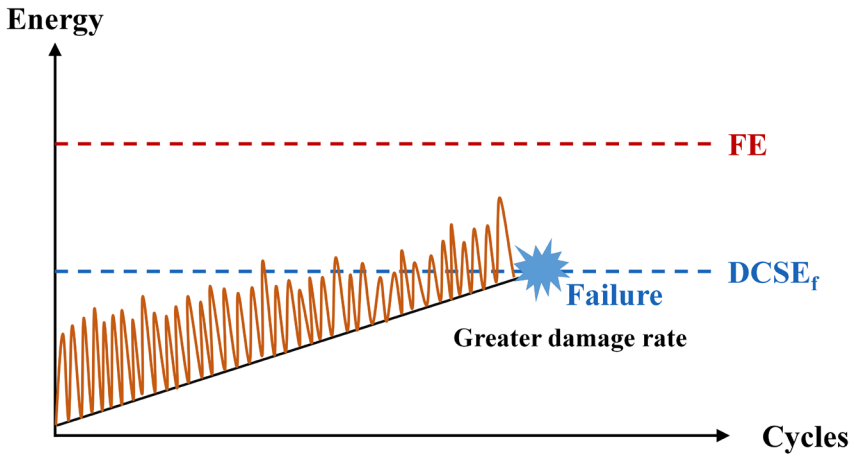

(a) ER-dominant failure mode

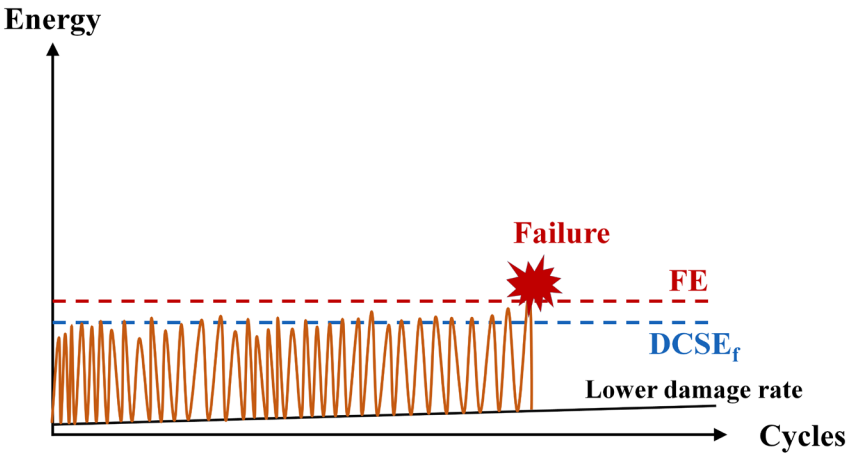

(b) FE limit-dominant failure mode

Figure 6-1. Comparison of failure mode

Figure 6-2 presents a comparison of creep compliance rate between today's mixtures and older mixtures. Mixtures from field cores obtained for 22 field sections (constructed in the 1980s) formed the group of older mixtures. These mixtures were used in the development and calibration of the energy ratio (ER) equation (Roque et al. 2004). Mixtures from the present study composed

the group of today's mixtures, including all eight PMA mixtures (20% RAP) conditioned with LTOA plus CPPC and two PMA mixtures (containing 20% C-I-#1 RAP and 20% I-I RAP, respectively) conditioned with LTOA only. As shown in Figure 6-2, today's mixtures exhibited significantly lower creep compliance rate, which is directly related to lower rate of damage accumulation, compared to older mixtures. It appears that the use of ER would be inappropriate for evaluating cracking performance of today's mixtures (i.e., RAP mixtures employed in the present study). Therefore, mixture fracture energy (FE_{mix}) was selected as the cracking performance indicator.

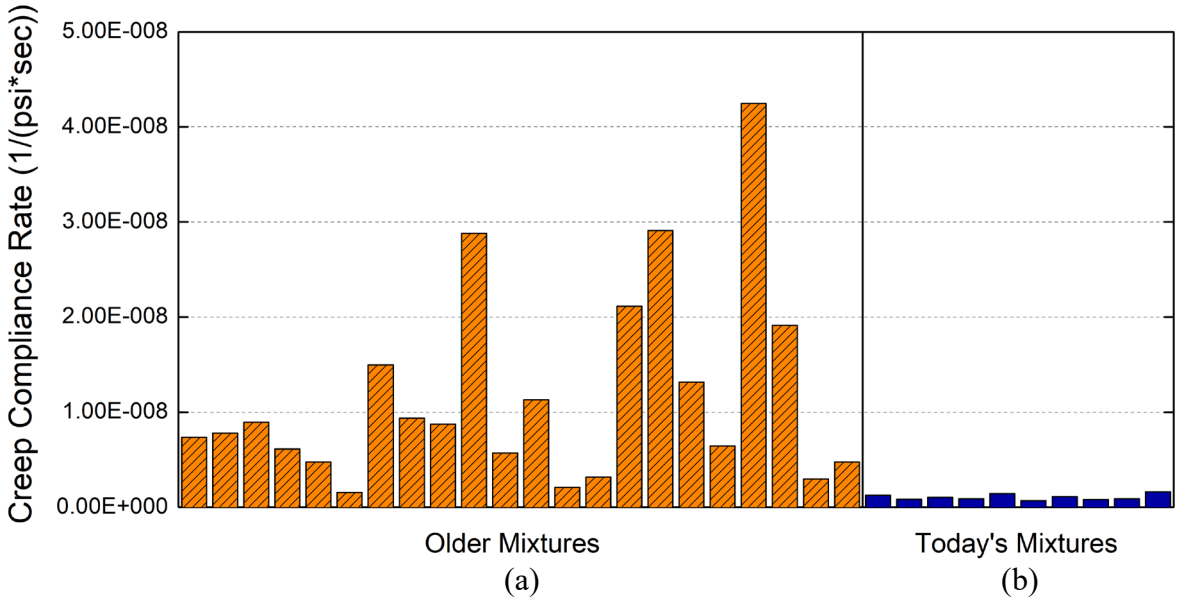

Figure 6-2. Comparison of creep compliance rate: (a) older mixtures and (b) today's mixtures

6.3 Fracture Energy of PMA Mixtures

Fracture energy was obtained from the Superpave IDT test for PMA mixtures with 20% RAP for all eight RAP sources. These FE_{mix} values were used to evaluate effects of RAP characteristics on cracking performance of PMA mixtures as well as to identify the FE limit at the mixture level. Additional PMA mixtures containing the maximum amount of RAP determined based on RAP fineness and RAP binder stiffness were designed and tested to verify the preliminary guideline for maximum RAP content proposed in CHAPTER 5.

6.3.1 Effect of RAP characteristics on PMA mixtures

Figure 6-3 shows fracture energy of PMA mixtures with 20% RAP was between 1.0 and 2.1 kJ/m^3 for all eight RAP sources. PMA mixtures with fine RAP sources generally exhibited lower FE_{mix} (1.1 to 1.3 kJ/m^3) compared to mixtures with intermediate and coarse RAP sources. For the three intermediate RAP sources which had a similar RAP fineness level, stiffer RAP binder resulted in lower FE_{mix}. For the coarse group, C-I-#1 mixture, which had coarser RAP, exhibited greater FE_{mix} than C-I-#2 mixture. The lowest FE_{mix} (1.0 kJ/m^3) among all 20% RAP mixtures was selected as the minimum acceptable FE_{mix} (Figure 6-3), since 20% is the maximum RAP usage currently allowed by FDOT. It should be noted that the minimum acceptable FE_{mix} of 1.0 kJ/m^3 is equivalent to the dissipated creep strain energy threshold ($DCSE_f$) of 0.75 kJ/m^3 specified to prevent poor cracking performance from especially brittle mixtures (Roque et al. 2004), which was determined based on long-term field observation and testing of field cores.

It is important to note that the minimum fracture energy limits at both the IC level (12 kJ/m^3 in Figure 5-7) and the mixture level (1.0 kJ/m^3 in Figure 6-3) were identified from the same PMA mixture design with RAP source I-I at 20% RAP content. The I-I RAP mixture had the JMF gradation with the highest coarseness among all mixture designs. As conceptually illustrated in Figure 6-4, when a RAP source was introduced to a coarse JMF gradation, the proportion of RAP within the IC range would be much higher compared to the same RAP introduced to a finer JMF gradation, leading to lower FE_{mix}.

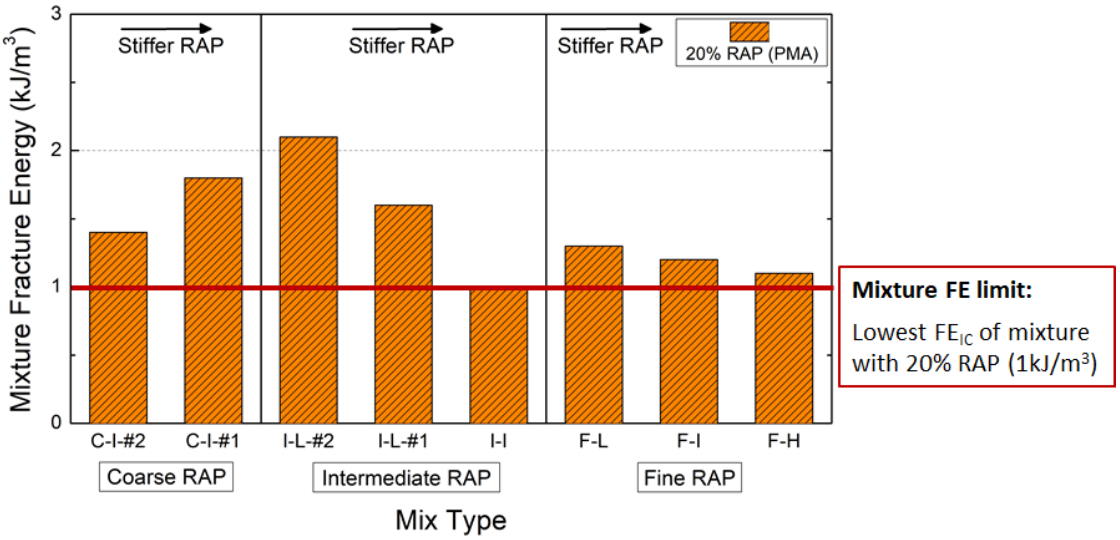

Figure 6-3. Fracture energy of PMA mixtures with 20% RAP

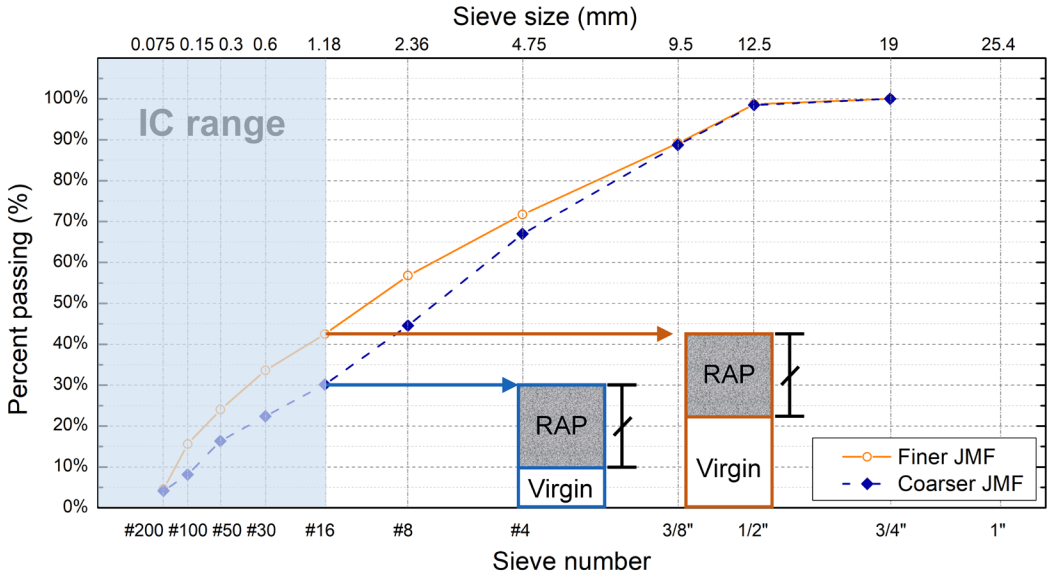

Figure 6-4. Schematic of JMF gradation effect on RAP distribution in the IC range

6.3.2 Verification of preliminary guideline for maximum allowable RAP content

Six RAP characteristics zones (Figure 6-5a) and corresponding RAP sources (Figure 6-5b) were selected to verify the preliminary guideline for maximum RAP contents as described below. The remaining three zones, i.e., Zone C-L (40% RAP), Zone C-H (30% RAP), and Zone I-H (20% RAP) were not considered due to unavailability of RAP sources.

- Zone C-I (35% RAP) with RAP source C-I-#1; C-I-#1 RAP was selected because it was determined to have a lower maximum RAP content than C-I-#2 based on FE_{IC} results (34.5% vs. 39.6%).
- Zone I-L (30% RAP) with RAP source I-L-#2; I-L-#2 RAP was selected because it was determined to have a lower maximum RAP content than I-L-#1 based on FE_{IC} results (32.3% vs. 38.1%).
- Zone I-I (20% RAP), Zone F-L (20% RAP), Zone F-I (20% RAP), and Zone F-H (20% RAP) with RAP sources I-I, F-L, F-I, and F-H, respectively; Only one RAP source is available for each of these zones.

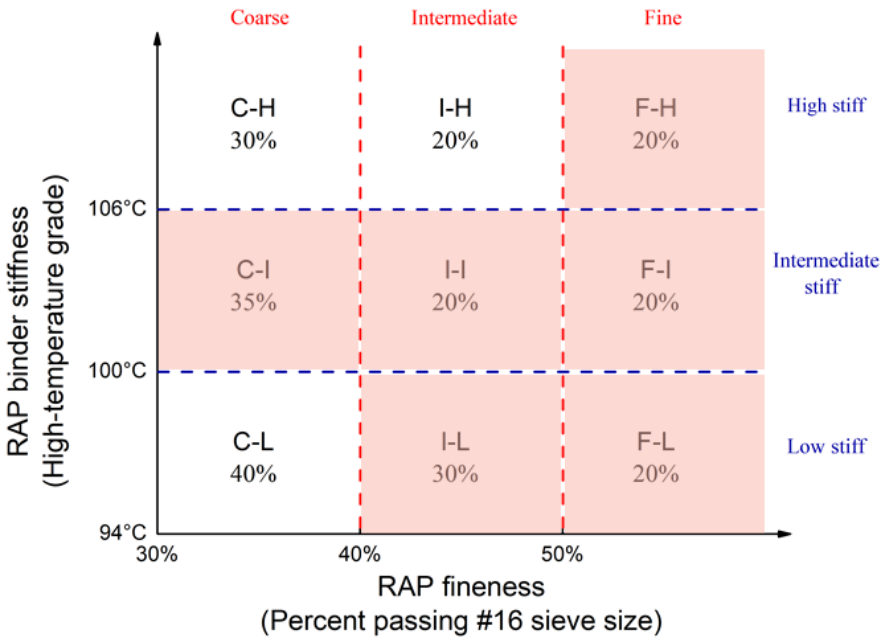

(a) RAP characteristics zones

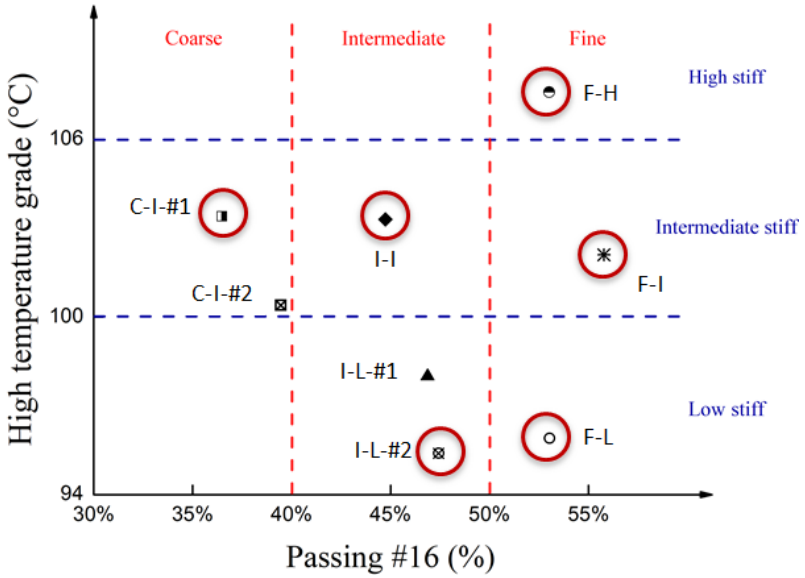

(b) RAP sources

Figure 6-5. Zones and RAP sources selected for verification of preliminary guideline

Figure 6-6 presents fracture energy for the six RAP mixtures with PMA binder. The RAP content of each mixture was determined following the preliminary guideline for selection of maximum RAP content based on RAP characteristics zone (defined by RAP fineness and RAP binder stiffness). The results clearly showed that all RAP mixtures, which were designed and

produced at the maximum RAP contents, satisfied the minimum FE_{mix} limit. It appeared that for all RAP sources included in this study, the preliminary guideline (i.e., RAP characteristics zones in Figure 6-5a) was able to satisfactorily determine maximum RAP contents in PMA mixtures. For Zone I-L, the PMA mixture containing 30% RAP exhibited greater FE_{mix} than the minimum FE_{mix} limit. It should be noted that the preliminary maximum RAP content (30%) for this zone was selected from the lower preliminary maximum RAP content of 32.3% determined for two RAP sources in the zone and rounded it down to the nearest 5%. If the PMA mixture is tested at 32.5% RAP content, the resulting FE_{mix} is expected to go down and get closer to the minimum FE_{mix} limit.

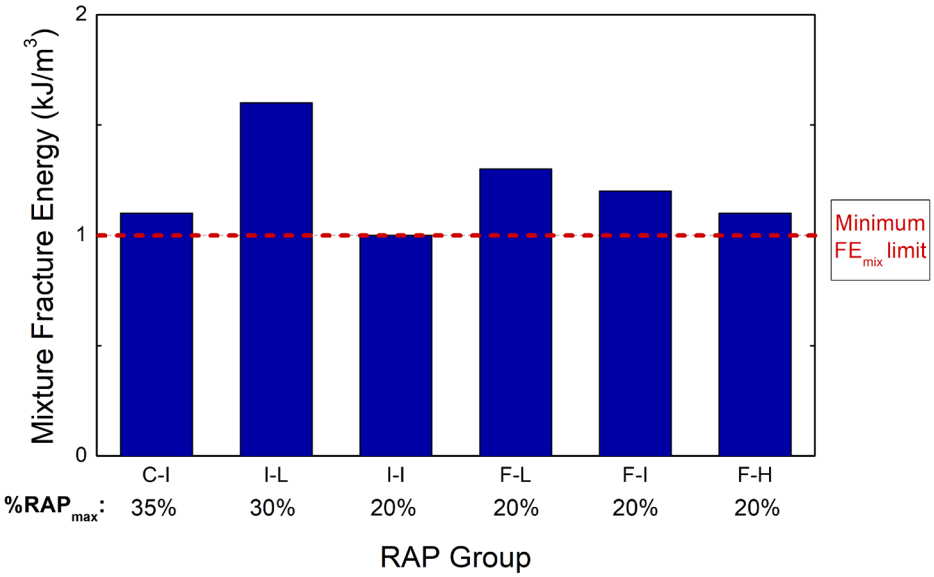

Figure 6-6. Fracture energy of PMA mixtures with recommended maximum amount of RAP

6.4 Fracture Energy of HP Mixtures

Fracture energy was obtained from Superpave IDT tests for HP mixtures containing 0% and 20% RAP for three RAP sources (C-I-#1, I-L-#2, and I-I). These FE_{mix} values were used to evaluate the finding from FE_{IC} results that use of HP binder may not ensure premium cracking resistance of asphalt mixtures with 20% RAP.

Three out of five coarse and intermediate RAP sources were selected based on FE_{IC} results of HP mix designs containing 20% RAP (Figure 5-10), including C-I-#1 RAP in Zone C-I which had higher FE_{IC} than C-I-#2 RAP from the same zone, I-L-#2 RAP in Zone I-L with higher FE_{IC}

than I-L-#1 RAP in the same zone, and I-I RAP in Zone I-I. Three fine RAP sources were not included in the mixture level evaluation since fine RAP resulted in clearly lower FE_{IC} compared to coarse and intermediate RAP, even though HP binder was used.

As shown in Figure 6-7, HP mixtures with 20% RAP satisfied the minimum FE_{mix} limit. Furthermore, HP mixtures exhibited greater FE_{mix} than PMA mixtures at 20% RAP content. This trend is consistent with the observation from FE_{IC} results. Figure 6-8 shows both C-I-#1 RAP and I-L-#2 RAP resulted in about 30% reduction in FE_{mix} with respect to the corresponding control mix designs (0% RAP). For I-I RAP, FE_{mix} reduced approximately 45% from the control mix design due to 20% RAP content. As mentioned earlier, coarser JMF gradation of I-I RAP mix design resulted in a greater reduction in FE_{mix} compared to C-I-#2 and I-L-#2 RAP mixtures. The results of 30% to 45% reduction in FE_{mix} along with 20% reduction in FE_{IC} indicated that use of HP binder may not ensure premium cracking resistance of asphalt mixtures with 20% RAP.

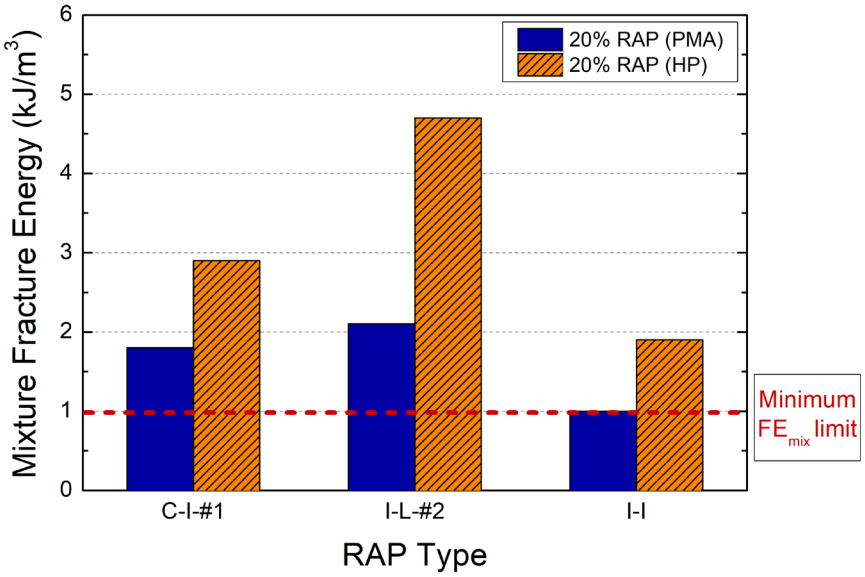

Figure 6-7. Fracture energy for HP and PMA mixtures with selected RAP sources (20% RAP)

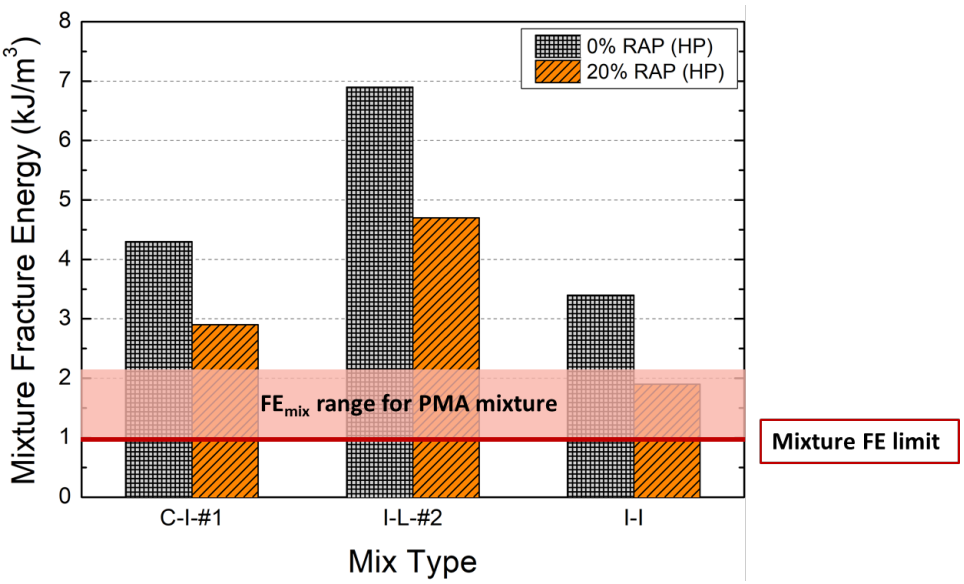

Figure 6-8 Fracture energy for HP mixtures: 20% vs. 0% RAP content

6.5 Concluding Remarks

Mixture fracture energy obtained from the Superpave IDT test was used to verify preliminary guidelines for maximum RAP content in PMA mixtures as well as to verify cracking resistance of HP mix designs with 20% RAP observed at the IC level. It was found that the preliminary guidelines based on RAP characteristics zones was able to satisfactorily determine maximum RAP contents in PMA mixtures. Furthermore, HP mixtures exhibited greater FE_{mix} than corresponding PMA mixtures at 20% RAP content. However, around 30% to 45% reduction in FE_{mix} indicated that incorporation of 20% RAP may preclude the premium cracking resistance expected of asphalt mixture with HP binder.

CHAPTER 7
CLOSURE

7.1 Summary and Findings

This research was conducted to achieve three primary objectives: (i) determine whether the current 20% maximum RAP content in PMA mixtures may be increased without adversely affecting cracking performance; (ii) determine whether additional RAP characterization is needed to implement the increase; and (iii) determine whether 20% RAP can be used in HP mixtures without significant loss in premium cracking performance associated with HP binder. In order to achieve these objectives, a comprehensive field sampling and laboratory experimental plan was developed, including eight RAP sources, two virgin binder types (PG 76-22 PMA and HP binders) and four RAP contents (0%, 20%, 30%, and 40%). Based on literature review, RAP binder stiffness and RAP fineness were identified as important characteristics related to cracking performance of RAP mixture. Twelve RAP sources were characterized using recovered RAP binder and aggregate to identify the range of these RAP characteristics for Florida RAP material. Eight out of 12 RAP sources, covering the range of RAP binder stiffness and RAP fineness encountered in Florida, were selected for further evaluation.

IC fracture energy (FE_{IC}) obtained from the ICDT test was used as a surrogate for a mixture fracture energy (FE_{mix}) to assess the effect of RAP binder stiffness and RAP fineness on cracking performance. FE_{IC} results were used to estimate preliminary maximum RAP content in PMA mixtures for each RAP source. The preliminary maximum RAP content of eight RAP sources was used to establish preliminary guidelines from which maximum RAP usage in PMA mixtures can be determined for any combination of RAP binder stiffness and RAP fineness. Moreover, the effect of 20% RAP on HP mixtures was evaluated using FE_{IC} to determine whether HP mixtures can maintain premium cracking performance. Preliminary guidelines and findings from FE_{IC} results were evaluated by Superpave IDT tests results for asphalt mixtures. A summary of findings based on results of tests and analyses is presented below:

- Finer RAP (RAP fineness greater than 50% passing the No. 16 sieve) was more detrimental to cracking resistance for both PMA and HP mixtures as compared to coarser RAP.
- Stiffer RAP binder generally reduced PMA mixture cracking performance.

- Proposed guidelines for maximum RAP usage (up to 40%) in PMA mixtures based on RAP binder stiffness and RAP fineness was verified with mixture testing.
- Introduction of 20% RAP in HP mixtures resulted in about 20% to 45% reduction in FE_{IC} and 30% to 45% reduction in FE_{mix} depending on RAP characteristics, even though RAP mixtures with HP binder exhibited better cracking performance than mixtures with PG 76-22 PMA binder.

7.2 Conclusions

Based on the findings of this study, the following conclusions were drawn:

- Characterizing RAP binder stiffness and RAP fineness is required to increase the current maximum RAP content (20%) in PMA mixtures.
- The specific maximum RAP limits based on RAP binder stiffness and RAP fineness, proposed in this study, may be used to successfully introduce up to 40% RAP in PMA mixtures.
- Incorporation of 20% RAP in HP mixtures would sacrifice the premium benefits of HP binder.

7.3 Recommendations and Future Work

Based on evaluations performed in this study, recommendations for further investigation are summarized below:

- It is recommended that guidelines for crushing RAP should be carefully considered to limit fineness of RAP.
- The proposed guidelines for maximum RAP usage in PMA mixtures should be continuously evaluated to consider potential changes in RAP material properties and RAP processing.
- More detailed laboratory study with better controlled variable is recommended.

LIST OF REFERENCES

AASHTO (2017). Stnadard Specification for Superpave Volumetric Mix Design, AASHTO M323

Advanced Asphalt Technologies, LLC. (2011). "A Manual for Design of Hot-Mix Asphalt with Commentary." *National Cooperative Highway Research Program (NCHRP) Report 673, Transportation Research Board, Washington D.C.*

Al-Qadi, I. L., Carpenter, S. H., Roberts, G., Ozer, H., Aurangzeb, Q., Elseifi, M., and Trepanier, J. (2009). "Determination of usable residual asphalt binder in RAP." *Illinois Center for Transportation (ICT). Final Report of Federal Highway Administration, FHWA-ICT-09031*

Anderson, R. M., King, G. N., Hanson, D. I., and Blankenship, P. B. (2011). "Evaluation of the relationship between asphalt binder properties and non-load related cracking." *Journal of the Association of Asphalt Paving Technologists*, 80, 615-664.

Asphalt Institute (2001). *Superpave mix design.* Asphalt Institute, Lexington, KY.

Beeson, M., Prather, M., and Huber, G. A. (2011). "Characterization of Reclaimed Asphalt Pavement in Indiana: Changing INDOT Specification for RAP." *Transportation Research Board 90th Annual Meeting,* Washington, D.C.

Bernier, A., Zofka, A., and Yut, I. (2012). "Laboratory evaluation of rutting susceptibility of polymer-modified asphalt mixtures containing recycled pavements." *Construction and Building Materials*, 31, 58-66.

Błażejowski, K., Wójcik-Wiśniewska, M., Peciakowski, H., and Olszacki, J. (2016). "The Performance of a Highly Modified Binders for Heavy Duty Asphalt Pavements." *Transportation Research Procedia*, 14, 679-684.

Bonaquist, R. (2007). "Can I run more RAP?" *HMAT: Hot Mix Asphalt Technology*, 12(5), 11-13.

Chen, J.-S., Wang, T. J., and Lee, C.-T. (2018). "Evaluation of a highly-modified asphalt binder for field performance." *Construction and Building Materials*, 171, 539-545.

Christensen, Jr. D., Pellinen, T., and Bonaquist, R. (2003). "Hirsch model for estimating the modulus of asphalt concrete." *Journal of the Association of Asphalt Paving Technologists*, 72, 97-121.

Chun, S., Zou, J., Roque, R., and Lopp, G. (2012). "Predictive relationships for HMA fracture properties based on mixture component characteristics." *Road Materials and Pavement Design*, 13(sup1), 140-160.

Copeland, A., D'Angelo, J., Dongré, R., Belagutti, S., and Sholar, G. (2010). "Field Evaluation of High Reclaimed Asphalt Pavement-Warm-Mix Asphalt Project in Florida." *Transportation Research Record: Journal of the Transportation Research Board*, 2179, 93-101.

Daniel, J. S., and Mogawer, W. S. (2010). "Determining the effective PG grade of binder in RAP mixes." NETCR78, Project No. 04-4.

FDOT (2018). "Standard Specifications for Road and Bridge Construction." Florida Department of Transportation (FDOT), Tallahassee, FL.

Guarin, A., Roque, R., Kim, S., and Sirin, O. (2013). "Disruption factor of asphalt mixtures." *International Journal of Pavement Engineering*, 14(5), 472-485.

Hajj, E., Salazar, L., and Sebaaly, P. (2012). "Methodologies for Estimating Effective Performance Grade of Asphalt Binders in Mixtures with High Recycled Asphalt Pavement Content." *Transportation Research Record: Journal of the Transportation Research Board*, 2294, 53-63.

Hajj, E. Y., Sebaaly, P. E., and Shrestha, R. (2009). "Laboratory Evaluation of Mixes Containing Recycled Asphalt Pavement (RAP)." *Road Materials and Pavement Design*, 10(3), 495-517.

Huang, B., Kingery, W., and Zhang, Z. (2004) "Laboratory study of fatigue characteristics of HMA mixtures containing RAP." *Proc. of International Symposium on Design and Construction of Long Lasting Asphalt Pavements, Auburn, Alabama, USA,* 501-22

Huang, B., Li, G., Vukosavljevic, D., Shu, X., and Egan, B. (2005). "Laboratory Investigation of Mixing Hot-Mix Asphalt with Reclaimed Asphalt Pavement." *Transportation Research Record: Journal of the Transportation Research Board*, 1929, 37-45.

Huang, B., Shu, X., and Vukosavljevic, D. (2011). "Laboratory Investigation of Cracking Resistance of Hot-Mix Asphalt Field Mixtures Containing Screened Reclaimed Asphalt Pavement." *Journal of Materials in Civil Engineering*, 23(11), 1535-1543.

IDOT (2016). "Standard Specifications for Road and Bridge Construction. "Illinois Department of Transportation (IDOT), Springfield, IL.

Isola, M., Chun, S., Roque, R., Zou, J., Koh, C., and Lopp, G. (2014). "Development and Evaluation of Laboratory Conditioning Procedures to Simulate Mixture Property Changes Effectively in the Field." *Transportation Research Record: Journal of the Transportation Research Board*, 2447, 74-82.

Kim, S., Roque, R., Birgisson, B., and Guarin, A. (2009). "Porosity of the Dominant Aggregate Size Range to Evaluate Coarse Aggregate Structure of Asphalt Mixtures." *Journal of Materials in Civil Engineering*, 21(1), 32-39.

Kim, S., Roque, R., Guarin, A., and Birgisson, B. (2006). "Identification and assessment of the dominant aggregate size range (DASR) of asphalt mixture (with discussion)." *Journal of the Association of Asphalt Paving Technologists*, 75, 789-814.

Kim, S., Sholar, G., Byron, T., and Kim, J. (2009). "Performance of Polymer-Modified Asphalt Mixture with Reclaimed Asphalt Pavement." *Transportation Research Record: Journal of the Transportation Research Board*, 2126, 109-114.

Kvasnak, A., West, R., Michael, J., Loria, L., Hajj, E., and Tran, N. (2010). "Bulk Specific Gravity of Reclaimed Asphalt Pavement Aggregate." *Transportation Research Record: Journal of the Transportation Research Board*, 2180, 30-35.

Kwon, O., Choubane, B., Greene, J., and Sholar, G. (2019). "Evaluation of the Performance of High-SBS Modified Asphalt Binder Through Accelerated Pavement Testing." *Florida Department of Transportation (FDOT), FL/DOT/SMO/18-588, Tallahassee, FL.*

Li, X., Gibson, N., Andriescu, A., and S. Arnold, T. (2017). "Performance evaluation of REOB-modified asphalt binders and mixtures." *Road Materials and Pavement Design*, 18(sup1), 128-153.

Ma, T., Mahmoud, E., and Bahia, H. (2010). "Estimation of Reclaimed Asphalt Pavement Binder Low-Temperature Properties Without Extraction." *Transportation Research Record: Journal of the Transportation Research Board*, 2179, 58-65.

McDaniel, R. S., Soleymani, H., Anderson, R. M., Turner, P., and Peterson, R. (2000). "Recommended Use of Reclaimed Asphalt Pavement in the Superpave Mix Design Method." NCHRP Web Document 30, TRB, National Research Council, Washington, D.C.

Mehta, Y., Nolan, A., Coffey, S., Dubois, E., Norton, A., Reger, D., Shirodkar, P., Sonpal, K., and Tomlinson, C. (2012). "High reclaimed asphalt pavement in hot mix asphalt." *Final Report of Federal Highway Administration, FHWA-NJ-2012-005*

MnDOT (2016). "Standard Specifications for Construction." Minnesota Department of Transportation (MnDOT), St.Paul, MN.

Mohammad, L. N., Negulescu, I. I., Wu, Z., Daranga, C., Daly, W. H., and Abadie, C. (2003). "Investigation of the Use of Recycled Polymer Modified Asphalt Binder in Asphalt Concrete Pavements." *Journal of the Association of Asphalt Paving Technologists*, 72, 551-594.

Mull, M. A., Stuart, K., and Yehia, A. (2002). "Fracture resistance characterization of chemically modified crumb rubber asphalt pavement." *Journal of Materials Science*, 37(3), 557-566.

Niu, T., Roque, R., and Lopp, G. A. (2014). "Development of a binder fracture test to determine fracture energy properties." *Road Materials and Pavement Design*, 15(sup1), 219-238.

Nukunya, B., Roque, R., Tia, M., and Mehta, Y. (2002). "Effect of Aggregate Structure on Rutting Potential of Dense-Graded Asphalt Mixtures" *Transportation Research Record: Journal of the Transportation Research Board*, 1798(1), 136-145.

ODOT (2013). "Construction and Material Specifications." Ohio Department of Transportation (ODOT), Columbus, Ohio.

Roque, R., Birgisson, B., Drakos, C., and Dietrich, B. (2004). "Development and field evaluation of energy-based criteria for top-down cracking performance of hot mix asphalt (with discussion)." *Journal of the Association of Asphalt Paving Technologists*, 73, 229-260.

Roque, R., Birgisson, B., Sangpetngam, B., and Zhang, Z. (2002). "Hot mix asphalt fracture mechanics: a fundamental crack growth law for asphalt mixtures." *Journal of the Association of Asphalt Paving Technologists*, 71, 816-827.

Roque, R., and Buttlar, W. G. (1992). "The development of a measurement and analysis system to accurately determine asphalt concrete properties using the indirect tensile mode (with discussion)." *Journal of the Association of Asphalt Paving Technologists*, 61, 304-332.

Roque, R., Buttlar, W. G., Ruth, B. E., Tia, M., Dickison, S. W., and Reid, B. (1997). "Evaluation of SHRP indirect tension tester to mitigate cracking in asphalt concrete pavements and overlays." *Final Report of Florida Department of Transportation, FDOT Contract No. B-9885, University of Florida, Gainesville FL.*

Roque, R., Chun, S., Zou, J., Lopp, G., and Villiers, C. (2011). "Continuation of Superpave projects monitoring." *Final Report of Florida Department of Transportation, FDOT Contract No. BDK-75-977-06, University of Florida, Gainesville FL*.

Roque, R., Isola, M., Chun, S., Zou, J., Koh, C., and Lopp, G. (2012). "Effects of laboratory heating, cyclic pore pressure, and cyclic loading on fracture properties of asphalt mixture."

Final Report of Florida Department of Transportation, FDOT Contract No. BDK75-977-28, University of Florida, Gainesville FL.

Roque, R., Yan, Y., Cocconcelli, C., and Lopp, G. (2015). "Perform an investigation of the effects of increased reclaimed asphalt pavement (RAP) levels in dense graded friction courses." *Final Report of Florida Department of Transportation, FDOT Contract No. BDU-77, University of Florida, Gainesville FL*.

Roque, R., Yan, Y., and Lopp, G. (2018). "Impact of Recycled Asphalt Shingles (RAS) on Asphalt Binder Performance." *Final Report of Florida Department of Transportation, FDOT Contract No. BDV31-977-36, University of Florida, Gainesville FL*.

Shah, A., McDaniel, R., Huber, G., and Gallivan, V. (2007). "Investigation of Properties of Plant-Produced Reclaimed Asphalt Pavement Mixtures." *Transportation Research Record: Journal of the Transportation Research Board*, 1998, 103-111.

Sharma, B. K., Ma, J., Kunwar, B., Singhvi, P., Ozer, H., and Rajagopalan, N. (2017). "Modeling the Performance Properties of RAS and RAP Blended Asphalt Mixes Using Chemical Compositional Information." *Illinois Center for Transportation (ICT). Final Report of Federal Highway Administration, FHWA-ICT-17-001*

Shirodkar, P., Mehta, Y., Nolan, A., Sonpal, K., Norton, A., Tomlinson, C., Dubois, E., Sullivan, P., and Sauber, R. (2011). "A study to determine the degree of partial blending of reclaimed asphalt pavement (RAP) binder for high RAP hot mix asphalt." *Construction and Building Materials*, 25(1), 150-155.

Singh, D., and Girimath, S. (2016). "Influence of RAP sources and proportions on fracture and low temperature cracking performance of polymer modified binder." *Construction and Building Materials*, 120, 10-18.

Singh, D., and Sawant, D. (2016). "Understanding effects of RAP on rheological performance and chemical composition of SBS modified binder using series of laboratory tests." *International Journal of Pavement Research and Technology*, 9(3), 178-189.

Swiertz, D., Mahmoud, E., and Bahia, H. (2011). "Estimating the Effect of Recycled Asphalt Pavements and Asphalt Shingles on Fresh Binder, Low-Temperature Properties Without Extraction and Recovery." *Transportation Research Record: Journal of the Transportation Research Board*, 2208, 48-55.

Timm, D., Sholar, G., Kim, J., and Willis, J. (2009). "Forensic Investigation and Validation of Energy Ratio Concept." *Transportation Research Record: Journal of the Transportation Research Board*, 2127, 43-51.

Timm, D. H., West, R. C., and Taylor, A. J. (2016). "Performance and Fatigue Analysis of High Reclaimed Asphalt Pavement Content and Warm-Mix Asphalt Test Sections." *Transportation Research Record: Journal of the Transportation Research Board*, 2575, 196-205.

Von Quintus, H., Mallela, J., and Buncher, M. (2007). "Quantification of Effect of Polymer-Modified Asphalt on Flexible Pavement Performance." *Transportation Research Record: Journal of the Transportation Research Board*, 2001, 141-154.

West, R., Kvasnak, A., Tran, N., Powell, B., and Turner, P. (2009). "Testing of Moderate and High Reclaimed Asphalt Pavement Content Mixes." *Transportation Research Record: Journal of the Transportation Research Board*, 2126, 100-108.

West, R., Willis, J. R., and Marasteanu, M. (2013). "Improved Mix Design, Evaluation, and Materials Management Practices for Hot Mix Asphalt with High Reclaimed Asphalt Pavement Content." *National Cooperative Highway Research Program (NCHRP) Report 752, Project 09-46*.

West, R. C. (2008). "Summary of NCAT Survey on RAP Management Practices and RAP Variability."Federal Highway Administration, Washington, DC.

West, R. C. (2015). "Best Practices for RAP And RAS Management." National Asphalt Pavement Association (NAPA), Lanham, MD.

West, R. C., and Copeland, A. (2015). "High RAP Asphalt Pavements: Japan Practice — Lessons Learned." National Asphalt Pavement Association (NAPA), Lanham, MD.

Williams, B. A., Copeland, A., and Ross, T. C. (2018). "Asphalt Pavement Industry Survey on Recycled Materials and Warm-Mix Asphalt Usage: 2017." *National Asphalt Pavement Association (NAPA) Report No. IS 138 (8e).*

Xie, Z., Tran, N., Julian, G., Taylor, A., and Blackburn, L. D. (2017). "Performance of Asphalt Mixtures with High Recycled Contents Using Rejuvenators and Warm-Mix Additive: Field and Lab Experiments." *Journal of Materials in Civil Engineering*, 29(10), 04017190.

Yan, Y., Hernando, D., Lopp, G., Rilko, W., and Roque, R. (2018a). "Enhanced mortar approach to characterize the effect of reclaimed asphalt pavement on virgin binder true grade." *Materials and Structures*, 51(2), 41.

Yan, Y., Preti, F., Romeo, E., Lopp, G., Tebaldi, G., and Roque, R. (2018b). "Fracture energy density of interstitial component of asphalt mixtures." *Materials and Structures*, 51(5), 118.

Yan, Y., Roque, R., Cocconcelli, C., Bekoe, M., and Lopp, G. (2017a). "Evaluation of cracking performance for polymer-modified asphalt mixtures with high RAP content." *Road Materials and Pavement Design*, 18(sup1), 450-470.

Yan, Y., Roque, R., Hernando, D., and Lopp, G. (2017b). "Development of a new methodology to effectively predict the fracture properties of RAP mixtures." *Road Materials and Pavement Design*, 18(sup4), 372-387.

Yildirim, Y. (2007). "Polymer modified asphalt binders." *Construction and Building Materials*, 21(1), 66-72.

Zhang, Z., Roque, R., Birgisson, B., and Sangpetngam, S. (2001). "Identification and Verification of a Suitable Crack Growth Law for Asphalt Mixtures." *Journal of Asphalt Paving Technologists*, 70, 206-241.

Zofka, A., Marasteanu, M., Li, X., Clyne, T., and McGraw, J. (2005). "Simple Method to Obtain Asphalt Binders Low Temperature Properties from Asphalt Mixtures Properties (With Discussion)." *Journal of the Association of Asphalt Paving Technologists*, 74, 255-282.

Zou, J., Roque, R., Chun, S., and Lopp, G. (2013). "Long-term field evaluation and analysis of top-down cracking for Superpave projects." *Road Materials and Pavement Design*, 14(4), 831-846.

APPENDIX A
RAP MANAGEMENT PRACTICES

West et al. (2013) reported that industry experts identified two major issues to be addressed to successfully use higher RAP contents in asphalt mixtures. One was the lack of guidance on RAP management (i.e., processing, handling and characterization) prior to mix design. The other was further improvement of the Superpave mix design method to better handle mixtures with RAP content above 25%. This need manifested by the industry resulted in the National Cooperative Highway Research Program (NCHRP) Report 752 (West et al. 2013).

With respect to management, West et al. (2013) reviewed the general methods to process RAP, which included minimal processing, crushing, mixing and fractionating (Table A-1). According to a survey conducted by NCAT on 81 contractors across the United States (West 2008), 74% of the respondents crushed to one size (52% crushed to a maximum particle size of one-half inch). West et al. (2013) underscored that "single-size crushing approach often leads to generating high dust contents, which can limit the amount of the RAP that can be successfully used in mix designs".

Based on information provided by the FDOT, crushing to pass a single screen size is the most common practice currently in the State of Florida. Crushing tends to generate excessive particles passing the 0.075 mm sieve size, which hinders the use of higher RAP contents. Fractionating the RAP source into various sizes not only reduces the variability in the gradation and binder content but also provides the flexibility to use specific components of the available RAP in different mixtures.

Table A-1. General methods for RAP processing (West et al. 2013)

Process	Description	Suitable conditions	Possible concerns
Minimal processing	Screening only to remove oversized particles (may be accomplished in line during feed of RAP to the plant)	RAP is from a single source	Single-source RAP piles are a finite quantity. When a stockpile is depleted, new mix designs will be needed with another RAP stockpile
Crushing	Breaking of RAP chunks, agglomerations, and/or aggregate particles to avoid large particles that do not break apart during mixing or particles that exceed the mix NMAS	RAP contains large chunks (anything larger than 2 inches) or RAP aggregate NMAS exceeds that of recycled mix	Generating excess dust and uncoated surfaces
Mixing	Using a loader or excavator to blend RAP from different sources; usually done in combination with crushing or fractionating	RAP stockpile contains materials from multiple sources	Good consistency of RAP characteristics must be verified with a RAP QC plan
Fractionating	Screening RAP into multiple size ranges	High RAP content mixes (above 30 to 40%) are routine	Highest cost, requires additional RAP bin(s) to simultaneously feed multiple fractions

The amount of dust (i.e., material passing the 0.075 mm sieve) in the RAP stockpile is not the only factor that governs the maximum RAP content that can be added to a mixture. According to a NCHRP study conducted by Advanced Asphalt Technologies (LLC 2011), additional factors include:

- *Amount of RAP available* The inventory of some contractors may limit the maximum amount of RAP to be introduced as part of new asphalt mixtures. Also, West (2015) pointed out that "there may be additional costs associated with higher RAP contents, such as additional materials testing, higher RAP processing costs, plant modifications, and higher plant maintenance costs".
- *Variability of the RAP material* Although one could think that RAP is a highly variable material, numerous studies have shown that processing a variety of sources into a large

stockpile can be made into a consistent material (West et al. 2013). West (2015) went further and stated that "some contractors have been able to develop RAP processing practices using continuously replenished stockpiles that have very consistent gradations, aggregate properties, and asphalt contents over a long period of time".

- *Properties of RAP binder and available virgin binders* Properties of the aged binder existing in the RAP, namely stiffness, may define the maximum RAP content to be combined with a particular virgin binder
- *Specification limits* In this regard, West and Copeland (2015) indicated that highway agency specifications should allow the use of RAP at the contractor's discretion and provide simple and clear criteria for ensuring pavement performance.
- *Capability of the hot-mix plant to dry, heat and effectively mix the RAP material* This involves both practical and safety concerns. West (2015) expressed that excess heat from the virgin aggregate used to dry and raise the temperature of RAP can create the potential for a fire in the mixer, or in the mixer section of the drum, if the feed of the RAP is disrupted due to a clogged gate, broken belt or clogged dryer entry and the virgin asphalt contacts superheated aggregate.

Another step included in proper management of RAP stockpiles is characterization through sampling and testing. West (2015) recommended to gather the following information, which can also be used later for mix design:

- Asphalt binder content
- Gradation of recovered aggregate
- Bulk specific gravity of RAP aggregate
- Superpave consensus properties of aggregate recovered from RAP
- RAP asphalt binder properties (for RAP contents above 25%)

APPENDIX B
MORTAR APPROACH FOR CHARACTERIZATION OF RAP BINDER STIFFNESS

Many previous studies have determined RAP binder properties using recovered RAP binder obtained from a solvent extraction and recovery procedure. However, the primary concern of solvent extraction and recovery is that binder properties may be altered by the presence of residual solvent after recovery and aging of binder at high temperature (Mehta et al. 2012; Swiertz et al. 2011). The process is labor intensive, and negative effects of the chemicals on health and environment are of concern. Therefore, a method for non-solvent based binder characterization was identified to estimate properties of RAP binder.

Researchers at the University of Wisconsin (UW) developed a new mortar testing procedure to determine RAP binder continuous grade without the need for extraction and recovery (Ma et al. 2010; Swiertz et al. 2011). However, recent research determined that the data interpretation method employed by UW resulted in underestimated high-temperature true grade and overestimated low-temperature true grade for RAP/RAS binder (Roque et al. 2018). A modified data interpretation and analysis procedure using a relationship between binder and mortar measurements was proposed. The modified method was evaluated by comparing predicted continuous grade to measured grade of recovered RAP binders. More accurate predictions of high and low-temperature continuous grade were obtained by the modified method for all virgin binder types, RAP sources and binder replacement ratios evaluated.

Specimen preparation

RAP material was broken down, dried and sieved to collect R_{100} material, which is passing No. 50 sieve (0.3 mm) and retained on No. 100 sieve (0.15 mm). The ignition oven test was conducted to determine RAP binder content of R_{100} material and to obtain recovered R_{100} aggregate following Florida Method of Test FM 5-563.

Figure B-1 shows a schematic diagram of two types of mortar (Mortar A and B). Both mortar samples have identical total binder content, virgin binder type and gradation. However, mortar A included R_{100} material and virgin binder, while mortar B was composed of recovered R_{100} aggregate and virgin binder. It is important to note that a minimum total binder content of

35% was recommended to obtain sufficient workability to produce mortar samples without air voids.

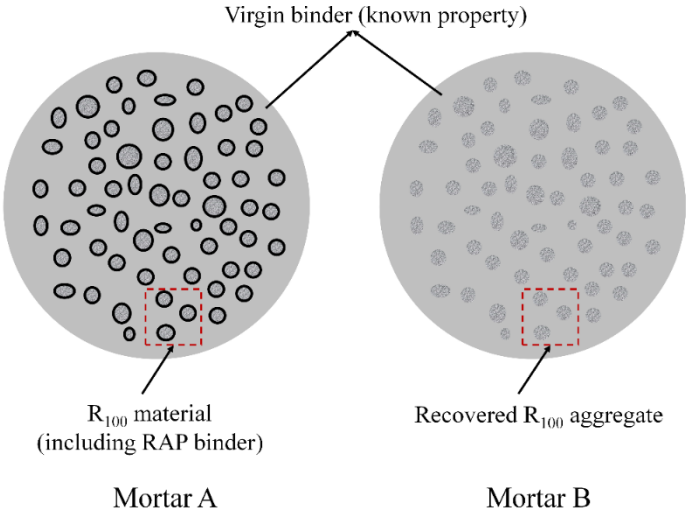

Figure B-1. Schematic diagram of two types of mortar

Figure B-2 illustrates specimen preparation procedure for virgin binder and all types of mortar samples including mortar with unaged virgin binder (fresh mortar), mortar with rolling thin-film oven (RTFO)-aged virgin binder (RTFO mortar) and mortar aged with pressure aging vessel (PAV), called PAV mortar. Fresh mortar A samples were R_{100} material mixed with unaged virgin binder, while recovered R_{100} aggregate was mixed with unaged virgin binder to produce fresh mortar B. RTFO mortar A samples were R_{100} material mixed with RTFO-aged virgin binder, while recovered R_{100} aggregate was mixed with RTFO-aged virgin binder to create RTFO mortar B. PAV mortar A and B samples were produced by aging the RTFO mortar A and B samples in the PAV at 100°C for 24 hours. The amount of mortar in each PAV pan was determined such that 50g of binder were present in the pan. For example, if the total binder content of the mortar is 35%, the amount of mortar in each PAV pan will be 143g.

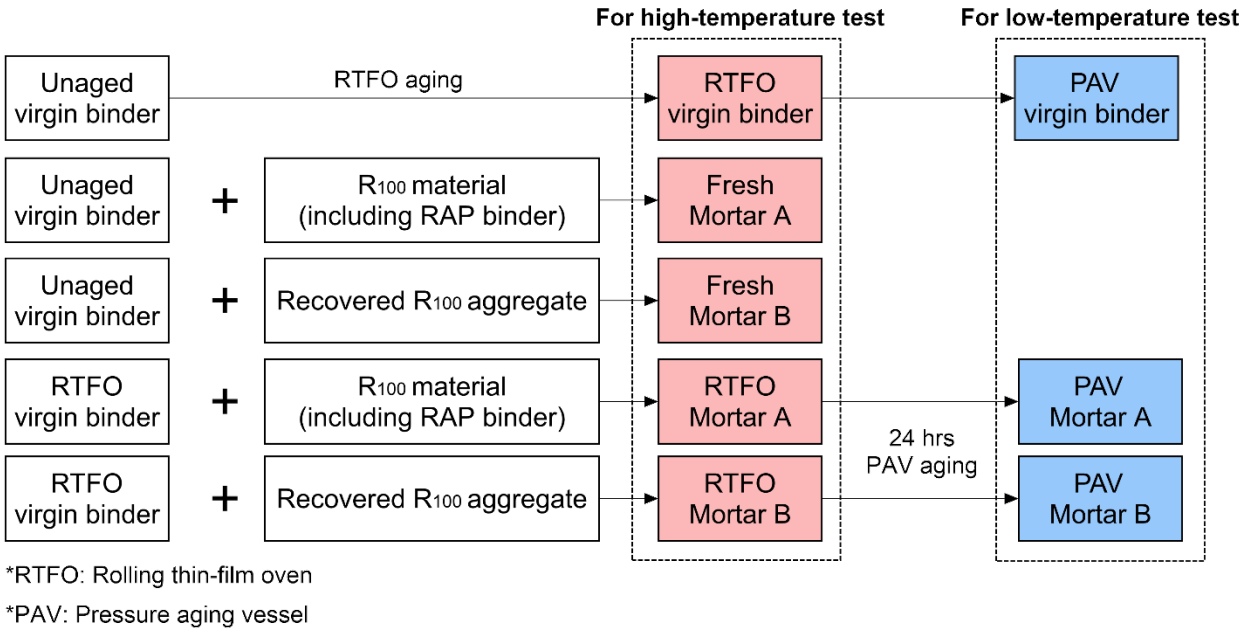

Figure B-2. Procedure of mortar specimen preparation

Determination of continuous grade for blended binder in mortar A

Continuous grade of blended binder (virgin binder + RAP binder) can be predicted from virgin binder and mortar properties measured using Superpave binder performance grade tests. Low-temperature properties (S and m-value) can be measured by performing bending beam rheometer (BBR) test, while the high-temperature property ($G^*/\sin\delta$) can be determined using dynamic shear rheometer (DSR) test. Intermediate-temperature testing will not be considered in this study because DSR measurements on PAV mortar samples were not repeatable due to specimen deficiencies, i.e., air voids at the edge of trimmed specimens (Roque et al. 2018).

For each temperature level (i.e., high and low), virgin binder and mortar samples are tested at two temperatures corresponding to virgin binder performance grade (PG) as summarized below.

- Testing temperatures for high-temperature properties
  - T_1: high PG of virgin binder
  - T_2: high PG of virgin binder plus 6°C
- Testing temperatures for low-temperature properties
  - T_1: low PG of virgin binder
  - T_2: low PG of virgin binder plus 6°C

As an example, Table B-1 presents two testing temperatures for each temperature level for mortar samples with PG 76-22 virgin binder type.

Table B-1. Example of mortar testing temperatures for each temperature level

Temperature level	**Virgin binder type**	**Mortar testing temperatures**	
		T_1	**T_2**
High-temperature	PG 76-22	76°C	82°C
Low-temperature		-12°C	-6°C

Blended binder properties can be predicted from mortar and virgin binder properties using the modified procedure developed by (Roque et al. 2018), as shown in Figure B-3. In Step 1, the following relationship is established between measured binder and mortar properties.

$$\log(P_{mortar}) = c \times \log(P_{binder}) + d \qquad Eq.B.1$$

where, P_{mortar} denotes mortar property, P_{binder} is binder property, and c and d are coefficients determined based on measured properties of virgin binder and mortar B at two temperatures T_1 and T_2 as described below.

$$c = \frac{\log(P_{mortar\ B1}/P_{mortar\ B2})}{\log(P_{binder\ 1}/P_{binder\ 2})}$$

$$d = \log P_{mortar\ B1} - c \times \log P_{binder\ 1}$$

where,

$P_{mortar\ B1}$ = mortar B property at T_1; $P_{mortar\ B2}$ = mortar B property at T_2;

$P_{binder\ 1}$ = virgin binder property at T_1; $P_{binder\ 2}$ = virgin binder property at T_2

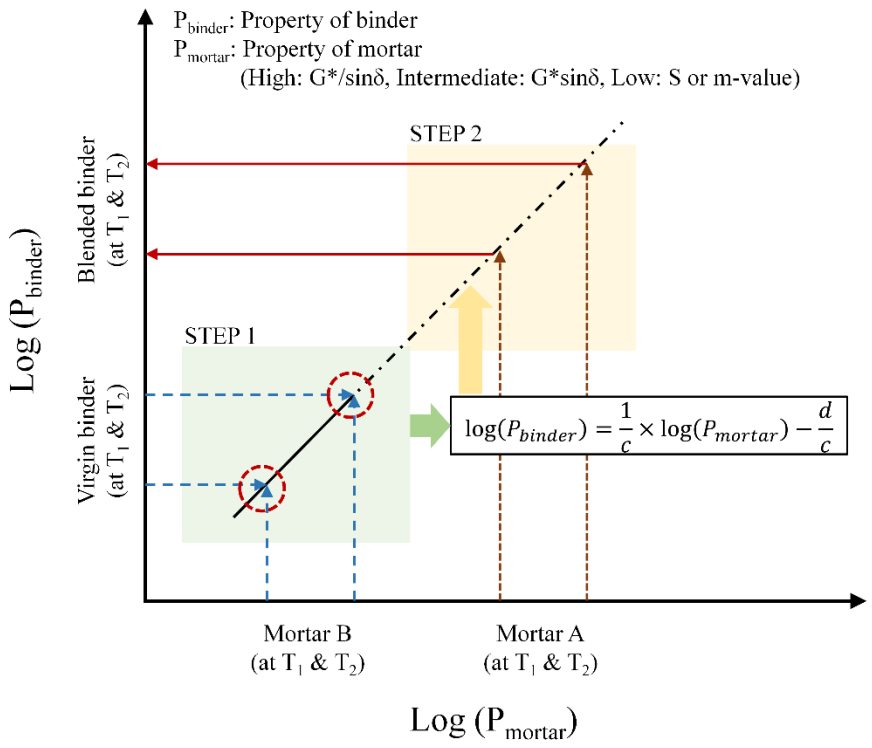

Figure B-3. Concept of predicting properties of blended binder

Coefficients c and d are dependent on the aggregate and binder volume fractions of mortar. Since the aggregate type and volume fractions are identical between mortars A and B, the difference in properties of these two mortars is caused by different binder properties. Therefore, the same relationship is used in Step 2 to predict properties of blended binder based on measured properties for mortar A by rewriting Equation B.1 in the following form:

$$\log(P_{blended\ binder}) = \frac{1}{c} \times \log(P_{mortar\ A}) - \frac{d}{c} \qquad Eq.B.2$$

Substituting mortar A property for P_{mortar} in Equation B.2, the blended binder property is obtained. Then, blended binder continuous grade can be determined by the predicted properties at two temperatures based on procedures set forth in ASTM D7643-16. It is important to note that the continuous grade of blended binder corresponds to the binder replacement ratio (BRR) of mortar A.

Prediction of continuous grade for RAP binder

Once the continuous grade of blended binder is determined for one BRR, the continuous grade of RAP binder alone can be obtained through linear extrapolation as shown in Figure B-4. It has been shown that binder replacement ratio and continuous grade of RAP binder are linearly related (Yan et al. 2018a). First, a grade change rate (GCR, °C/%replacement) is calculated as the change in continuous grade (°C) over the change in binder replacement ratio as shown in the following equation.

$$\mathrm{GCR} = \frac{Blended\ binder\ C.G. - Virgin\ binder\ C.G.}{BRR} \qquad Eq.B.3$$

where,

Blended binder C.G. = estimated continuous grade of blended binder (°C);

Virgin binder C.G. = measured continuous grade of virgin binder (°C);

BRR = binder replacement ratio (%) in the blended binder

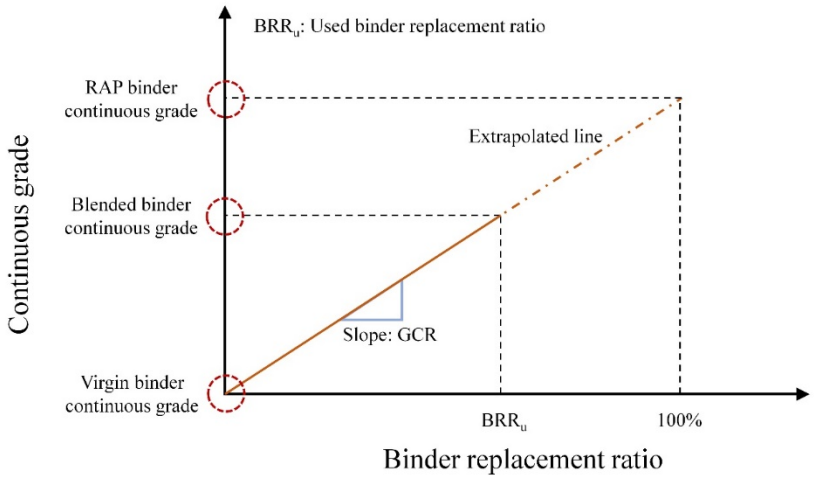

Figure B-4. Prediction of RAP binder continuous grade using grade change rate

The GCR can then be used to predict the high and low-temperature continuous grade of blended binder at any binder replacement ratio including 100%, which is RAP binder alone.

APPENDIX C

RECOVERED RAP GRADATION

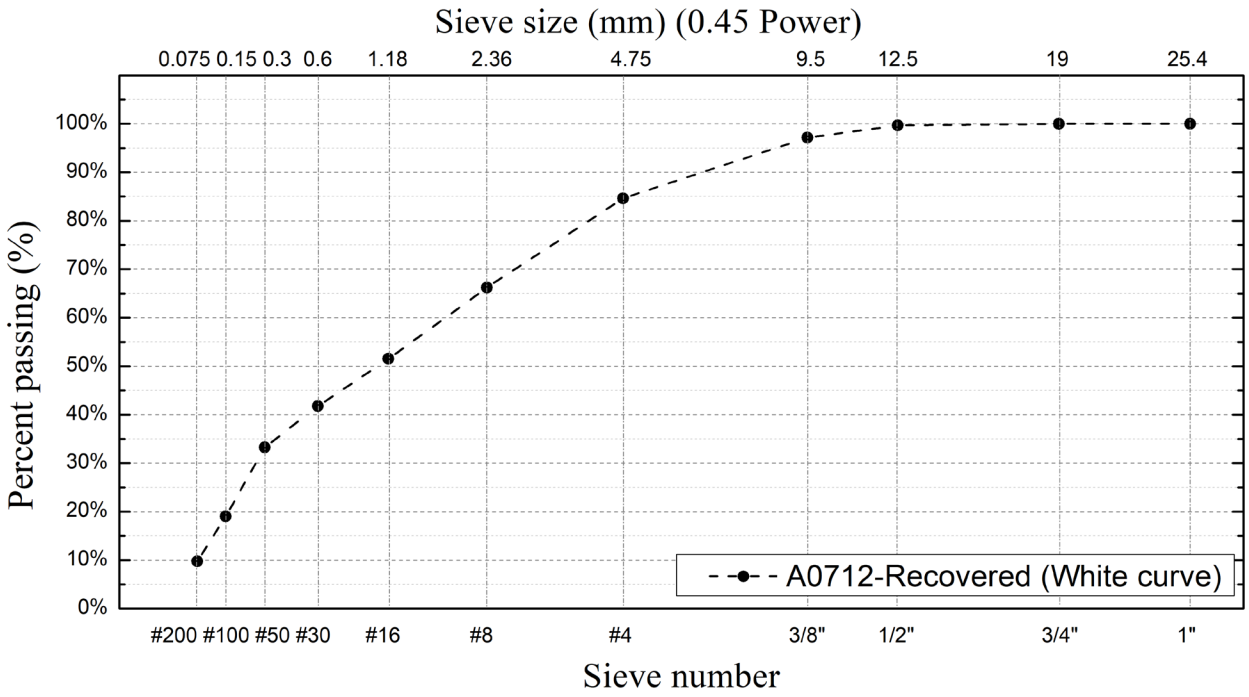

Figure C-1. Recovered RAP gradation of A0712 RAP stockpile

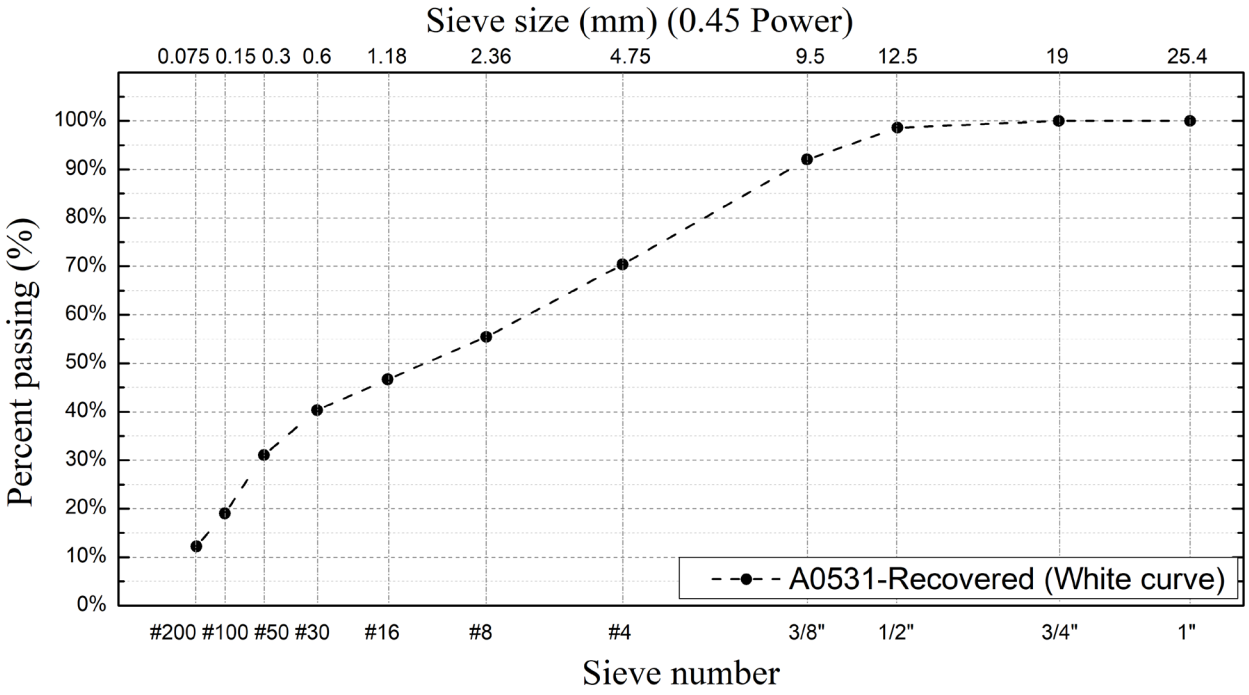

Figure C-2. Recovered RAP gradation of A0531 RAP stockpile

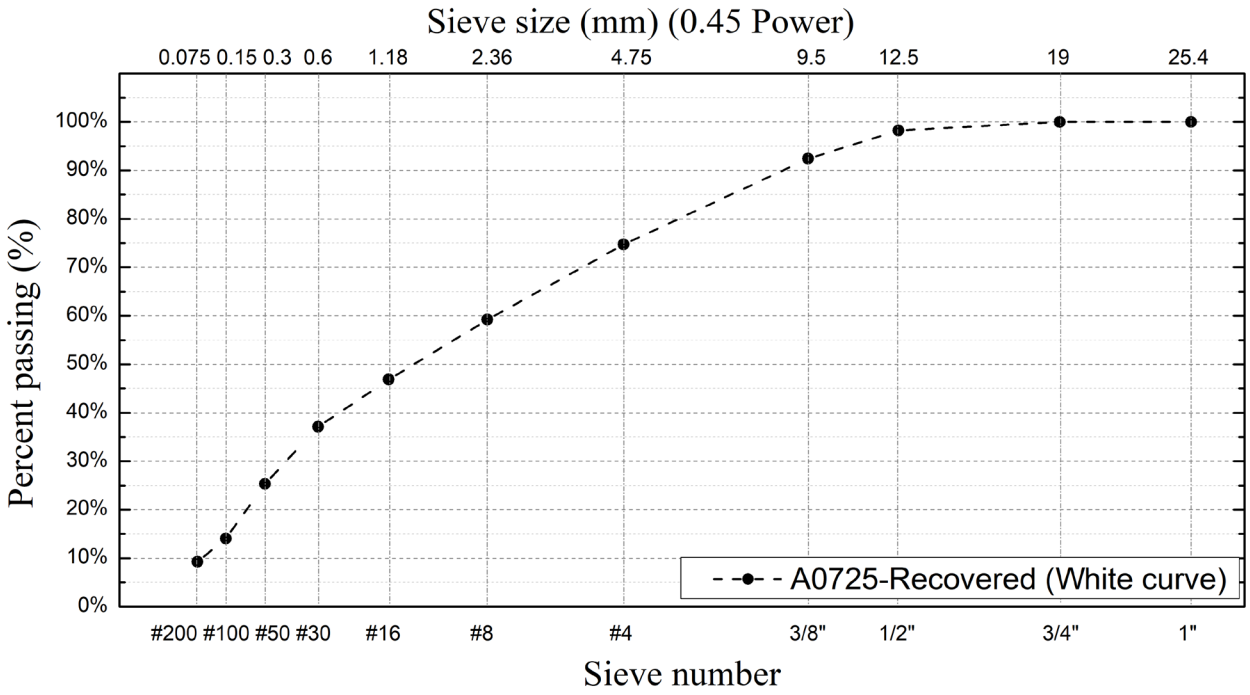

Figure C-3. Recovered RAP gradation of A0725 RAP stockpile

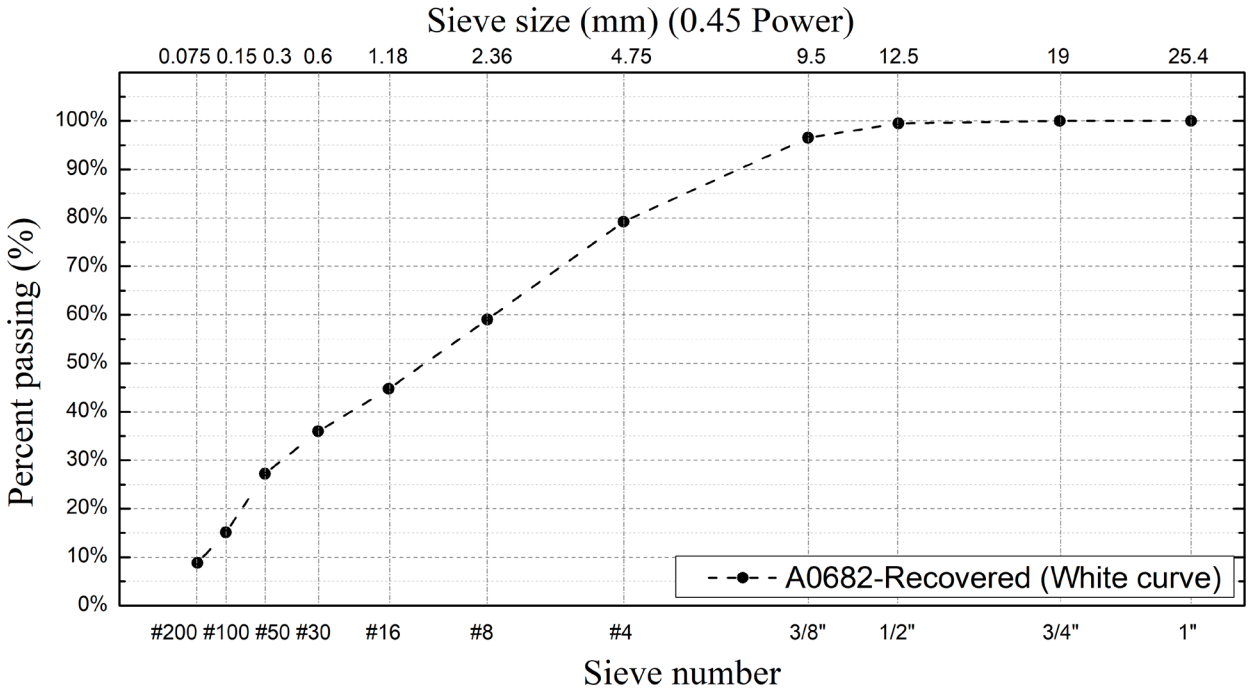

Figure C-4. Recovered RAP gradation of A0682 RAP stockpile

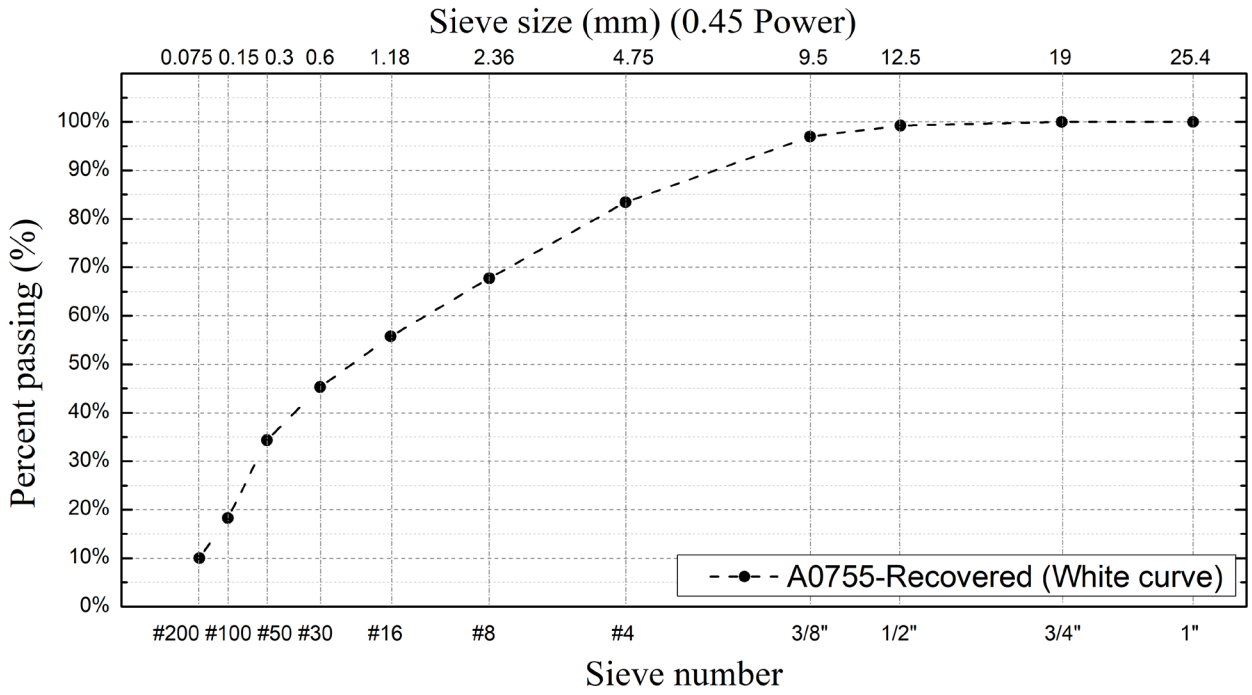

Figure C-5. Recovered RAP gradation of A0755 RAP stockpile

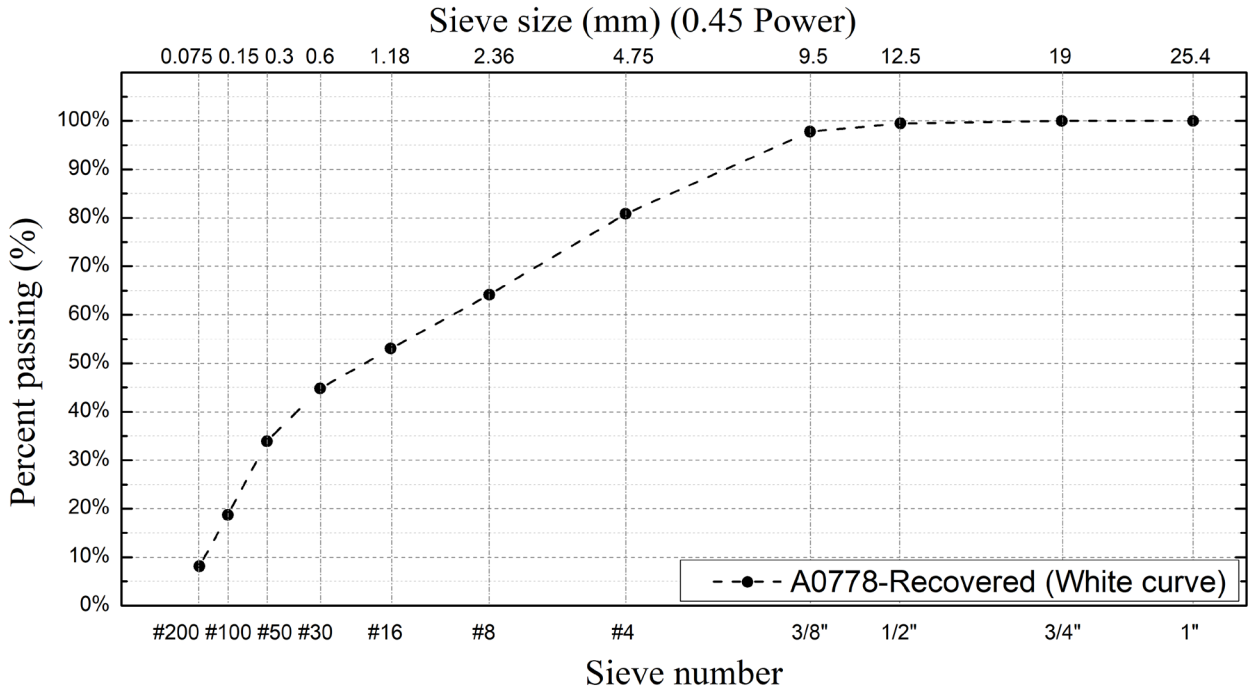

Figure C-6. Recovered RAP gradation of A0778 RAP stockpile

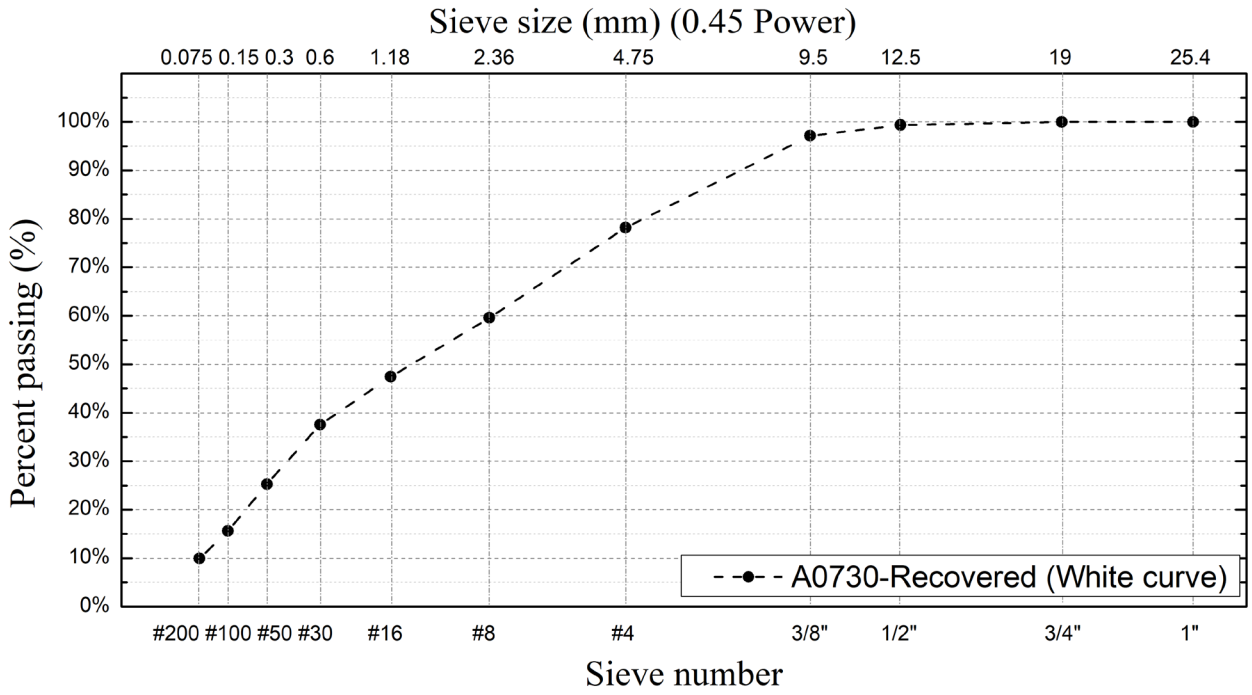

Figure C-7. Recovered RAP gradation of A0730 RAP stockpile

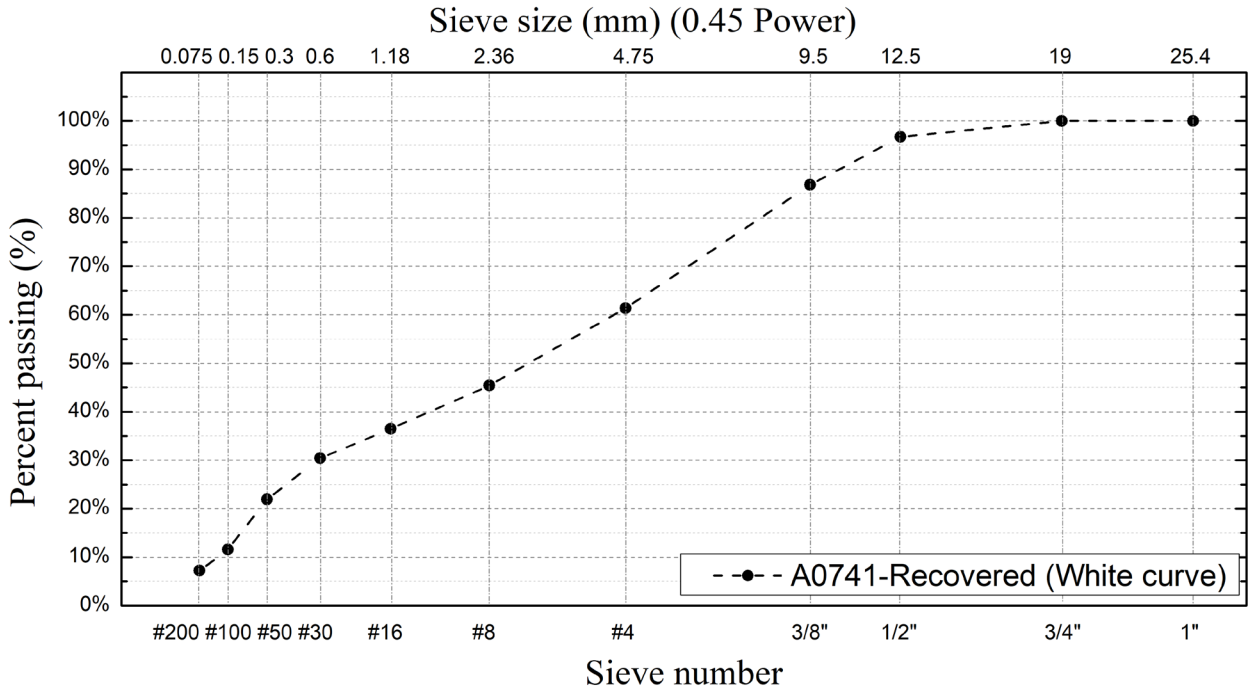

Figure C-8. Recovered RAP gradation of A0741 RAP stockpile

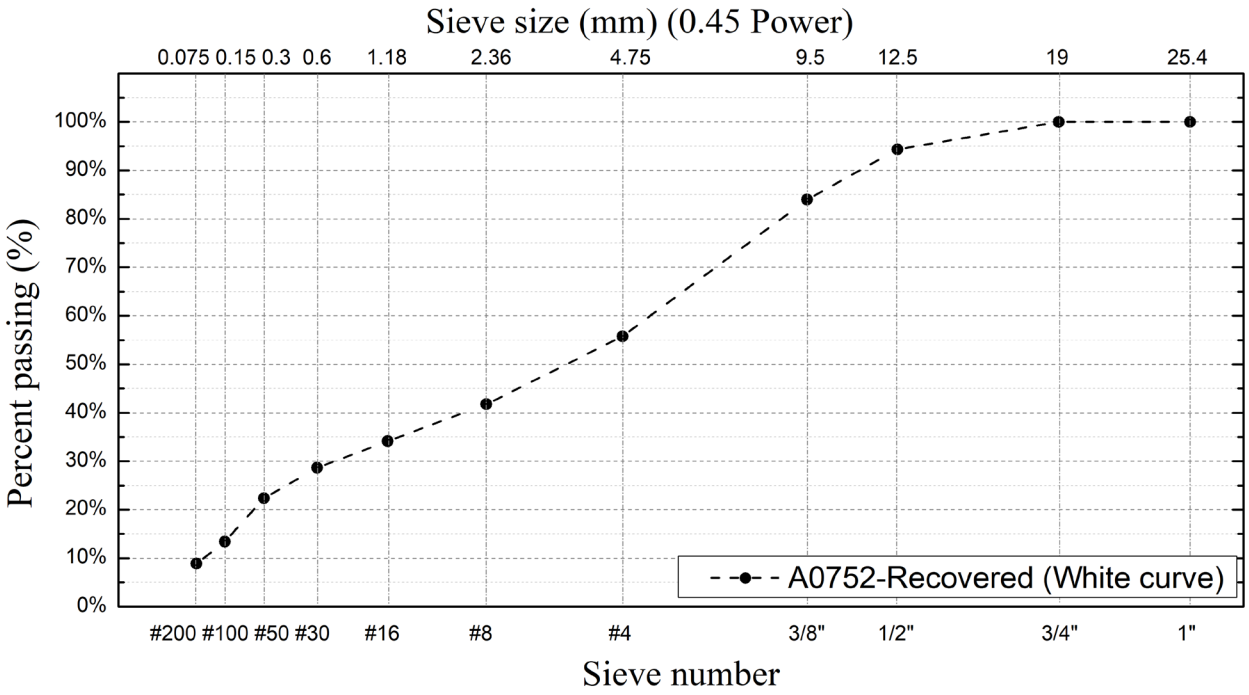

Figure C-9. Recovered RAP gradation of A0752 RAP stockpile

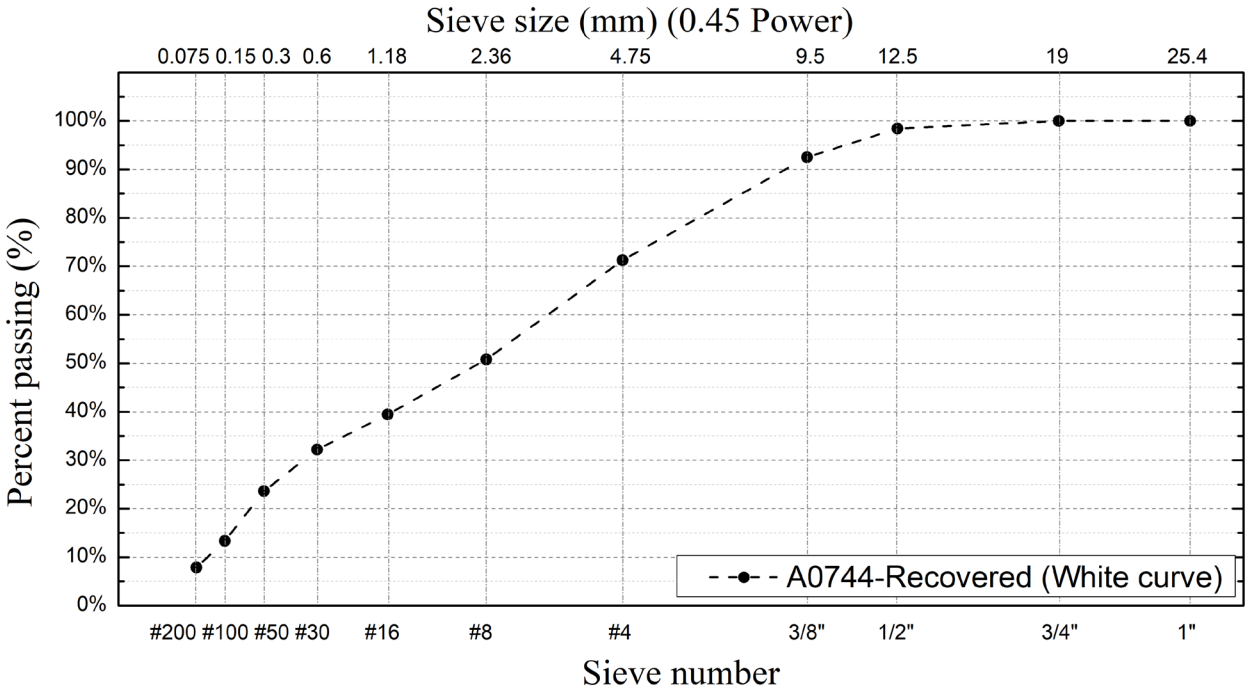

Figure C-10. Recovered RAP gradation of A0744 RAP stockpile

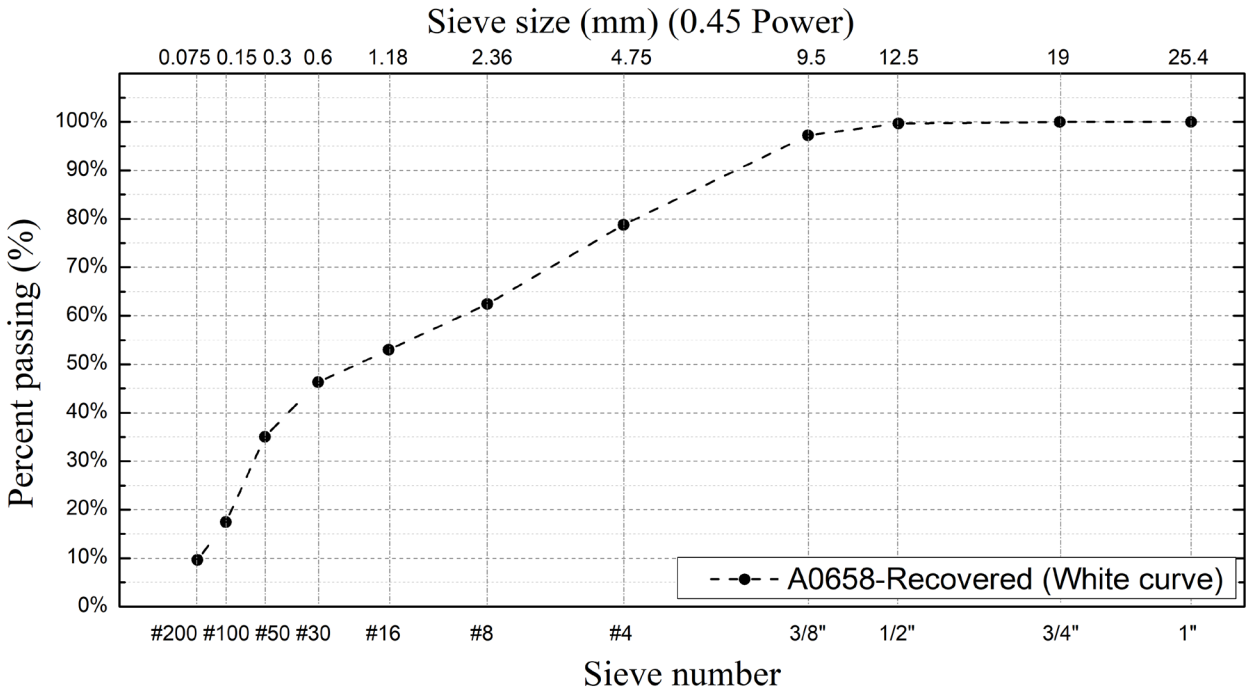

Figure C-11. Recovered RAP gradation of A0658 RAP stockpile

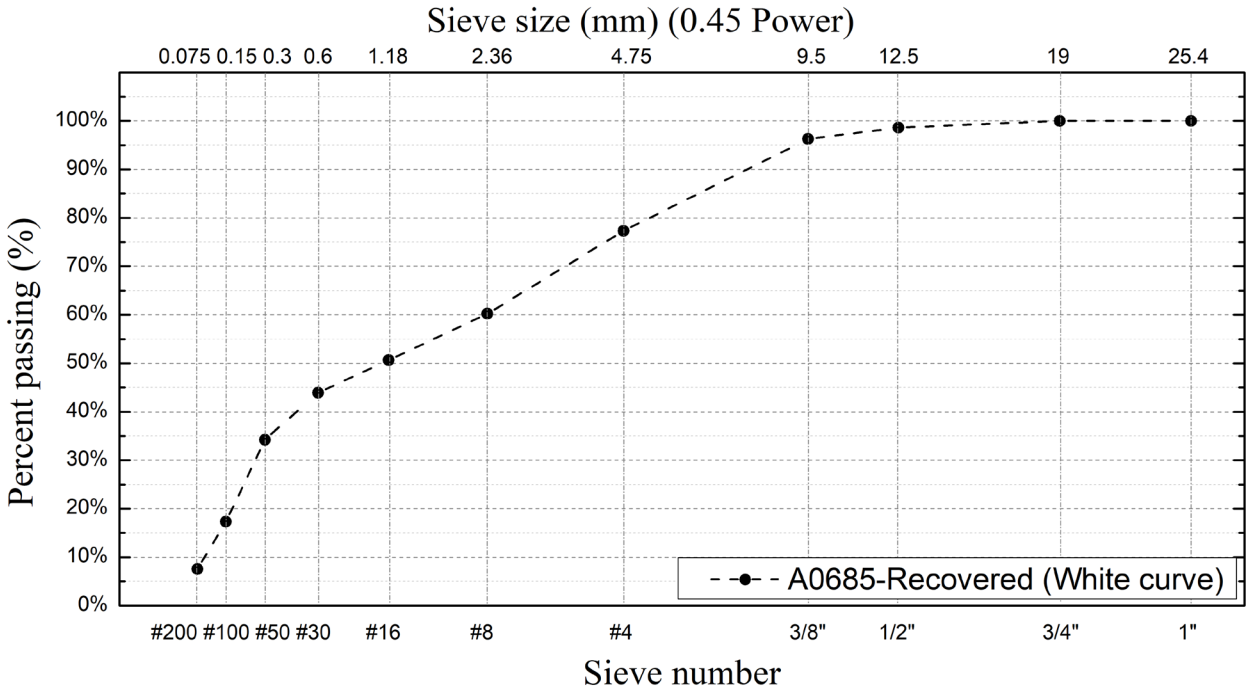

Figure C-12. Recovered RAP gradation of A0685 RAP stockpile

APPENDIX D

RECOVERED RAP BINDER TESTING RESULTS

Table D-1. Absolute viscosity test results

RAP material	Absolute viscosity at 60°C (poise)
A0712	965,322
A0531	653,203
A0725	501,799
A0682	651,431
A0755	755,280
A0778	222,064
A0730	260,790
A0741	901,291
A0752	412,835
A0744	716,101
A0658	1,336,673
A0685	561,914

Table D-2. High-temperature continuous grade of the 12 sampled RAP

RAP material	High-temperature continuous grade (°C)
A0712	101.1
A0531	95.9
A0725	98.0
A0682	103.3
A0755	102.1
A0778	95.9
A0730	95.4
A0741	103.4
A0752	100.4
A0744	100.4
A0658	107.6
A0685	99.6

APPENDIX E

RAP FINENESS RESULTS

Table E-1. RAP fineness (% Passing No. 16 sieve) of sampled RAP

RAP material	RAP fineness (% Passing No. 16 sieve)
A0712	51.52%
A0531	46.71%
A0725	46.87%
A0682	44.74%
A0755	55.78%
A0778	53.03%
A0730	47.43%
A0741	36.48%
A0752	34.13%
A0744	39.45%
A0658	53.01%
A0685	50.67%

APPENDIX F

BLENDED AGGREGATE GRADATAION (JMF)

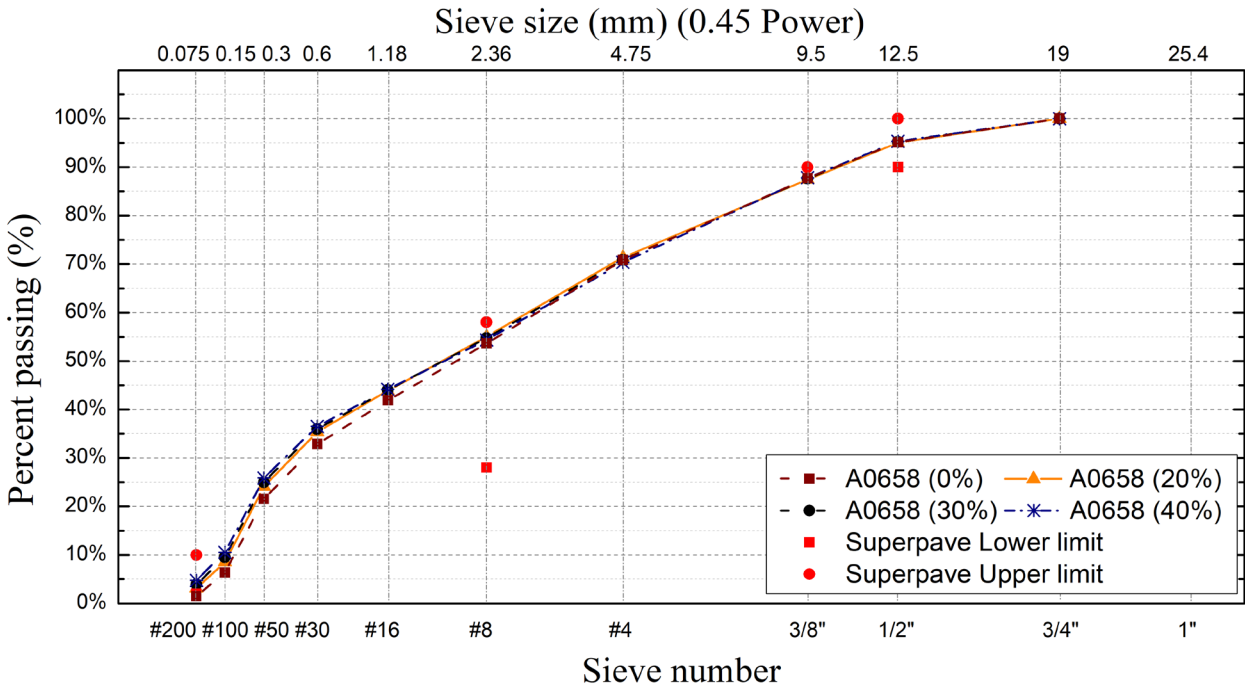

Figure F-1. Blended aggregate gradations (JMF) of A0658 RAP mix design

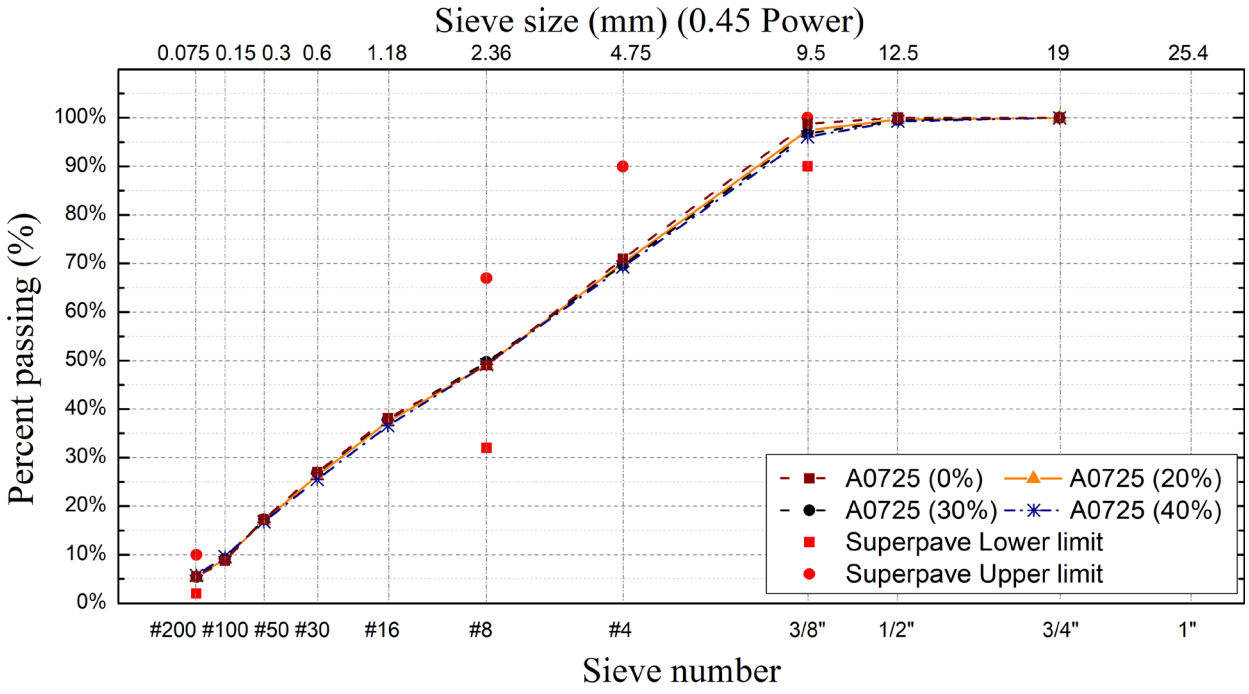

Figure F-2. Blended aggregate gradations (JMF) of A0725 RAP mix design

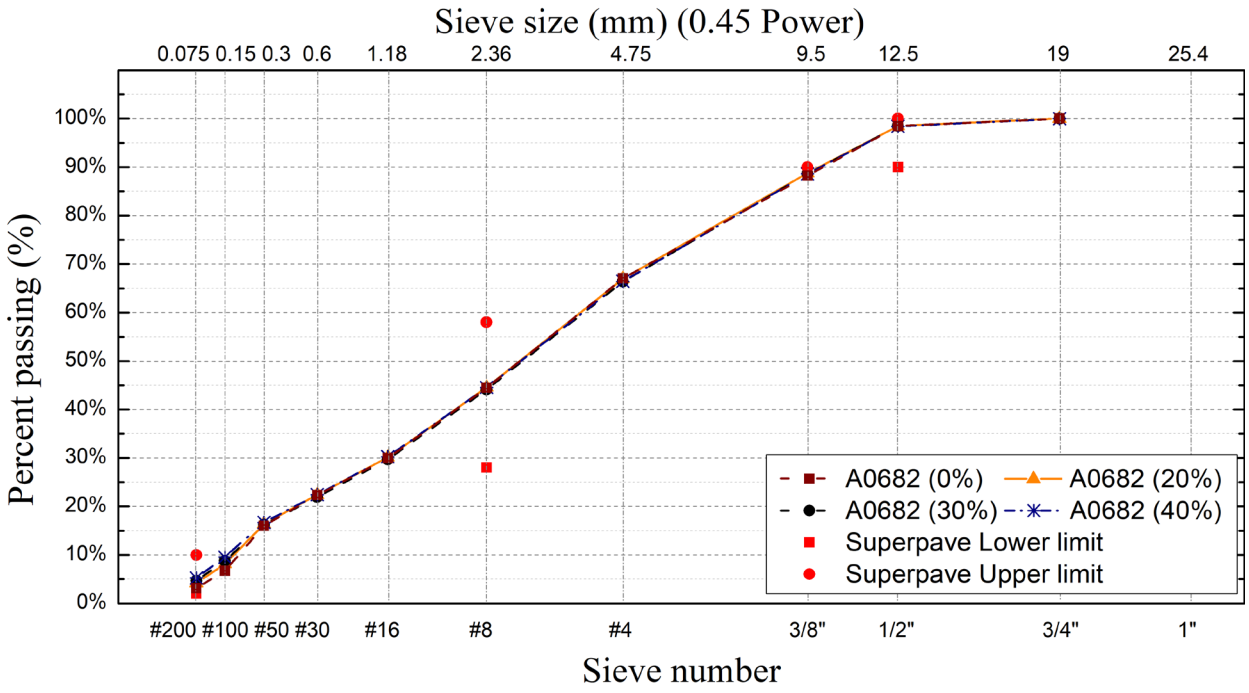

Figure F-3. Blended aggregate gradations (JMF) of A0682 RAP mix design

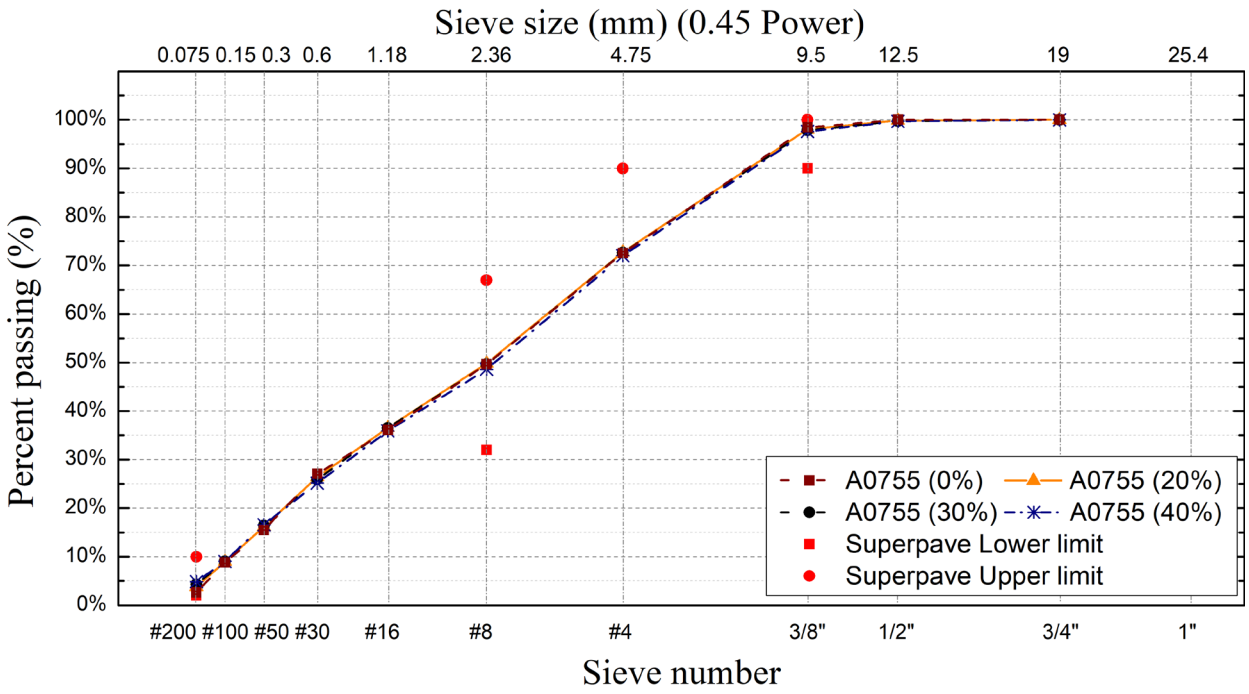

Figure F-4. Blended aggregate gradations (JMF) of A0755 RAP mix design

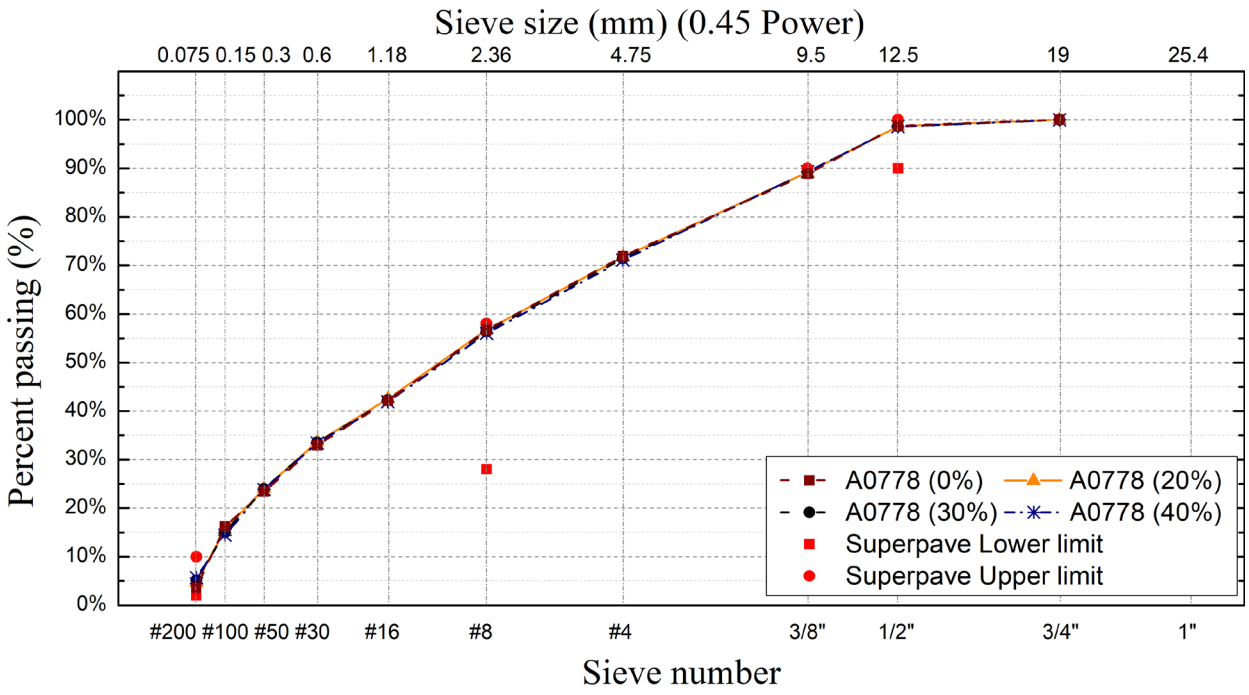

Figure F-5. Blended aggregate gradations (JMF) of A0778 RAP mix design

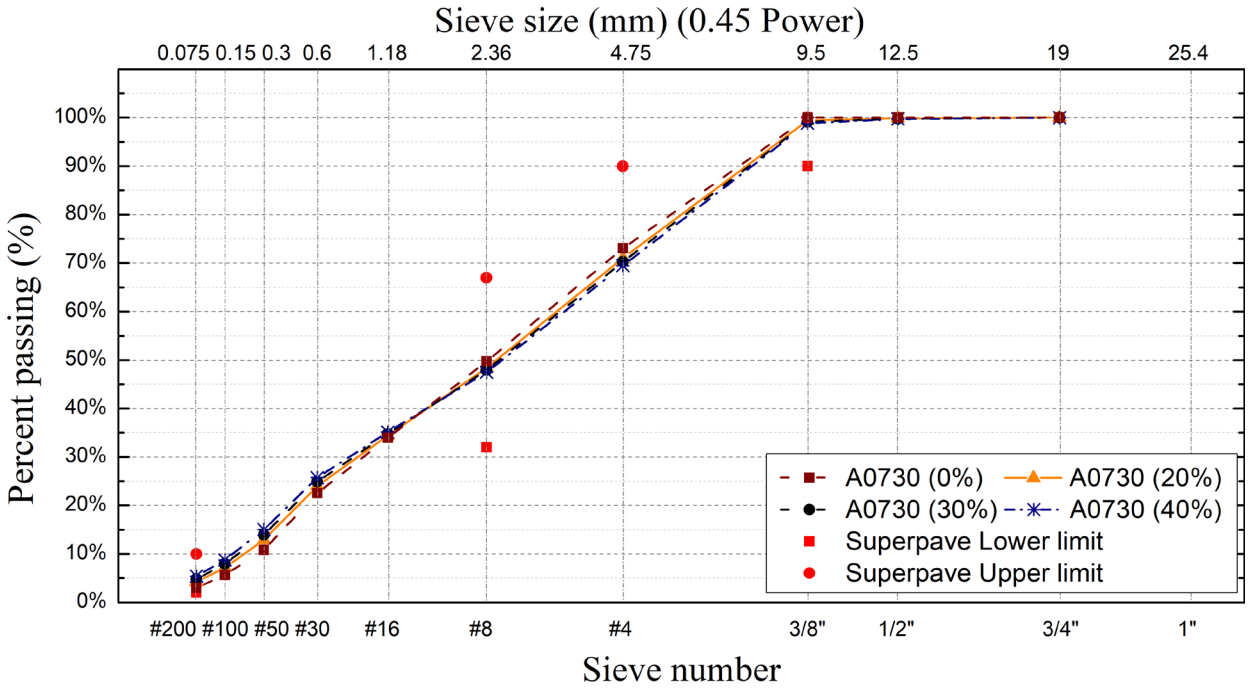

Figure F-6. Blended aggregate gradations (JMF) of A0730 RAP mix design

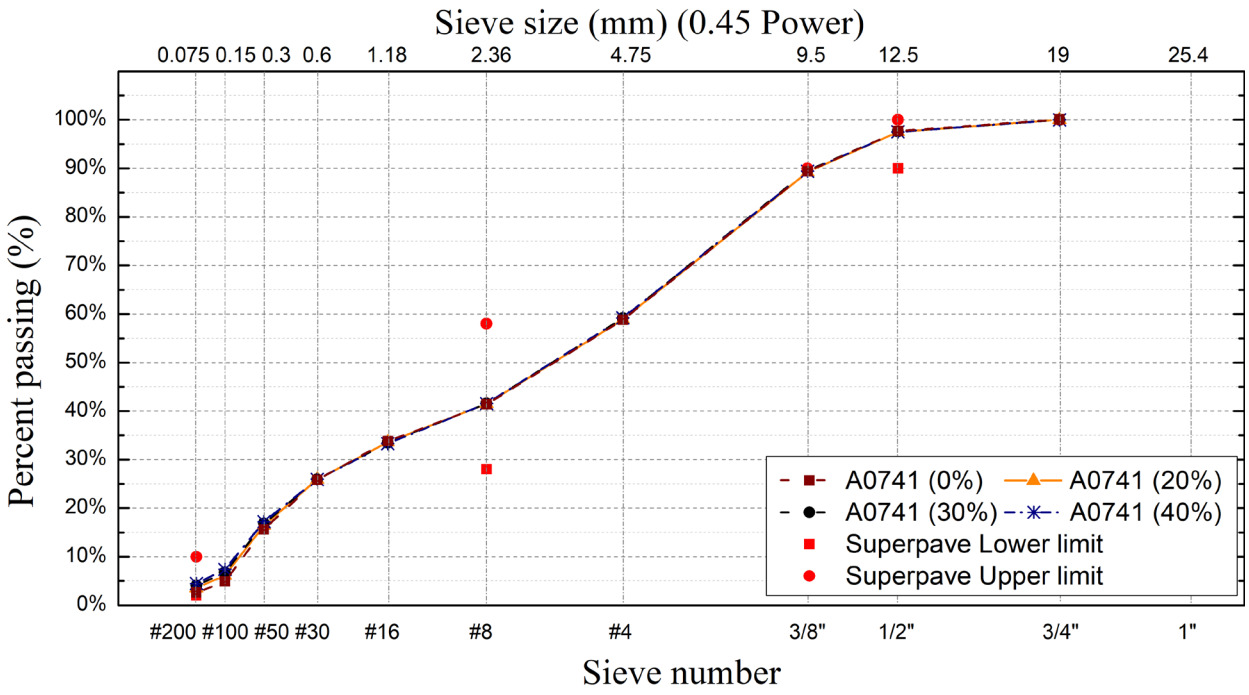

Figure F-7. Blended aggregate gradations (JMF) of A0741 RAP mix design

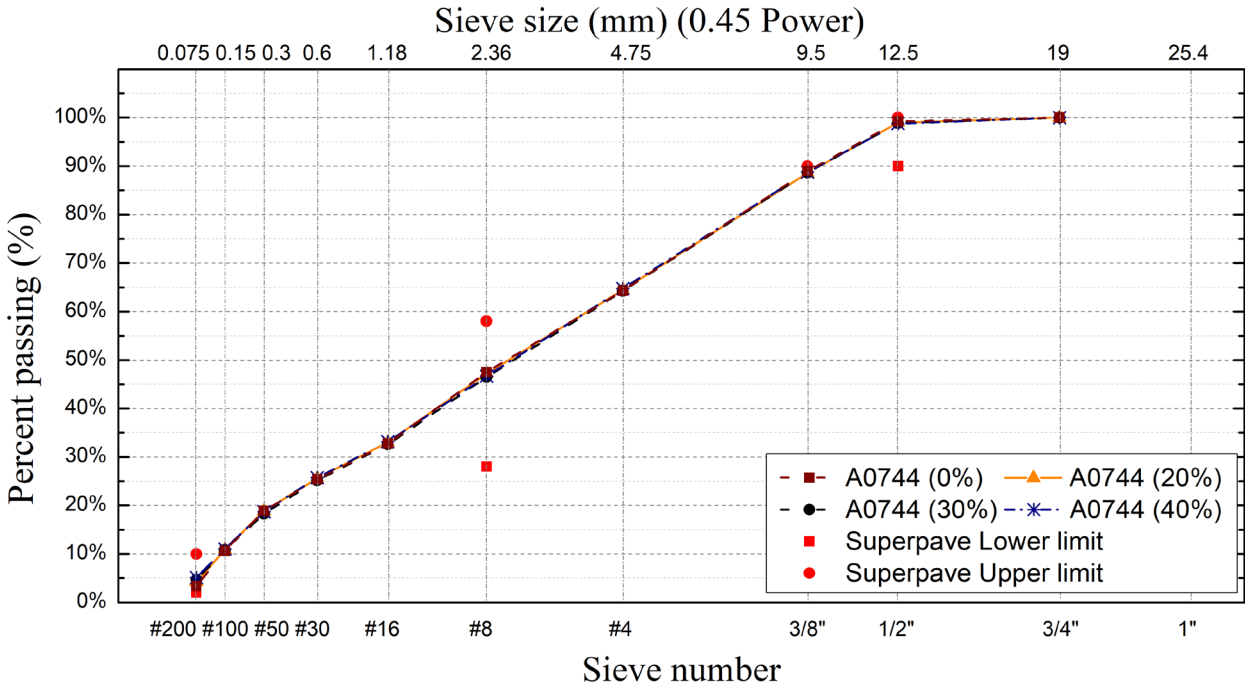

Figure F-8. Blended aggregate gradations (JMF) of A0744 RAP mix design

APPENDIX G

IC FRACTURE ENERGY RESULTS

Table G-1. IC fracture energy results

RAP type	Virgin binder type	IC fracture energy (kJ/m^3)			
		RAP content			
		0%	20%	30%	40%
C-I-#1	PMA binder (PG 76-22)	21.16	14.97	13.07	11.33
	HP binder	78.71	64.70	-	-
C-I-#2	PMA binder (PG 76-22)	25.52	20.10	16.35	11.89
	HP binder	53.08	44.30	-	-
I-I	PMA binder (PG 76-22)	31.40	12.16	11.30	10.06
	HP binder	81.31	64.82	-	-
I-L-#1	PMA binder (PG 76-22)	28.04	16.71	13.77	11.89
	HP binder	52.23	40.54	-	-
I-L-#2	PMA binder (PG 76-22)	20.98	14.82	12.92	10.30
	HP binder	76.13	60.25	-	-
F-H	PMA binder (PG 76-22)	11.04	4.90	4.41	2.62
	HP binder	25.27	12.61	-	-
F-I	PMA binder (PG 76-22)	17.85	4.55	5.46	5.19
	HP binder	35.24	23.93	-	-
F-L	PMA binder (PG 76-22)	17.40	6.88	4.36	3.76
	HP binder	19.23	11.23	-	-

APPENDIX H

SUPERPAVE IDT TESTS RESULTS

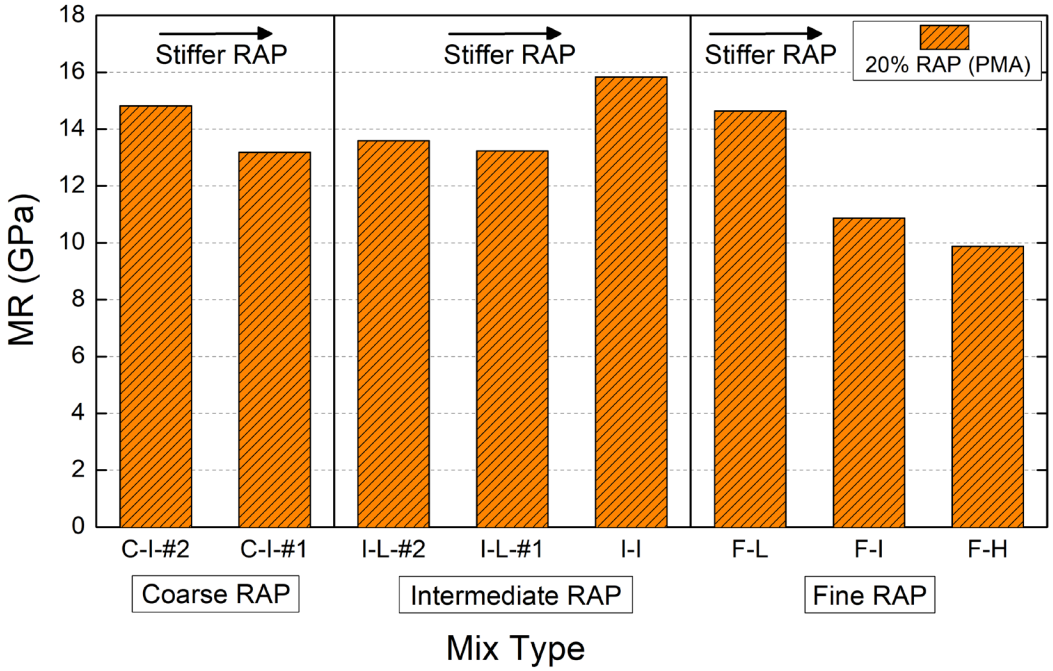

Figure H-1. Resilient modulus for PMA (PG 76-22) mixture with 20% RAP (LTOA+CPPC)

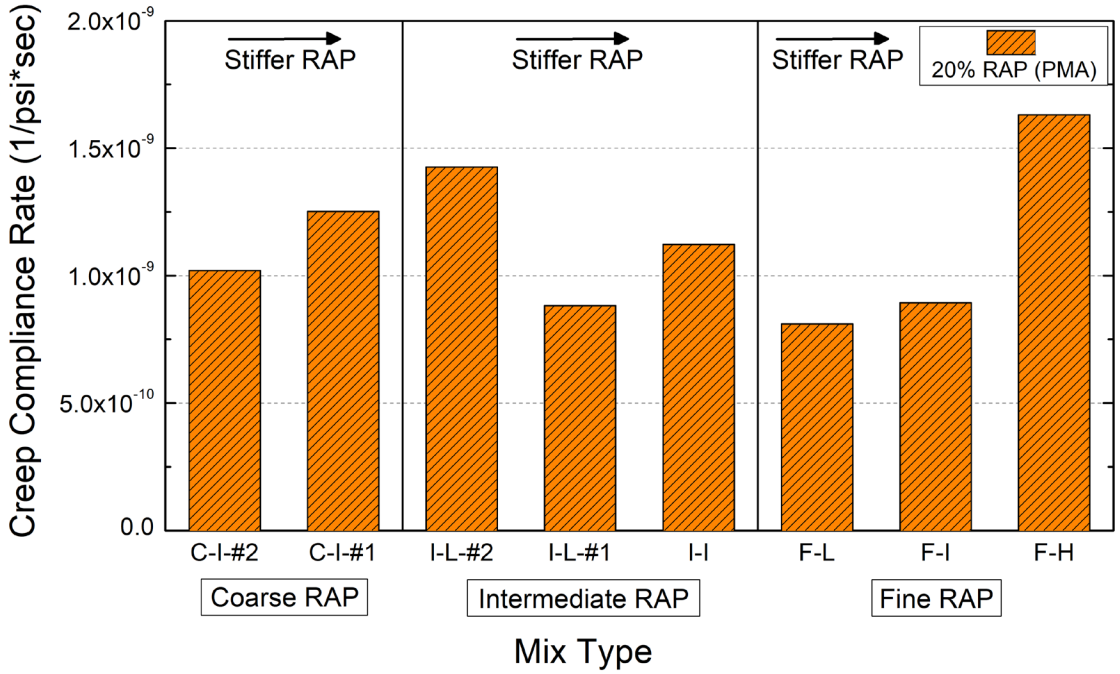

Figure H-2. Creep compliance rate for PMA (PG 76-22) mixture with 20% RAP (LTOA+CPPC)

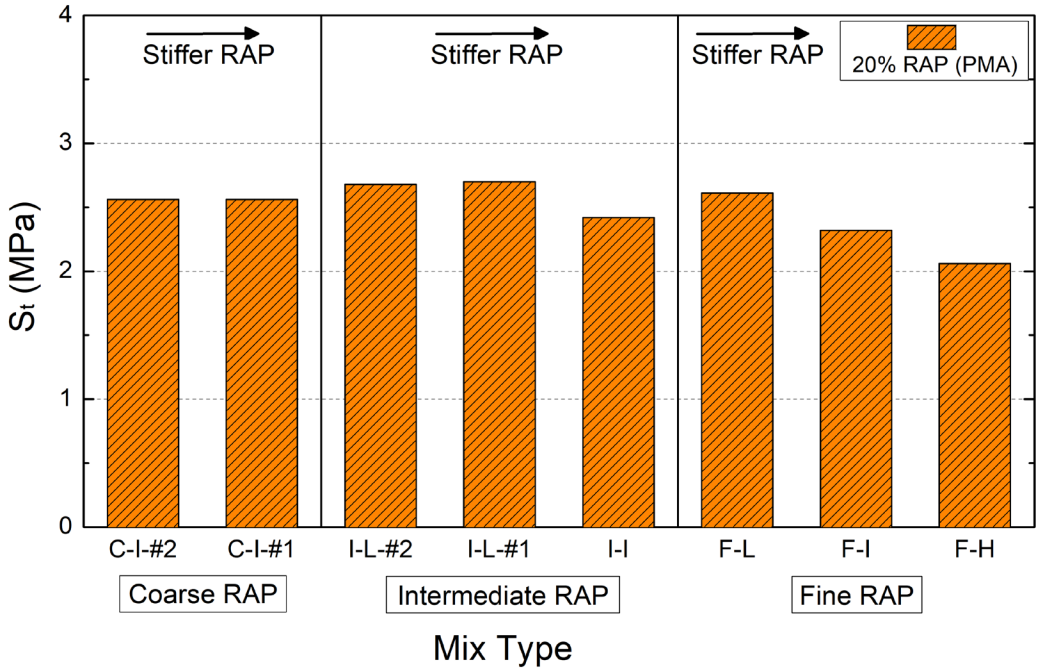

Figure H-3. Tensile strength for PMA (PG 76-22) mixture with 20% RAP (LTOA+CPPC)

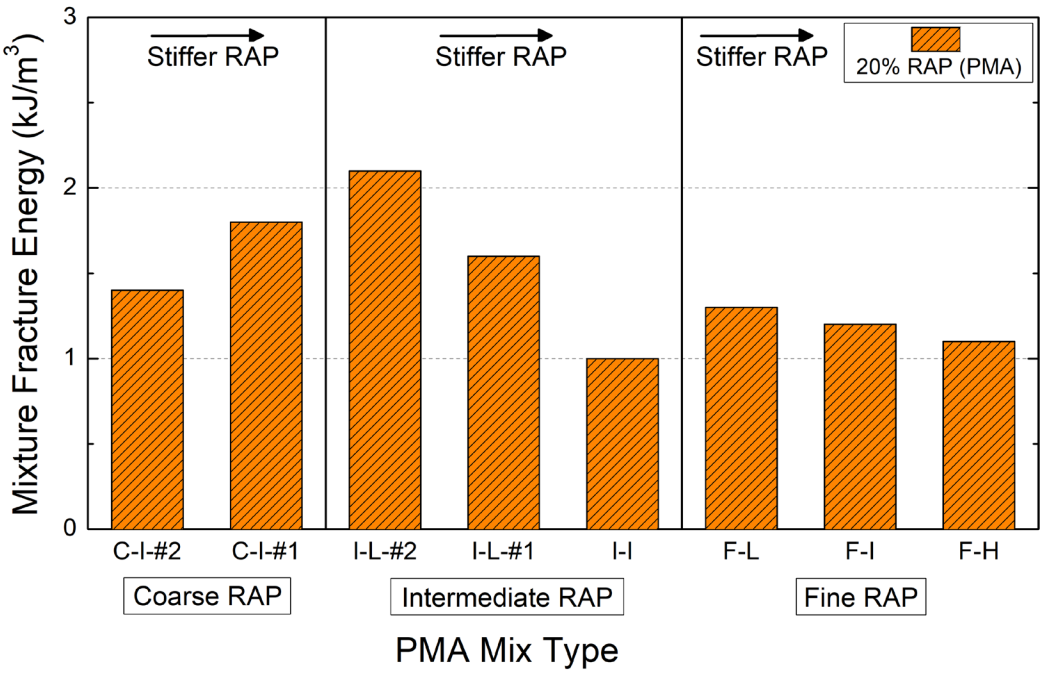

Figure H-4. Mixture fracture energy for PMA (PG 76-22) mixture with 20% RAP (LTOA+CPPC)

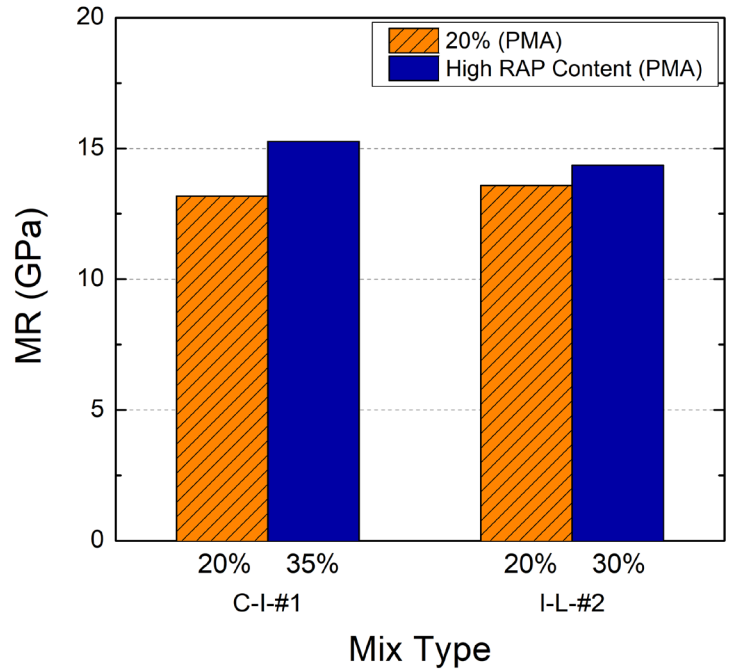

Figure H-5. Resilient modulus comparison between PMA (PG 76-22) mixture with 20% RAP and high RAP (LTOA+CPPC)

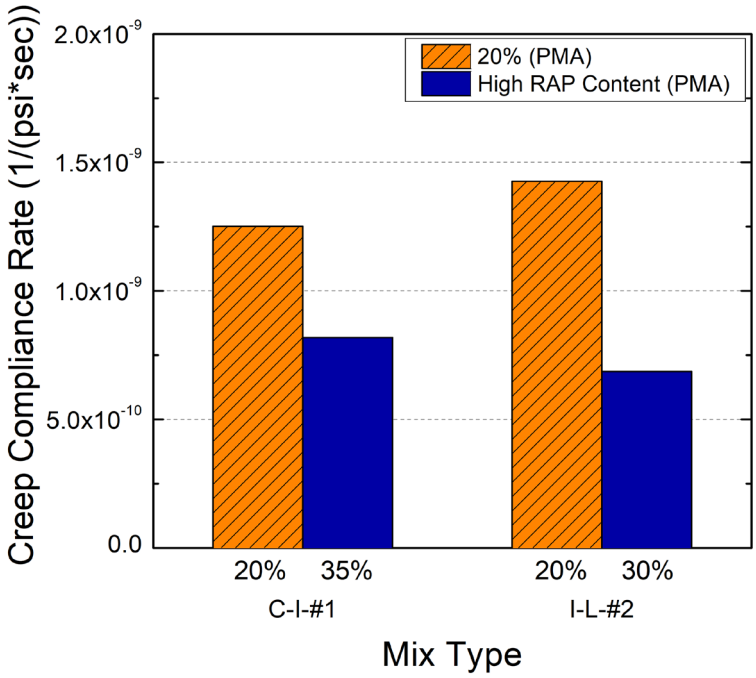

Figure H-6. Creep compliance rate comparison between PMA (PG 76-22) mixture with 20% RAP and high RAP (LTOA+CPPC)

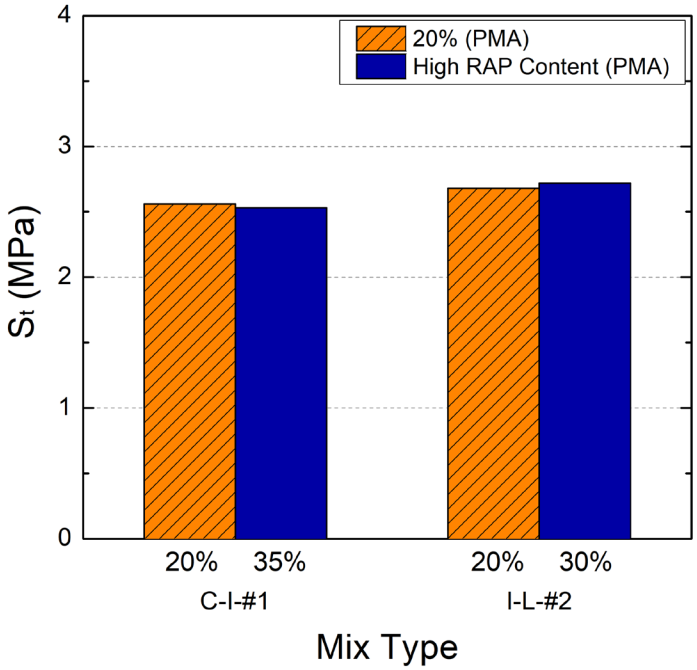

Figure H-7. Tensile strength comparison between PMA (PG 76-22) mixture with 20% RAP and high RAP (LTOA+CPPC)

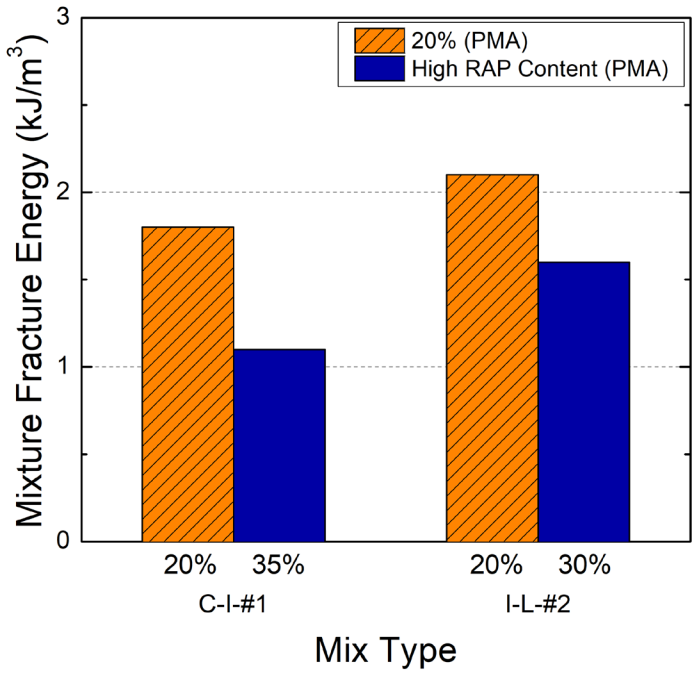

Figure H-8. Fracture energy comparison between PMA (PG 76-22) mixture with 20% RAP and high RAP (LTOA+CPPC)

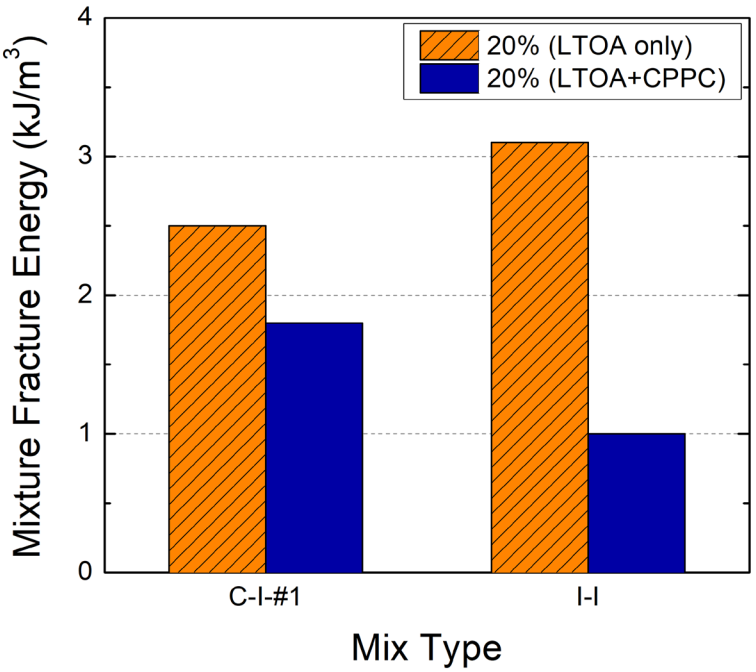

Figure H-9. Effect of CPPC conditioning on fracture energy

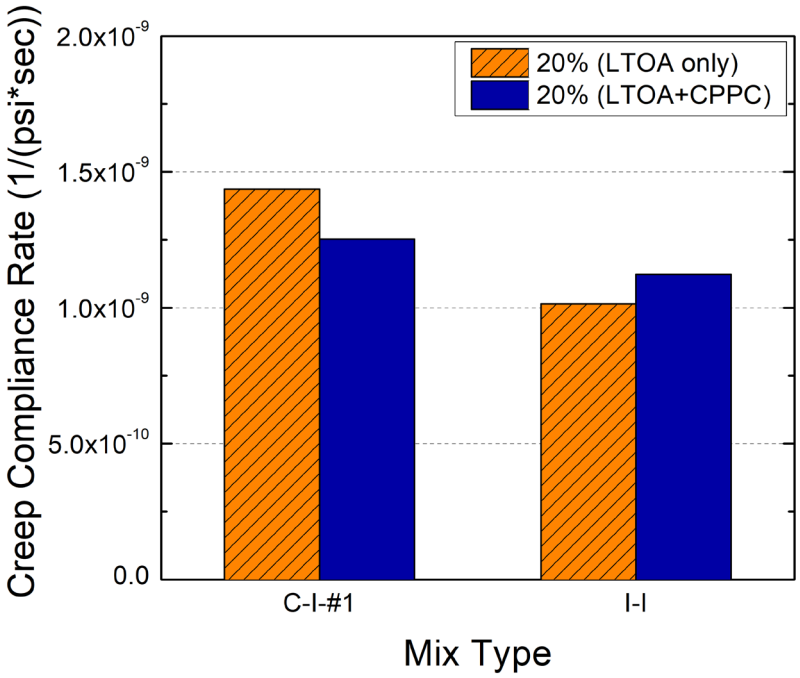

Figure H-10. Effect of CPPC conditioning on creep compliance rate

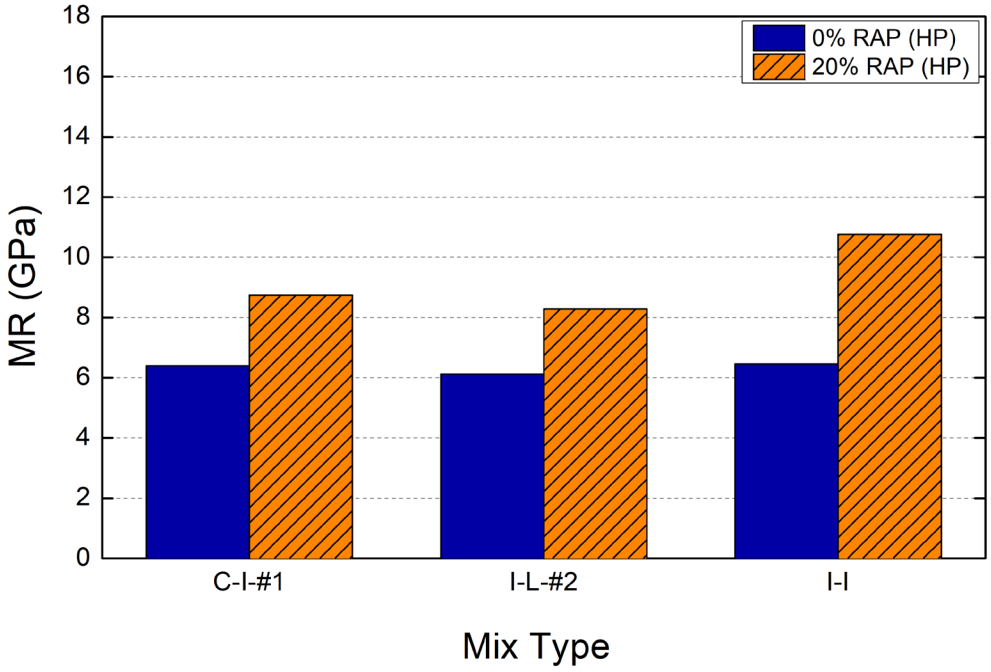

Figure H-11. Resilient modulus results for HP mixtures (LTOA+CPPC)

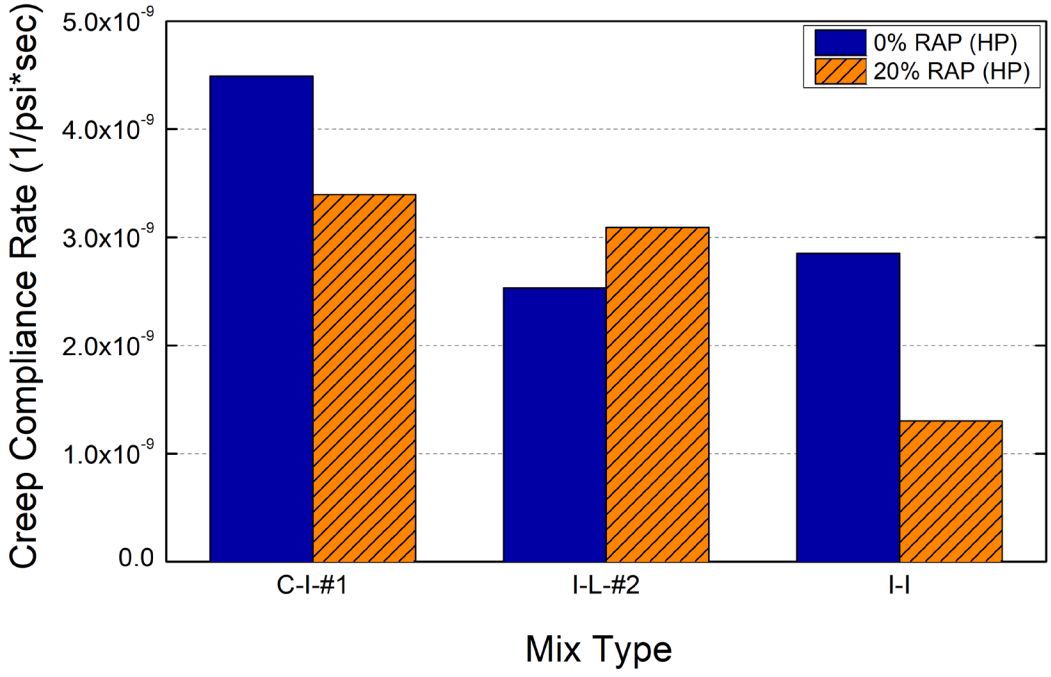

Figure H-12. Creep compliance rate results for HP mixtures (LTOA+CPPC)

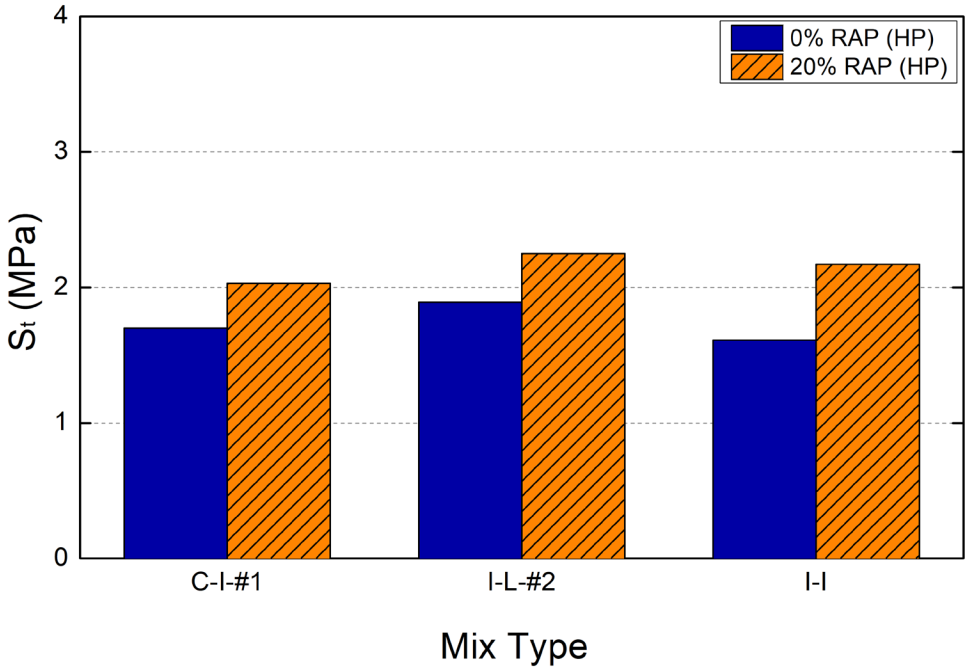

Figure H-13. Tensile strength results for HP mixtures (LTOA+CPPC)

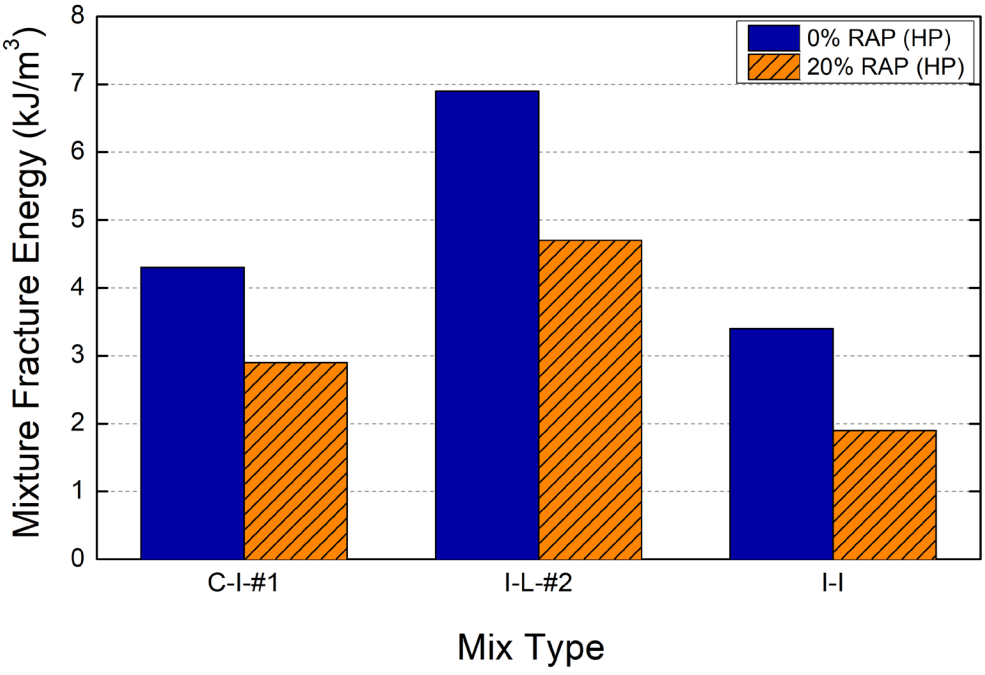

Figure H-14. Mixture fracture energy results for HP mixtures (LTOA+CPPC)